GEOELECTROMAGNETIC EXPLORATION FOR NATURAL RESOURCES: MODELS, CASE STUDIES AND CHALLENGES

MAXWELL A. MEJU
Geo-Optimization & Geoelectromagnetism Facility, Department of Geology, University of Leicester, Leicester LE1 7RH, England
E-mail: mxw@le.ac.uk

(Received 14 December 2000; Accepted 13 December 2001)

Abstract. This paper presents a tutorial review of electrical and electromagnetic (herein collectively called geoelectromagnetic) methods as applied in the search for natural resources. First, the paper discusses the technical problems and advances in geoelectromagnetic methods in the last decade. A scheme for integrating electrical and electromagnetic depth sounding data is suggested. Then, for natural resources exploration, it focuses on three themes: (1) understanding geological models of resource targets, their physical properties, and the development of conceptual geoelectromagnetic exploration models, (2) overview of geoelectromagnetic case studies in resource exploration, and (3) outstanding challenges in exploration. For brevity, model development is restricted to groundwater, geothermal and hydrocarbon resources, metallic ore-bodies (exemplified by volcanogenic massive sulphides, porphyry coppers, and epithermal and Archaean greenstone belt gold deposits) and diamonds. In the treatment of resource exploration in this paper, the unifying theme is that geochemical processes of weathering and hydrothermal alteration form clayey products that may render natural resource targets directly or indirectly detectable by their resistivity characteristics. Since hydrated clays are an important feature of most resource types and are major causes of low resistivity anomalies in geoelectromagnetic exploration, they may be taken as providing detectable marker horizons or pathfinders and a basis for developing a consistent investigative approach for natural resources. However, it is recognised that no single resource model or standard approach may be universally applicable. Natural resource systems are inherently 3D and require large numbers of depth soundings at high station densities to image adequately. Thus, developing methods of increasing the productivity of data acquisition, the development of better 3D software tools and lowering costs are seen as the major challenges facing the use of geoelectromagnetic methods for natural resource exploration.

Keywords: geochemical alteration, geoelectromagnetic (GEM) prospecting, mineral deposit models, resistivity characteristics, weathering

1. Introduction: Definition of Problems and Prospects

Mineral, geothermal and hydrocarbon resources are genetically related by water and heat. The physical property of subsurface materials that is most affected by changes in water content and temperature is electrical conductivity. Thus, important and in many respects unique information about economic natural resource targets can be deduced from measurements of their electrical conductivity. Numerous field techniques are used for conductivity measurements and the salient features are schematised in Figure 1. Basically, the ground is energised using

Surveys in Geophysics **23:** 133–205, 2002.

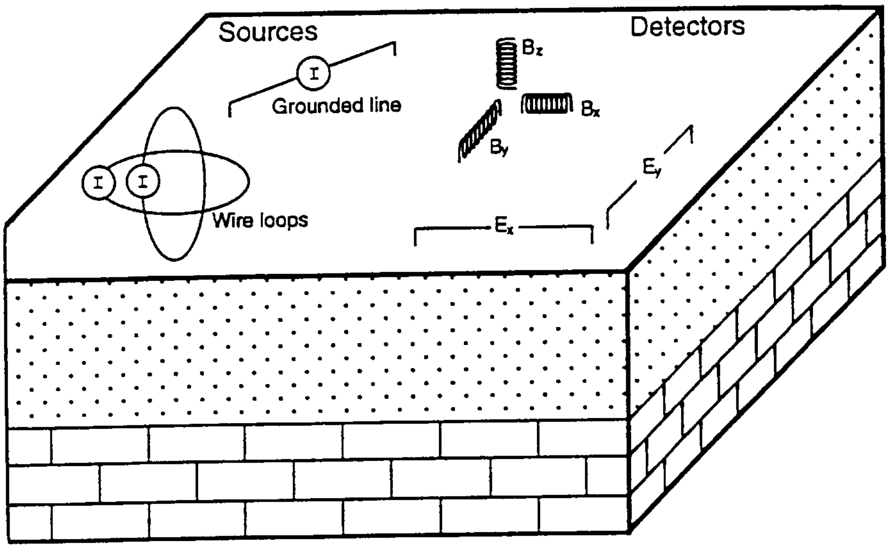

Figure 1. Geometry of typical GEM signal sources (transmitters) and receivers.

an inductive or galvanic source and the response is detected using suitable receivers (induction coils or grounded electric dipoles); the recorded data bear the conductivity signature of the subsurface. The electrical methods commonly used for subsurface investigations include the dc resistivity, induced polarisation (IP), spontaneous polarisation (SP) and magnetometric resistivity (MMR) techniques. The inductive or electromagnetic (EM) methods consist of frequency-domain and time-domain techniques. The frequency-domain electromagnetic (FEM) techniques include the natural source magnetotelluric (MT) and controlled source MT (CSMT) methods, as well as shallower-probing techniques that employ portable vertical- and horizontal-dipole EM sources (Figure 1). The time-domain techniques include the transient electromagnetic (TEM) method and the ground probing radar technique (not emphasised in this paper). The various techniques have downhole and/or airborne adaptations. The electrical and electromagnetic (herein collectively dubbed geoelectromagnetic or GEM) methods are central tools in the search for natural resources.

1.1. Overview of Problems and Developments in GEM Methods of Exploration

The TEM method is now widely used in natural resource investigations. The use of vertical-component TEM data is very common in non-mining investigations (e.g., Fitterman and Stewart, 1986; Buselli et al., 1988, 1990, 1992; Sinha, 1990; Meekes and van Will, 1991; Sandberg, 1993; Goldman et al., 1991, 1994; Christensen and Sorensen, 1994; Sorensen et al., 1995; Meju et al., 1999; Yang et al., 1999; Shtivelman and Goldman, 2000). It is now relatively straightforward to interpret the vertical-component data in terms of resistivity-versus-depth information (e.g., Christensen, 1995; Zhdanov et al., 1995; Meju, 1998) enabling approximate depths to subsurface targets to be determined (a vital piece of information for optimised post-survey drilling). Interestingly, numerous field studies in complex mining environments (e.g., Fokin, 1971; Fouques et al., 1986; Peters and de Angelis, 1987), and numerical and physical-scale modelling studies (e.g., Newman et al., 1987; Wilt and Williams, 1989), have shown that the horizontal components of the TEM response can pin-point the location of anomalous conductivity or geological contacts. With the commonly available single-component receivers, 3-component data are collected by sequentially orienting the axis of a receiver coil in the respective component directions. This is a laborious time-consuming process that is prone to operator errors especially for large transmitter loop sizes. Efficient 3-component broadband TEM receivers are now commercially available. With state-of-the-art TEM equipment (e.g., Geonics PROTEM47-67, Sirotem Mk3, Zonge GDP32-NT20 and ARTEMIS), it is now possible to image target features of exploration significance from a depth of a few metres to over 500 m depth using portable transmitters and 3-component receivers. Barnett (1984) and Macnae (1984) describe the interpretation of fixed-source, moving receiver, 3-component TEM data. Smith and Keating (1996) provide an insightful discussion of the usefulness of 3-component airborne TEM measurements in mining geophysics, specifically for the offset transmitter-receiver geometry used commonly in fixed-wing aircraft surveying. Multi-component data sets are especially useful in model selection in noisy or geologically complex areas. The ratio of the horizontal-to-vertical component TEM response (Spies, 1988) can be used as a dimensionality indicator in layered-earth interpretations. Annan et al. (1996) and Smith et al. (1996) show that measurements made while the transmitter is switched on, can provide valuable additional resistivity information in airborne TEM surveying in resistive terrains. Sorensen et al. (1995) and Sorensen (1997) describe novel pulled array TEM techniques that appear to offer considerable advantages over the conventional electrical and portable frequency-domain EM methods (e.g., greater penetration depth, improved logistics and anomaly resolution).

The classical tensor MT methods (e.g., Vozoff, 1972, 1991) require more time for field set-up than TEM and shallow-depth FEM techniques such as the horizontal-loop EM (HLEM) method. However, the recent availability of sophisticated multi-channel MT systems which are capable of simultaneous measurements at a base station and several remote stations or continuous EM array profiling - EMAP – (Torres-Verdin and Bostick, 1992) and the high frequency controlled source adaptations (e.g., Geometrics-EMI Stratagem model EH-4) hold good promise for increased productivity in natural resource investigations. The well-established high-power CSMT systems (such as those manufactured by Zonge Engineering & Research Organisation, Phoenix Geophysics and Metronix) are still the industry standard where accuracy, high productivity and deep penetration are demanded.

The electromagnetic methods have some practical advantages over electrical methods especially in difficult terrains. However, the availability of automatic electrode switching devices has meant that electrical surveys can be easily and much more efficiently done using a microcomputer controlled data acquisition system (e.g., Goebuchi et al., 1988; Halvorsen et al., 1988; Griffiths et al., 1990; Olayinka and Barker, 1990; Meju and Montague, 1995; Shima et al., 1996). Advanced adaptations can be found in novel mobile electrical and electrostatic arrays (Sorensen, 1996; Panissod et al., 1998).

Traditional prospecting for natural resources using widely spaced GEM sounding stations (herein referred to as 'discrete soundings') face the problem of galvanic distortion of the apparent resistivity soundings curves - the so-called static shift or lateral effects in MT or dc resistivity parlance (see e.g., Barker, 1981; Jones, 1988; Sternberg et al., 1988). Fortunately, new advances in digital technology and concurrent developments in optimised multi-dimensional numerical modelling (e.g., Newman et al., 1986; Druskin and Knizhnerman, 1988; Wannamaker, 1991; Rijo, 1993; Sugeng et al., 1993; Mackie and Madden, 1993; Spitzer, 1993; Ellis and Oldenburg, 1994; Zhang et al., 1995; Druskin et al., 1999; Weller et al., 2000; Sasaki, 2001) and instrumentation (e.g., Goebuchi et al., 1988; Griffiths et al., 1990; Shima et al., 1996; Sorensen et al., 1995; Sorensen, 1996, 1997; Constable et al., 1998) have led to improved data acquisition (especially high productivity 'continuous array profiling') and interpretation techniques as well as brought these popular methods within range of their theoretical resolving capability (Meju, 2000a). It is now possible to collect field data sets of the highest achievable quality so as to push the methods to their limits and hence quantify their utility and resolving power in natural resource investigations. The previously undesirable near-surface 3D bodies that cause galvanic distortions of sounding curves may now be identified or mapped using 3D surveys with a dense network of observational stations and appropriate sounding frequencies or electrode spacings. From a practical viewpoint, the most important development in the use of GEM methods in natural resource exploration is the availability of software for 2D and 3D interpretation of field data from both the commercial (e.g., Druskin and Knizhnerman, 1988; Oldenburg and Li, 1994; Loke and Barker, 1996) and non-commercial sectors (e.g., deGroot-Hedlin and Constable, 1990; Uchida and Murakami, 1990; Smith and Booker, 1991; Mackie and Madden, 1993; Spitzer, 1993; Mackie, 1996).

However, in spite of the aforementioned developments, the effectiveness of each individual GEM method varies from one geological terrain to another and there is still the problem of integrating the numerous surface and downhole methods to obtain a consistent form of data presentation (see e.g., Spies and Eggers, 1986) or a uniform investigative approach in natural resource investigations as in the seismic community. Based on numerical modelling and comparisons of dc resistivity, TEM and MT field data, Meju (1996b) suggests that Schlumberger vertical electric

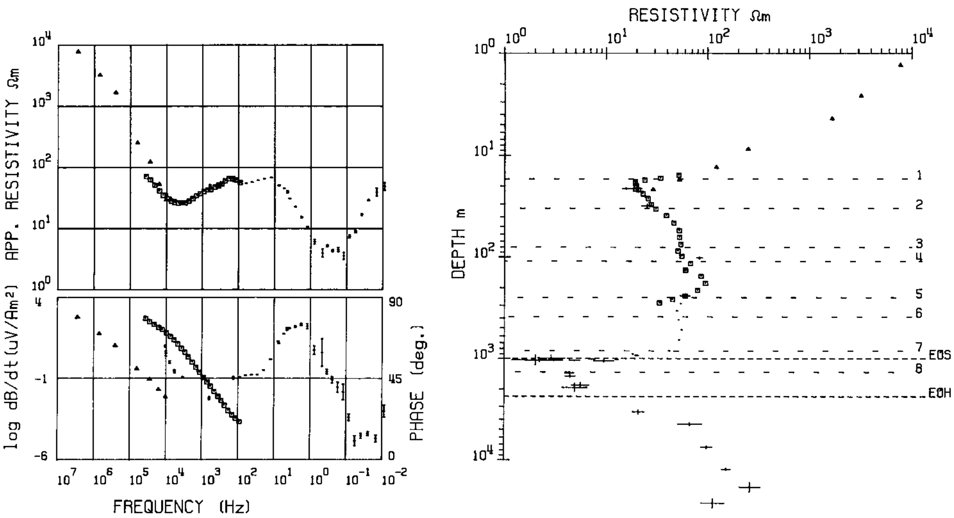

Figure 2. Example of integration of VES, TEM and MT sounding curves. The VES (triangles), TEM (squares), and MT (shown with error bars) ρ_a data are presented in the left-hand top panel using a common-scale based on Equations (1) and (2). Other field responses (phases and log resistance and voltage decay) are shown in the bottom panel. The result of simple depth transformations of the ρ_a data are compared in the right-hand plot with lithological data (sequentially numbered formation boundaries) from a nearby borehole (see Meju et al., 1999, Figure 9). EOH = end of hole. EOS = base of an important shaly formation.

sounding (VES) and TEM apparent resistivity data may be compared or combined using the scaling relation

$$\log_{10} t \cong 2\log_{10}(L) - \log_{10}(\rho_i/(k\mu_o)), \quad (1)$$

where the transient time t is in milliseconds, L (= AB/2) is the distance from the centre of the array to a current electrode in metres, $\mu_0 = 4\pi \times 10^{-7}$ H/m, $k = 1500$, and ρ_i is the subsurface resistivity at the appropriate (ith) depth (which may be conveniently approximated by apparent resistivity in practice). Also, TEM and MT soundings may be combined using the scaling relation (cf. Meju, 1996a)

$$T \cong 3.92t, \quad (2)$$

where the transient time t is in seconds and T is the equivalent MT period in seconds. The above empirical relations work well especially in quasi-1D environments and may serve for integrating electrical and EM vertical depth sounding data as shown in Figure 2. Note that Meju et al. (1999) employed a variant of Equation (1) with a fixed value for ρ_i corresponding to the average value for the uppermost geoelectric section (100–150 Ωm) imaged by VES in their study region.

1.2. Towards a consistent investigative approach

It is well known that within a given tectonic environment, lithology, stratigraphy and structure exert important controls on the occurrence of natural resources. Thus, successful and cost-effective applications of GEM methods depend upon our understanding and imaginative application of geological models of resource systems. This, and the recently available capability for acquiring and interpreting 3D GEM data, hold the key to fully understanding resistivity images of natural resource targets. The main motivation in this review paper is therefore to find a common thread that binds the various natural resource targets within a geoelectromagnetic framework, and a tutorial approach is deemed necessary. The well-established concepts in exploration geology and geochemistry are combined with the available petrophysical data to develop analogous geoelectromagnetic models for natural resources with emphasis on the role of hydrothermal and weathering processes in the development of clayey conductive targets. Those elements of the exploration models that could be sought in practical settings are stressed in a naive attempt to encourage the development of a consistent investigative approach. Currently outstanding and anticipated future challenges in geoelectromagnetic prospecting are presented for each resource type.

2. Groundwater Resources

2.1. Geological setting of groundwater resources

Groundwater is the water filling the pore spaces in rocks. Sedimentary materials and fractured crystalline rocks commonly form aquifers or reservoirs (saturated permeable geological units that can transmit significant quantities of water under ordinary hydraulic gradients). Clays, shales, intrusive igneous bodies and metamorphic rocks are common aquitards or aquicludes (relatively impermeable rock materials that serve as seals or caps for aquifers) and are typically characterised by insignificant interconnected pore spaces. The nature and distribution of aquifers and aquitards are controlled by geological and geomorphological factors (see e.g., Freeze and Cherry, 1979, Chap. 4). Typical geological environments for groundwater occurrence include alluvial fill and gravel beds overlying crystalline bedrock or other impervious material, sand and gravel lenses in glacial till, and fault and fracture zones in crystalline basement rocks.

Sand, gravel, conglomerate and carbonate aquifers are the most important water sources in sedimentary environments (Freeze and Cherry, 1979). The main forms of occurrence of groundwater targets in soft-rocks are illustrated in Figure 3. Glacial terrains are characterised by complex stratigraphy with sand and gravel lenses in till being the most important targets. In carbonate terrains, the main features are the zones of fracture concentration (in particular, fracture intersections and lineaments) and rock dissolution (karst cavities) that may contain significant quantities

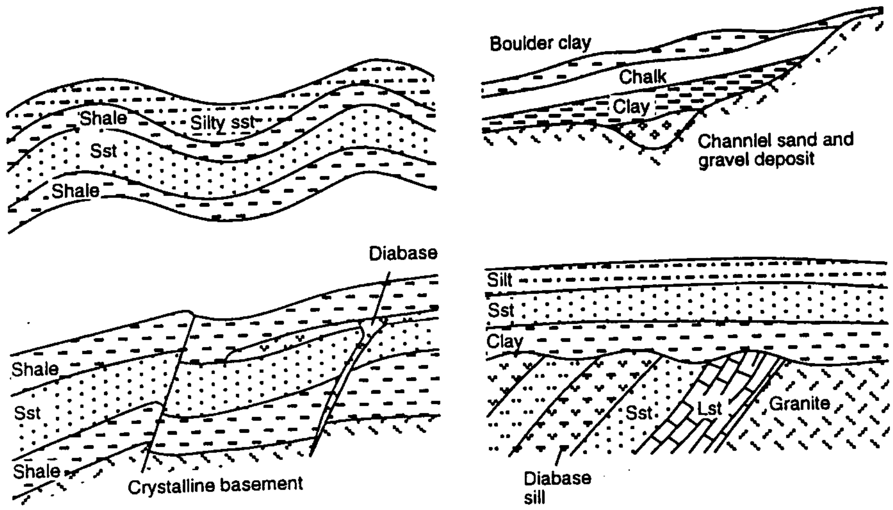

Figure 3. Common stratigraphic and structural groundwater traps. The structural traps shown consist of conformable shale and sandy formations affected by folding (top left), and by faulting and igneous intrusion (bottom left). The stratigraphic traps consist of pinch-out chalk unit and unconformable channel fill deposits over crystalline basement (top right), and steep basement formations with unconformable cover sequence (bottom right). Sst = sandstone. Lst = limestone.

of groundwater (e.g., Lattiman and Parizek, 1964) or may sometimes be back-filled with overburden materials (e.g., Vogelsang, 1987). It is pertinent to mention that a solution cavern in massive carbonate rock may be filled with groundwater containing significant amounts of dissolved solids (e.g., products of intensive rock dissolution) and the cavern may be recharged via a myriad of fracture-zones in the hanging-wall which themselves constitute an indirect pathfinder for the cavern. The main elements of a groundwater resource system of exploration interest are the nature of the aquifer (its permeability, thickness and lateral extent), the nature and integrity of the aquitards or confining layers, the water table, water quality, fluid flow and the attendant structural controls on water distribution (e.g., presence of faults, folds, dikes or sills, depressions or buried channels in the bedrock which determine flow characteristics), the presence of perched or connected multi-level aquifers in geologically complex formations, the recharge sources, and the presence of salt or brackish water especially in coastal regions.

The geology of aquifers in fractured and weathered metamorphic or intrusive igneous rocks is quite different from the above. The attendant processes vary with climate, rock composition and structure, groundwater regime and topography (e.g., Palacky et al., 1981; Jones, 1985) but a fully developed weathering profile may consist of an upper zone of completely weathered rocks and an underlying transition zone (see upper diagram in Figure 4). The completely weathered mass may contain a water-saturated chloritisation zone (dubbed the saprolite zone) and an upper leached zone depending on the type of lithology. The transition zone may contain slightly weathered rocks in the upper part and broken rock fragments of identical mineral composition as the parent rocks in the lower part. The upper part of this zone may be up to 10 m thick and is characterised by maximum intergranular porosity and permeability (formed by a process of selective mineral decomposition and drainage); its position typically varies from 15 to over 70 m below the surface in the basement complex of Africa and in Northern Brazil (see e.g., Jones, 1985; Meju et al., 2001). In many parts of the world, there may be a useable aquifer in the transition zone and in the underlying steep fracture-zone which itself may be a few metres to tens of metres across. Note that the thickness, morphology, and composition of the weathered mass vary over different bedrock materials (Palacky, 1987). Deep weathering is common in tropical and subtropical shields or basement complexes, but it is not unusual to find preserved weathered layers in areas that are not presently favourable to the processes of deep weathering such as Scandinavia and Canadian shield (Palacky, 1987).

2.2. Resistivity characteristics of aquiferous targets

Although the electrical resistivity, permittivity and polarizability characteristics of the common aquiferous and confining materials vary from one geological terrain to another, there is some consistent pattern in the variation between, for example, freshwater bearing sand and gravel formations (which tend to be moderately resistive) and clayey confining rocks which tend to have lower resistivities (see Figure 5). There is a direct relationship between the bulk electrical conductivity σ_b of an aquifer (of total porosity ϕ and fractional pore saturation S) and the conductivity of its saturating fluid, σ_w (Archie, 1942), namely

$$\sigma_b = a\sigma_w \phi^m S^n + \sigma_s, \tag{3}$$

where a, m and n are specific constants for a given rock formation and σ_s is the solid conductivity. This proves the suitability of GEM methods to groundwater exploration. However, the above equation does not take the clay content of the aquifer into account; and the presence of clays is often the determining factor in the hydraulic and electrical conductivities of many groundwater aquifers. In sedimentary (or soft-rock) terrains, an unconfined freshwater aquifer typically consists of an upper resistive unsaturated zone and an underlying less resistive saturated zone, with the zone of water table fluctuations being the most conductive (since it is the zone of initial accumulation of materials leached from above) and easily detectable. In confined aquifers, the decrease in resistivity at the water table is often subdued and difficult to detect using surface GEM measurements especially if the upper confining aquitard is clayey. However, there is usually a marked contrast in relative permittivity (exploited by the ground probing radar (GPR) method) and chargeability between water-bearing and barren aquiferous materials. It is remarked that clay aquitards are highly desirable marker horizons for the delineation of aquifers (Meju et al., 1999); the base of a freshwater aquifer may be mapped much more

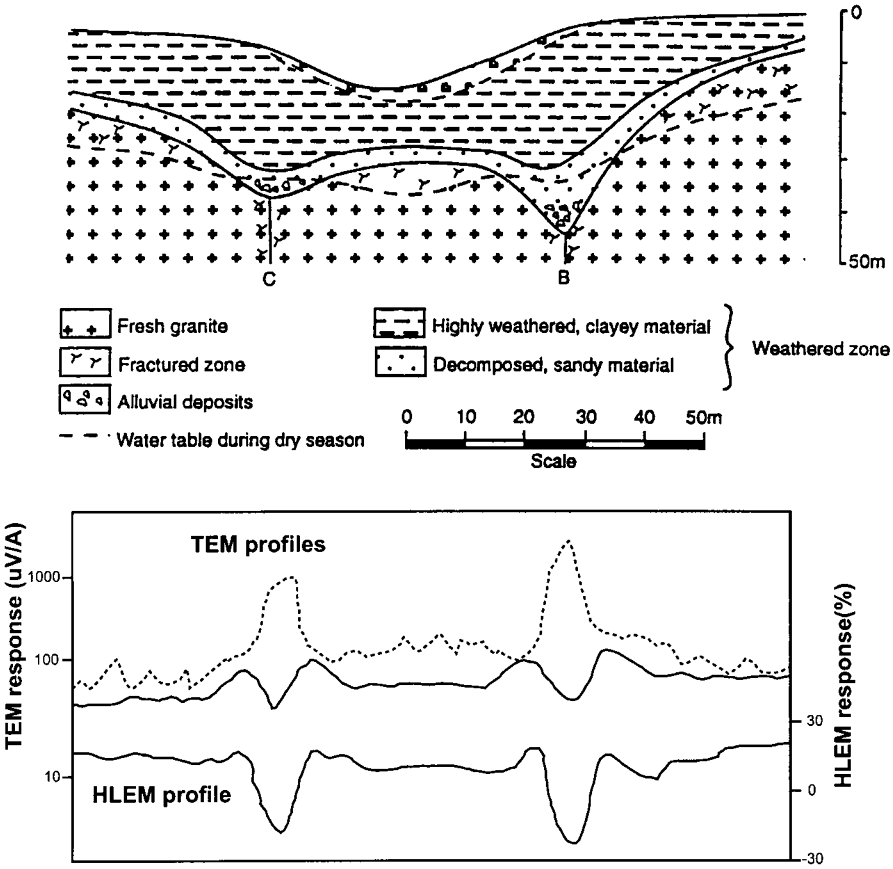

Figure 4. Idealised weathering profile and electromagnetic responses over a fractured granitic basement (Meju et al., 2001). The Upper diagram shows the distribution of aquifers in the basal part of weathered zones and deep bedrock fracture-zones. The lower diagram shows the expected TEM early-time single-peak anomalies over zones of thickened saprolitic overburden (upper dashed line) and later-time twin-peak anomalies over the steep fracture-zones (middle solid line); the classical HLEM signature of steep fracture-zones (bottom solid line) is also shown for comparison.

easily if a conductive clay substrate rather than a resistive crystalline basement is present.

In crystalline basement complexes, the areas of deep weathering and broken rock fragments above localised fracture-zones usually have higher transmissivities than the surrounding areas (Jones, 1985). The typical fracture-zone target may take the form of a tabular or elongate preferentially weathered surficial mass (consisting of a relatively resistive leached or mottled upper zone and an underlying highly conductive saprolite zone) with a moderately resistive transition zone of partial weathering above fresh bedrock of higher resistivity (see e.g., Palacky et al., 1981; Peric, 1981; Palacky, 1987). The saprolite zone is a very important marker horizon identified in many regions of the world as the most conductive layer in a weathered

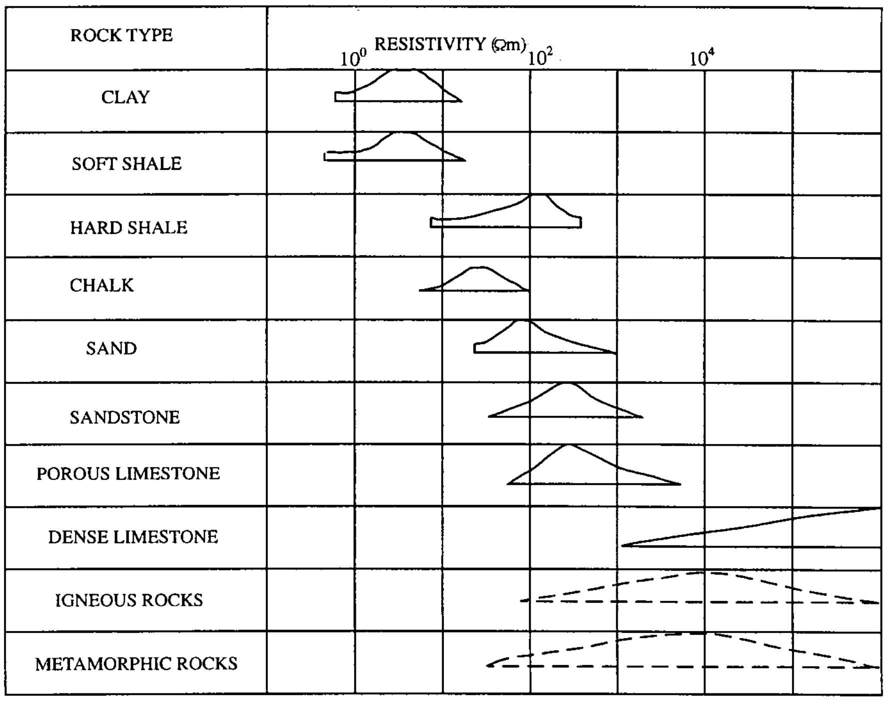

Figure 5. Schematic of resistivity ranges of common materials that form aquifers and confining layers.

section (e.g., Peric, 1981; Palacky, 1987), and will be best developed over the zone of intense fracturing in a given rock mass yielding a 'valley-shaped' conductive structure across the fracture-zone (Meju et al., 2001). It is of exploration interest that, owing to differences in rock susceptibility to weathering, the saprolite layer formed over mafic igneous rocks is always thicker and more conductive than that formed over felsic rocks (Palacky, 1987). The saprolite formed over gneiss does not appear to be very conductive while that formed over schists varies substantially (Palacky, 1987). This dependence of saprolite resistivity on the underlying lithology, and the relatively shallow depth (<100 m) and steep mode of occurrence of fracture-zone targets make GEM methods suitable for groundwater exploration in hard-rock terrains (see lower diagram in Figure 4). Note that a solution cavern in massive carbonate rock that is filled with groundwater containing significant amounts of dissolved solids could be likened to a relatively conductive body embedded in a moderately resistive host; the roof of the cavern may be permeated by small-size solution paths thus providing a relatively conductive marker zone for GEM prospecting.

2.3. Case studies and developments in groundwater exploration

Geophysical prospecting for groundwater entails searching for suitably confined materials with good storage capability (and potential for recharge). GEM methods are still the most popular geophysical tools for routine groundwater investigations due to their ease of use, low cost and the fact that these methods essentially measure physical property variations related to changes in pore fluid content and chemistry in the subsurface. GEM methods have been adapted to all aspects of groundwater resource evaluation and development (e.g., Raiche et al., 1985; McNeill, 1987; Vogelsang, 1987; Edet, 1990; Hawkins and Chadha, 1990; Ross et al., 1990; Olayinka and Barker, 1990; Beres and Haeni, 1991; Goldman et al., 1991; Meekes and van Will, 1991; Ritzi and Andolsek, 1992; Sandberg, 1993; Sorensen et al., 1995; Frohlich et al., 1996; Fontes et al., 1997; Yang et al., 1999; Shtivelman and Goldman, 2000). The main areas of current application of GEM methods in soft-rock terrains are summarised in Table I. Some novel practical approaches have been developed and improvements made on the existing acquisition techniques. Sorensen et al. (1995) and Sorensen (1996) show interesting applications of rapid continuous profiling systems to groundwater studies in Denmark. The recent availability of efficient software for 2D and 3D interpretation of GEM data is an important development in hydrogeophysics. 2D resistivity and IP imaging of subsurface aquifers using densely sampled measurements is now routine practice in small-scale studies (e.g., Lane et al., 1995; Atekwana et al., 2000 and references therein) but discrete soundings are still popular in regional groundwater investigations especially in the developing countries (e.g., Carrasquilla et al., 1997; Meju et al., 1999).

Vertical-component TEM sounding is used widely for groundwater investigations in soft-rock terrains (e.g., Stewart and Gay, 1986; Goldman et al., 1991, 1994; Christensen and Sorensen, 1994; Yang et al., 1999; Meju et al., 1999, 2000). An emerging practice in TEM ground surveys is to acquire multi-geometry or three-component data at each sounding position but model resolution is still hampered by the lack of efficient full-domain 2D/3D software tools for routine data interpretation; Zhdanov et al. (1995) present a simple approximate 2D imaging scheme for vertical-component TEM data. There are numerous symposia presentations of the result of EMAP-type 2D imaging of aquifers using the Stratagem model EH-4 equipment (e.g., Nichols et al., 1994; Unsworth et al., 1997). This is an exciting development since it extends the depth range covered by the traditional MT method for which there are freely available multi-dimensional interpretation codes (e.g., Smith and Booker, 1991; Mackie and Madden, 1993; Mackie, 1996). Meju et al. (1999) combine discrete MT, EMAP, TEM and dc resistivity soundings for regional groundwater studies in northeast Brazil, and found it necessary in their field studies to define conductive marker horizons (shaly formations) for better regional correlations.

In glacial terrains, the commonest exploration problem is the delineation of sand and gravel lenses in till. Due to the heterogeneous nature of till, EM methods

TABLE I

Current uses of GEM methods in soft-rock hydrogeological investigations. PACEP stands for pulled array continuous electric profiling (Sorensen, 1996). AEM = airborne EM.

GEM method	Exploration targets
Electrical	
SP	Fluid flow, compositional and thermal gradients
IP	Structure, stratigraphy, water table, water quality, clay-saltwater distinction
Dc resistivity/PACEP	Structure, stratigraphy, water table, water quality, aquifer porosity-permeability variation, aquifer vulnerability, saltwater intrusion
Electromagnetic	
AEM, HLEM, GPR	Lineaments, faults, shallow aquifers, aquifer vulnerability, karst features, shallow saltwater intrusions
TEM/CSMT	Structure, stratigraphy, karst features, water quality, porosity-permeability distribution, aquifer vulnerability, freshwater- saltwater interface
MT/EMAP	Deep regional aquifers, basement architecture, faults, lineaments
Downhole methods	Rock type and boundaries, water table and quality, freshwater-saltwater interface, porosity distribution

are sometimes preferred to dc resistivity techniques but combining both types of measurements may be a better approach to target verification in such environments. For shallow-depth glacial targets, the portable, multi-geometry (vertical and horizontal dipole) FEM systems (e.g., Geonics EM31) are used for rapid profiling (e.g., Mathers and Zalasiewicz, 1994). Broadband FEM and TEM systems (e.g., Geonics EM34-3 and PROTEM47; APEX MaxMin; Zonge GDP32-NT20, Sirotem MK3, ARTEMIS or Bison TDEM-2000, Stratagem EH-4) are used for deep targets. Sample result of joint VES and PROTEM47 soundings over an aquifer with thick glacial cover can be found in Meju et al. (2000, Figure 12). The combined use of GEM and seismic methods in hydrogeological studies (Meekes and van Will, 1991; Sandberg, 1993; Shtivelman and Goldman, 2000) is an important approach to optimised prospecting. Note that downhole GEM logging can also serve for better hydrogeological characterisation and correlations especially in granular environments with pre-existing wells (e.g., Mwenifumbo, 1993).

In the case of crystalline basement terrains, case histories employing the HLEM and dc resistivity systems dominate the literature on groundwater exploration especially in regions with hot climate and low rainfall (e.g., Palacky et al., 1981; Lindqvist, 1987; McNeill, 1987; van Lisa et al., 1987; Beeson and Jones, 1988; Hazell et al., 1988; Edet, 1990; Lane et al., 1995). Multichannel and three- component TEM techniques have recently been used for well-siting in basement terrains and appear to offer some advantages over the conventional electrical and HLEM methods. Meju et al. (2001) show that it is possible to accurately locate deep fracture-zones using modern highly portable TEM field equipment (Geonics PROTEM47 and Sirotem Mk3) with small (5–20 m-sided) transmitter loops. The single-loop TEM voltage profiles recorded across a prolific (21000 l/h) fracture-zone in granite covered by about 60 m of lateritic weathered materials are shown in Figure 6. Note the anomalous TEM responses over the position of the fracture-zone.

2.4. Some challenges for hydrogeophysics

The issue of world water shortages is currently of great concern to the international community, as population growth exerts further pressure on already limited reserves. More than 1000 million people do not have access to a safe water supply; and it is estimated that in the next 20 years, water use by humans will increase by about 40 percent, and that 17 percent more water will be needed to produce enough food for the growing population while a further 20–70 percent steep rise in industrial demand is to be expected (Second World Water Forum, The Hague, 17–22 March, 2000). More than half of the world's rivers are polluted or running dry; in many parts of Mexico, India, Yemen and China, the water tables are falling by as much as a metre a year (Second World Water Forum, The Hague, 17–22 March, 2000). There will thus continue to be increasing demands for groundwater especially in the developing countries and it is logical to expect that there will be a

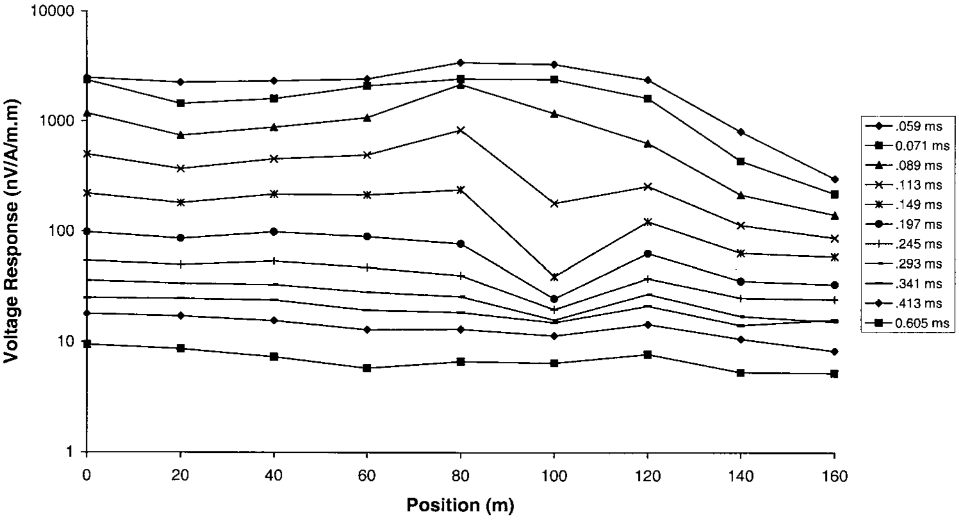

Figure 6. Single-loop TEM voltage profiles across a prolific (21,000 l/h) fracture zone in granite covered by ca. 60 m of weathered overburden in northeast Brazil (Meju et al., 2001). The fracture-zone is located at profile position 100 m.

corresponding need to locate deep (~1 km) groundwater aquifers of regional extent especially in semi-arid terrains (e.g., Meju et al., 1999). Airborne EM surveys (e.g., Sengpiel and Siemon, 1998) will play more pivotal roles in groundwater resource exploration in unexplored or inaccessible terrains in future but faces the problem of distinguishing between mineralised and unmineralised water-bearing fracture-zones in basement areas. Combining airborne EM profiling with thermal imaging of faults might be the best approach since it is well-known that wet faults cool down much faster than dry faults at night yielding dark strips in typical thermal image profiles flown at night-time.

Salt-water intrusion is a major threat to water quality in coastal fresh water aquifers and GEM techniques have been used to map the configuration of the freshwater-saltwater interface (e.g., Stewart, 1982; Goldman et al., 1991, 1994; Yang et al., 1999). The main problem is that the location of this interface is not always easy to define using only surface GEM sounding. A practical solution to this problem of target discrimination is to incorporate structural constraints provided by GPR or shallow seismic reflection data in the analysis of GEM data (e.g., Shtivelman and Goldman, 2000). An alternative solution is to develop an efficient automated method for 2D/3D joint inversion of GEM and seismic data. Such a development may lead to improved predictions of the petrophysical properties of aquifers. Realistic prediction of groundwater chemistry from surface GEM soundings is a topical issue that has cost-saving implications. Some relationships between fluid conductivity, total dissolved solids and chloride concentrations have been proposed by several workers (e.g., Ebraheem et al., 1990; Meju, 2000b), but the various empirical formulae require some site-specific constants. It is highly desirable to develop theoretical relationships that will be valid for all groundwater environments.

The integration of 3D sedimentological and GEM data in hydrofacies modelling of granular aquifers will become important since the effective evaluation of groundwater flow problems requires knowledge of the spatial distribution of hydraulic conductivity or permeability (among other hydrogeological parameters). The conventional point sampling methods in hydrogeology yields scanty data sets with attendant uncertainties in spatial interpretations. Since electrical conductivity is related to ionic transport in fluids while the sought parameter, hydraulic conductivity, is related to fluid transport, the information furnished by GEM soundings can serve for updating the permeability field for granular aquifers. High resolution 3D GEM mapping can furnish continuous images of the subsurface and may be integrated with grid-type sedimentological point samples in a stochastic joint inversion process to effectively constrain the subsurface permeability distribution. Actual estimates of the hydraulic conductivity, K, from direct measurement on cores can be augmented with those obtained indirectly from GEM conductivity models via the Kozeny–Carman equation (Domenico and Schwartz, 1990)

$$K = (d^2/180)[\phi^3/(1-\phi^2)], \tag{4}$$

where ϕ is the aquifer porosity and may be approximated using Archie's law (Equation (3)), and d is the effective grain size (in cm) of the granular aquifer determined from borehole or outcrop samples. Note that an additional term $(\delta_w g/\mu)$ appears in the right-hand side of Equation (5) in the variant called the Kozeny–Carman–Bear relation (Domenico and Schwartz, 1990) used by Aristodemou and Thomas-Betts (2000) to estimate K from resistivity models; this requires the fluid density, δ_w and dynamic viscosity, μ. g is the acceleration due to gravity.

3. Geothermal Resources

3.1. Geologic setting of geothermal systems

Geothermal energy is the natural heat stored in rock and water within the Earth. Under favourable geological conditions, geothermal energy can be tapped in wells (usually less than 3 km deep) located in sedimentary basins or along fault zones where deep circulation of groundwater of meteoric, connate or magmatic origin occurs. Geothermal systems are more commonly associated with areas of young tectonism and volcanism (mainly along active plate margins and intraplate hot spots) than stable cratonic regions. An idealised geothermal system (Figure 7) would consist of: (a) a heat source, (b) groundwater for transporting the heat, and (c) a suitably capped reservoir of adequate volume and sufficient permeability to facilitate convective transport or store the heat. The system would have associated

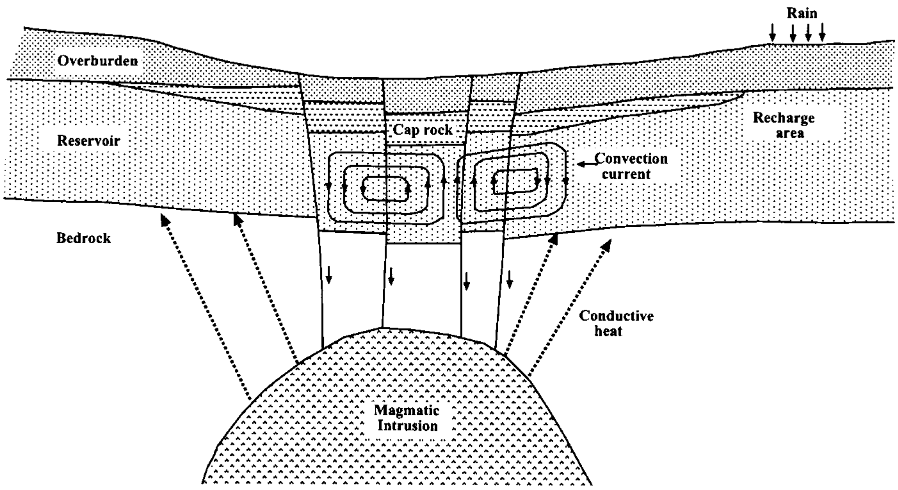

Figure 7. A model of an idealised geothermal system.

regional tectonic controls. Two convenient primary types of geothermal resources are recognized, depending on whether or not they are related to the emplacement of magma in the upper crust: (1) non-volcanic sediment-hosted resources, and (2) magmatic or volcanic-associated resources.

Nonvolcanic occurrences of geothermal resources typically result from redistributed heat in regional aquifers and include (Muffler, 1975): (a) geothermal reservoirs in low-porosity thermally conductive environments, (b) reservoirs in low-porosity conductive environments modified by deep circulation of meteoric water along faults and fractures, (c) reservoirs in high porosity, convective environments at hydrostatic pressure, and (d) geopressured resources or reservoirs in high permeability convective environments at pressures greater than hydrostatic (and approaching lithostatic) pressure. The resources related to volcanism or igneous intrusions include hydrothermal convective systems, magmas or partial melts, and hot dry rocks (Muffler, 1975). In terms of geographic distribution, magma generation is common along spreading zones, inter-arc basins, subduction zones and hot spots (intraplate melting anomalies). Such environments have good potential for geothermal resource formation. In subduction-related environments (e.g., west coast of South America and the Himalayan geothermal belt), the pods of magma produced by the melting of a subducted plate are injected into the upper plate forming potential heat sources for geothermal systems. Active geothermal systems also occur in major rift zones (e.g., East African Rift and Rio Grande Rift). Rift zones consist of fractured and brecciated rocks that create good reservoir conditions for convective cells (Warner, 1975). The commonly associated volcanism can furnish the heat source for convective and conductive transport to shallow reservoirs. Radiating subsidiary faults may augment the reservoir capability of the main rift by directing percolating meteoric waters towards the rift and heat source, and the continued movement along them ensures continued fracturing and rotation of reservoir rocks with the attendant enhancement of permeability (Warner, 1975).

Note that there may be no requirement for a cap to the reservoirs of some high temperature volcanic-associated geothermal resources. The geothermal reservoirs are active features with heat and fluid entering and leaving each system so that in their natural state, the reservoirs are in quasi-static equilibrium with their surroundings. While it is true that the argillic alteration that is almost always found near the surface of a high temperature geothermal reservoir will tend to reduce the permeability near the surface, almost all high-temperature liquid-dominated geothermal systems are 'once through' convective systems (T.G. Caldwell, pers. comm., 2001). The fluid, which is dominantly meteoric, is not re-circulated as suggested by Figure 7. After being heated at depth, the fluid rises convectively to near the surface where it is entrained into the overall pattern of groundwater flow or discharged joining the surface drainage. For example, Bibby et al. (1995) note that all but one of the twenty liquid dominated geothermal systems in New Zealand's Taupo Volcanic Zone are 'once through'. Also, in areas of high relief such as characterise the volcanic geothermal systems of the Philippines and Indonesia, large subsurface outflows of geothermal fluid occur, with hot springs occurring at distances of up to 10 km from the source or up-flow region.

The consequences of fluid and heat transport include: (1) the leaching of primary minerals and formation of secondary mineral assemblages that are stable in the resulting hydrothermal environment, (2) modification of the physical properties (notably permeability) of reservoir rocks especially by argillic alteration (due to the presence of high temperatures and acidic fluids), silicification (due to precipitation of silica as heat is removed from the ascending hot fluids) and densification (due to low grade hydrothermal metamorphism), and (3) the formation of surface discharge features such as fumaroles, hot springs and steaming grounds. In the case of high temperature volcanic-associated geothermal systems, the near-surface hydrothermal (clay) alteration (of what are normally fairly recent volcanic rocks), the slightly acidic and saline geothermal water and the high temperature all cause the subsurface resistivity to drop. The geothermal system may be mineralised (e.g., Goff and Gardner, 1994). It is these processes acting in concert that make the near-surface extent of a high temperature geothermal system easy to map electrically.

3.2. Resistivity characteristics of geothermal targets

It is well known that large volumes of rocks at elevated temperatures underlie all the major geothermal areas. The temperature characteristics of some resource types are summarised in Table II. The most important physical characteristic of a geothermal system is its base temperature (i.e., the highest temperature of the thermally uniform part of the reservoir). A large body of experimental evidence has

TABLE II

Thermal characteristics of geothermal resources (modified after White and Williams, 1975; Wright et al., 1985).

Resource type	Temperature characteristics
Magmatic associated resources	
Convective hydrothermal systems	
Hot-water dominated	About 30° to over 350 °C
Vapour-dominated (dry-steam)	About 240 °C
Hot rock systems	
Hot dry rock	90° to 650 °C
Partial melt	Over 600 °C
Radiogenic related hydrothermal	About 30° to over 150 °C
Nonvolcanic sediment-hosted resources	
Hot fluids in large-scale reservoirs	About 30° to 200 °C
Hot fluids in geopressured reservoirs	About 90° to 200 °C

shown that at high temperatures, the relationship between electrical conductivity and temperature takes the form

$$\sigma = \sigma_i \exp(-E_i/\kappa T), \tag{5}$$

where σ is the conductivity of a rock or mineral at temperature T (K), κ is the Boltzmann's constant, E_i is the activation energy and σ_i is a constant (related to mobility) that depends on the conduction mechanism (impurity, intrinsic or ionic). At high temperatures, semiconduction through mineral grains is assumed. At temperatures below 700 °C, typical activation energies are about 1 eV and hence solid conduction is unimportant. However, T may be specified in terms of the geothermal gradient s and depth z in the form (Petrick et al., 1977)

$$T(K) = sz + 300. \tag{6}$$

Typical resistivities of geothermal reservoir fluids range from 0.01 to 10 Ωm (Moskowitz and Norton, 1977). The direct relationship between electrical conductivity and temperature of a rock or between the electrical conductivity of a rock and its saturating fluids (Archie, 1942) proves the suitability of GEM methods to geothermal exploration.

In many cases and for reasons outlined in the previous section, the position of the geothermal manifestation is characterised by low resistivities (see Berktold, 1983; Wright et al., 1985; Strack et al., 1990; Martinez-Garcia, 1992 and references therein). Hydrothermal alterations usually lead to the formation of conductive

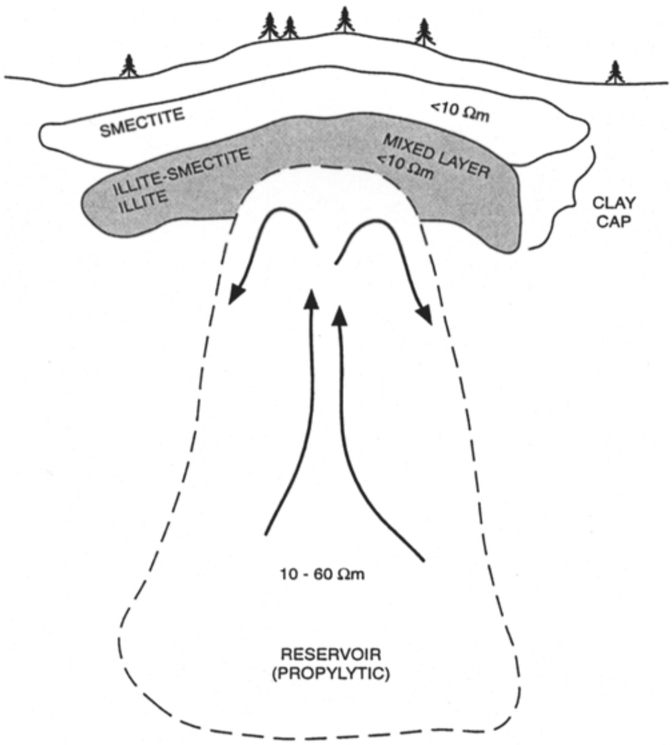

Figure 8. Conceptual resistivity model of a convective hydrothermal system with well developed alteration zones (after Pellerin et al., 1996).

clays (illite, smectite, montmorilonite) or densification (with attendant increase in resistivity) of host sediments and may thus impart a discernible zonation in mineralogy and resistivity across a potential reservoir as schematised in Figure 8. The composite structure may consist of a steep roughly cylindrical to oval core zone of sericitic or propylitic alteration (depending on the host materials), and an envelope of argillic (clay) alteration of low resistivity. Note that the reservoir has a relatively higher resistivity than the clay cap (a marker horizon) in the idealised system depicted in Figure 8 but this may not always be the case. For some fracture-zone aquifers, the relevant model may consist of a local flow system that is recharged and discharged vertically along faults or fracture-zones of high permeability and heated at depth during residence in more permeable rock formations (cf. Donaldson, 1962, 1970; White, 1973). The local flow system would consist of a resistive vapour-dominated upper section (cf. Olhoeft, 1981) and a less resistive liquid-dominated part at depth. The boiling interface between these two zones would be an important geoelectrical marker if the structure of the host rock is fairly simple.

3.3. Case studies and developments in geothermal exploration

Some of the numerous GEM studies carried out in the last 2 decades or so are summarised in Table III. This short list is only meant to highlight the widespread use of GEM methods in geothermal studies and the reader is referred to Berktold (1983), Wright et al. (1985) and Martinez-Garcia (1992) for more detailed reviews of GEM applications in geothermal exploration. It is important to understand and to articulate the role of electrical methods in geothermal exploration, which is primarily the accurate location of the reservoir. The presence of hydrothermal activity and hydrothermal clay alteration at the near-surface (a potential marker horizon) along with the associated geochemical and geological analysis usually indicates the general area of the reservoir. The practical challenge for the electrical geophysicist is to refine this location and indicate the precise area for drilling. In this regard, many of the MT surveys conducted for geothermal exploration in the early days (especially pre-1985) were poorly conceived and of little practical benefit to the geothermal industry. In New Zealand, the Philippines and Indonesia the early ('discovery or reconnaissance phase') geothermal exploration was done with conventional long-wire Schlumberger resistivity mapping (see references in Bibby et al., 1995). These surveys were highly successful, technically easy and cheap. It is only in recent years (post-1985), as the requirement for more detailed information about the internal structure of the geothermal reservoir has become more important, that MT surveys and other 'deep penetration' techniques have become useful. It is the post-1985 developments in lightweight instrumentation, signal processing and attendant dramatic increase in MT data quality that have made and will continue to make MT/EMAP and perhaps LOTEM surveys useful for detailed geothermal resource exploration. It is comforting that 3D predictive modelling of simple geothermal targets (e.g., Newman et al., 1985; Pellerin et al., 1996) now serve for improved survey design and especially for selection of GEM methods with optimum potential for reservoir mapping in geothermal prospecting.

It would appear from some of the recent GEM field studies (Table III) that magmatic systems and overlying hydrothermal alteration zones are the most prospective. A feature of the models presented for surveys over geothermal fields in volcanic regions (Table III) is the presence of very low resistivities at great depth (heat source?). For example, the 2D resistivity models (derived using different initial models) for an MT profile across the Rehai geothermal field near Tengchong in southern China (Bai et al., 2001) are shown in Figure 9. The Rehai field lies in an area of Quaternary volcanism in the Himalayan geothermal belt near the Indo-Eurasian collision zone. The models show strong lateral changes in resistivity in the subsurface. Note the anomalous, ca. 2 km wide, carrot-shaped, steep zone of low-resistivity ($<10\ \Omega$m) confined to the 6–17 km depth range underneath stations T08 and T07. The projected surface position of this low-resistivity feature lies within the known confines of the Rehai geothermal field (i.e., positions T09 to T03). This feature was interpreted as the magmatic heat source (Bai et al., 2001)

TABLE III
GEM methods currently applied to various geothermal exploration targets.

GEM method	Exploration targets
Electrical	
SP	Heat and fluid flows.
IP	Hydrothermal alterations, mineralisations.
dc resistivity	Saline fluids, faults, hydrothermal alterations.
Electromagnetic	
AEM, shallow FEM/TEM	Hot brines, faults, lineaments, alterations, mineralisations, outflow zones, clay cap.
MT/CSMT/LOTEM	Structural controls, conductivity distribution, clay cap, hot brines, intrusive bodies, magma chamber, partial melt.
Borehole methods	Rock type and boundaries, porosity and permeability, heat flow, hot brines, faults and fractures, alterations.

and was emphasised much more than the anomalous conductors in the top 2 km (near stations T10 and T08) that could be pointers to, or candidates for, the elusive geothermal reservoirs. It is remarked that while many such model interpretations are of academic interest, they provide little practical comfort to the explorationist working in the geothermal industry. The various elements of a geothermal system that are currently sought using GEM methods are given in Table IV; the practical targets in geothermal exploration should relate to the groundwater or transport medium and associated alterations, and the permeable geothermal reservoirs.

3.4. Main challenges in geothermal prospecting

Geothermal systems are inherently 3D and require large numbers of depth soundings at high station densities to image adequately. Developing methods of increasing the productivity of data acquisition in the field, the development of better 3D software tools and lowering costs are the major problems facing the use of EM methods in geothermal resource exploration. The multi-channel MT/EMAP systems currently being deployed may mark a significant watershed in the EM exploration of geothermal resources. Multi-polarization active-source rather than natural source techniques may offer a way of increasing data productivity but will require the development of 3D forward and inverse computation codes for non-plane wave sources. The more exotic challenges in geothermal applications of GEM methods would include: accurate mapping of alteration zones especially in neovolcanic systems (cf. Bibby et al., 1995), prediction of base temperatures, and the provision of other auxiliary data to aid optimal design of well spacings and pumping rates.

4. Petroleum Resources

The seismic reflection method is the most powerful tool for structural and stratigraphic prospecting for hydrocarbons. However, the use of seismic methods may sometimes be hampered by the presence of thick surface volcanics or high velocity carbonate rocks. Pre-Cambrian overthrust terrains, areas of rugged or steep topography and difficult statics, and permafrost are typical ‘seismic poor-record’ areas. The need for more useful information in seismic poor-record areas have led to the adaptation of deep probing EM methods to some exploration problems. For a different reason, there was also a resurgence of interest in GEM exploration for oil and gas in the early 1980s after significant geoelectrical anomalies were found over known oil fields (e.g., Snyder et al., 1981a, b). These anomalies appeared to confirm the evolving hypothesis that measurable distinct near-surface geochemical conditions are prevalent in the sedimentary section above oil and gas fields possibly due to the formation of the metallic mineral pyrite. If such conditions obtain in a prospective region, then the relatively low-cost GEM methods can be deployed in the search for hydrocarbons.

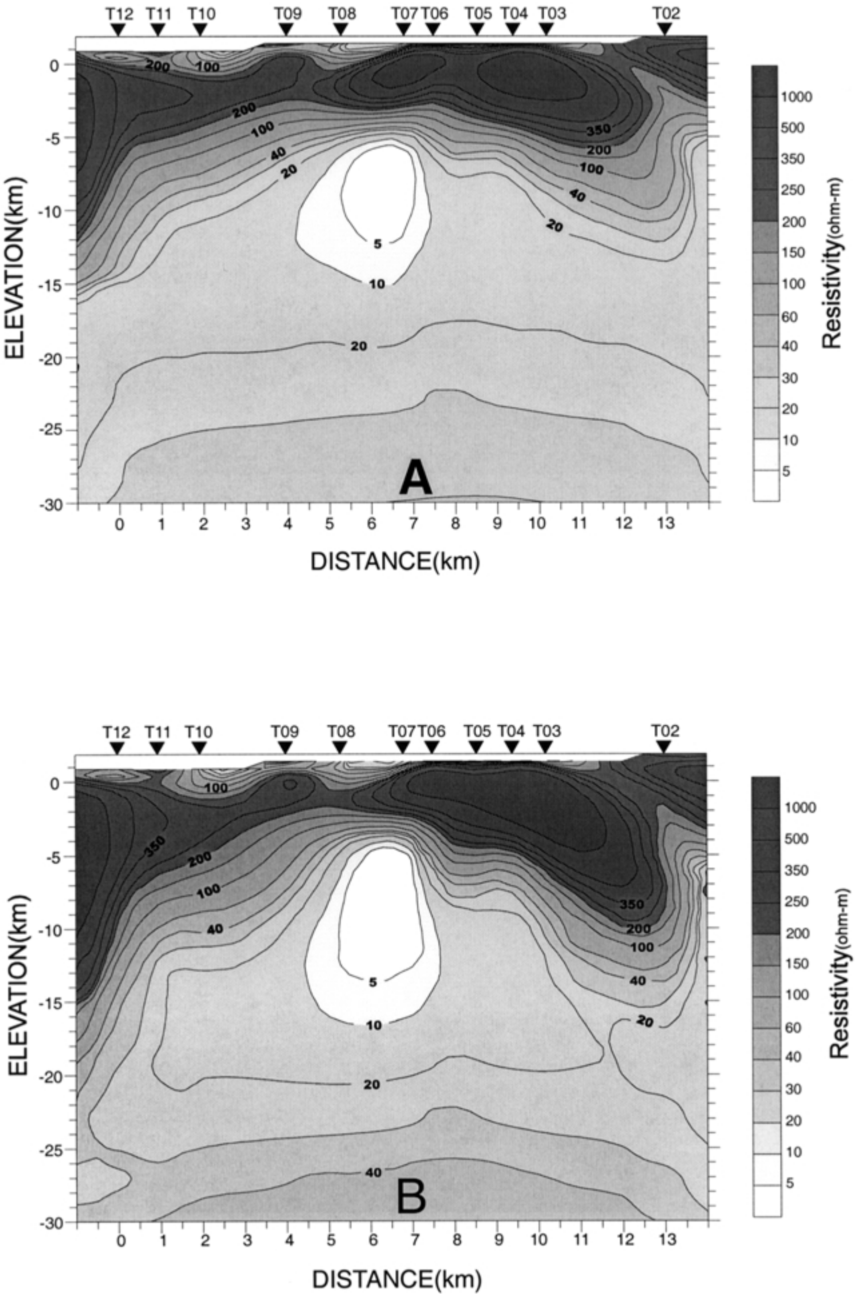

Figure 9. 2-D MT resistivity models for the Rehai geothermal field near Tengchong, China (Bai et al., 2001). The statistically equivalent 2D models were derived by inversion using an initial half-space model of: (a) 50 Ωm and (b) 100 Ωm. Note that both models are similar.

TABLE IV
Sample case histories of geothermal investigations in different geographical regions.

Country/locality	GEM method used	Investigators
NEW ZEALAND		
Broadlands-Ohaaki	MT	Ingham (1991)
Taupo Volcanic Zone	Tensor CSMT (4–4000 Hz)	Bromley (1993)
		Bibby et al. (1995)
USA		
Snake River Plain, Yellowstone	MT (0.004–250 s)	Stanley et al. (1982)
Nevada	FEM (0.001–1000 Hz)	Wilt et al. (1983)
Jamez Volcanic Zone, New Mexico	MT/AMT (10.2 KHz–2000 s)	Ander et al. (1984)
Newberry Volcano, Oregon	TEM	Fitterman and Neev (1985)
Cove Fort-Sulphurdale, Utah	Dipole-dipole resistivity	Ross and Moore (1985)
Valles Caldera, New Mexico	MT	Jiracek et al. (1993)
Valles Caldera, New Mexico	CSMT	Wannamaker (1997a, b)
ITALY		
Travale, Tuscany	MT	Hutton et al. (1985)
Travale, Tuscany	MT	Schwarz et al. (1985)
GERMANY		
Urach	MT/GDS	Berktold et al. (1982)
Urach and Black Forest	LOTEM	Strack et al. (1990)
ICELAND		
	MT (0.1–3600 s)	Hersir et al. (1984)
JAPAN		
Hatchobaru	Mise-a-la-masse	Tagomori et al. (1984)
Hatchobaru	MT/CSMT	Ushijima et al. (1986)
GREECE		
Genisea	Dc resistivity	Thanassoulas et al. (1986)
Milos Iland	MT	Haak et al. (1989)
Milos Island	MT	Galanopoulos et al. (1991)
CHINA		
Rehai-Tengchong	MT (0.004–4096 s)	Bai et al. (1994, 2001)

4.1. Tectonic setting of hydrocarbon accumulations

The major hydrocarbon accumulations are genetically related to the large-scale rifting and break-up of the continents during Mesozoic and Cenozoic times. For instance, the Mesozoic rifting in the South Atlantic resulted in the break-up of Pangea and the development of several basins with similar tectono-stratigraphic pattern of evolution. In many of these basins, the initial history can be attributed to an early phase of rift faulting, with contemporaneous basaltic magmatism in response to a thermal anomaly in the mantle (Furlong and Fountain, 1986), and subsequent thermal recovery of the lithosphere sometimes with some important deviations from the classic homogeneous simple stretching model (McKenzie, 1978). The intensity of the pattern of rift faulting and the behaviour of the different fault blocks determine the shape and internal structure of the basins. Oil and gas are sourced by organic materials deposited in such basinal environments. The basins may be marine, brackish, lacustrine or continental but significant accumulations of hydrocarbons require the presence of source rocks, reservoir rocks (e.g., sands, fractured limestones and chalk) and cap rocks or seal (e.g., shales, evaporites and volcanic rocks or structural barriers) in favourable juxtaposition to form traps (comparable to those shown in Figure 3 for groundwater). The useful organic debris in source rocks are mostly contributed by plants. A combination of biogenic, chemical and thermal processes act on the organic debris in the sediments converting them into hydrocarbons. (Petroleum forms when the temperatures reach ca. 35–150°C; the higher the temperature, the greater the proportion of gas produced. Above 180°C, the hydrocarbons are converted to methane and graphite). The hydrocarbons are expelled from the source rocks, and migrate to suitable accumulation sites in reservoir rocks entrained in water from which they ultimately become segregated aided by their buoyancy. The geological structures that serve for the entrapment of oil and gas in petroliferous basins include the so-called structural, stratigraphic and volcanic traps (cf. Figure 3) but regional or local structural trapping mechanism is dominant in the major oil producing basins. The amount of post-depositional deformation, uplift and erosion experienced by a prospective region dictate to a large extent whether or not commercial quantities of hydrocarbons are likely to be present in existing traps. The different basin types of current exploration interest include thrust belts, volcanic arc basins, intra-cratonic and foreland basins, passive margins and rift basins.

In general, hydrocarbon traps are not leakproof. Hydrocarbons leak from their loci of entrapment by slow episodic seepage or continuous effusion, modifying the physico-chemical properties of overlying sediments during their upward migration. Seeps may manifest onshore as concealed bitumen impregnations and electrochemical alteration haloes (cf. Sassen, 1980). In terms of seepage potential, the most leaky basins are thrust belts followed by volcanic arc basins and diapiric passive margins. The least leaky basins are the intra-cratonic and foreland basins with the rift basins and undeformed passive margins lying between the two extreme groups.

4.2. Generalised electrical models for oil and gas systems

The geological basis for employing GEM methods in structural or lithological prospecting for hydrocarbons is the fact that prospective basins tend to have successions of source or cap rocks (dominantly shaly formations) and reservoir rocks (typically sandy or carbonate formations) which have contrasting electrical properties (cf. Figure 5); shales and other fine clastics are usually highly conductive (generally $<30\ \Omega$m) while sandstones and carbonate rocks are highly resistive (usually $>30\ \Omega$m). In a hydrocarbon trap, oil and gas (which are electrically resistive, $>10^5\ \Omega$m) may rest on brines which are highly conductive (typically 0.01–1 Ωm), and their contact may provide a good target or marker horizon for the GEM methods especially in shallow-depth occurrences.

For seepage-related geochemical alterations, it is possible to construct a generalised model as illustrated in Figure 10. Essentially, light hydrocarbons (mainly methane) migrate upward along permeable pathways (fractures, faults, contact point) and through porous materials. As they rise upward they create a vertical reducing zone (referred to as a reduced plume or chimney). Near the surface, the plume undergoes a number of changes dependent on the local geology. A suite of minerals are deposited as a result of exsolution in oxidizing meteoric waters and/or geochemical interactions with the host rocks in the presence of anaerobic bacteria (e.g., Donovan, 1974; Donovan et al., 1981; Sassen, 1980; Oehler and Sternberg, 1984). In some cases the resultant mineralisation and soil gases create halo-shaped features around the periphery of the reducing plume. The alteration phenomena (and their electrical effects) that are of exploration interest include pyrite mineralisation (high polarisation), clay alteration (low resistivity, low polarisation), calcite cementation (high resistivity) and brine effects (low resistivity, high polarisation). The net effect of all possible alterations is the formation of physicochemically distinct zones (elliptic- to crescent-shaped in plan) that may take the form of conductive and/or resistive, relatively polarizable features of considerable vertical and lateral dimensions. Oil/gas-water contacts and leakage-related near-surface manifestations of hydrocarbon reservoirs (and the major structural controls on the seepage process) constitute important marker zones for the GEM methods.

4.3. Case histories of hydrocarbon exploration

4.3.1. *Oil-water contact and alteration mapping*

The TEM method has been used to map geochemical anomalies and oil-water contacts in various shallow reservoir settings (see e.g., Spies, 1983; Bertin et al., 1981; Wightman et al., 1983; Nekut and Spies, 1989). The use of surface GEM methods as direct indicators of hydrocarbon plumes in oil and gas exploration was prompted by the detection of subtle geoelectrical anomalies in several petroliferous areas. Although there has been several earlier suggestions of this association (e.g., publicity IP reports by Colfax Surveys Ltd in the mid-70s in *Oilweek*, 1976, 1978; IP results over Lambert Field in Northern Texas described by Snyder et al., 1981a,

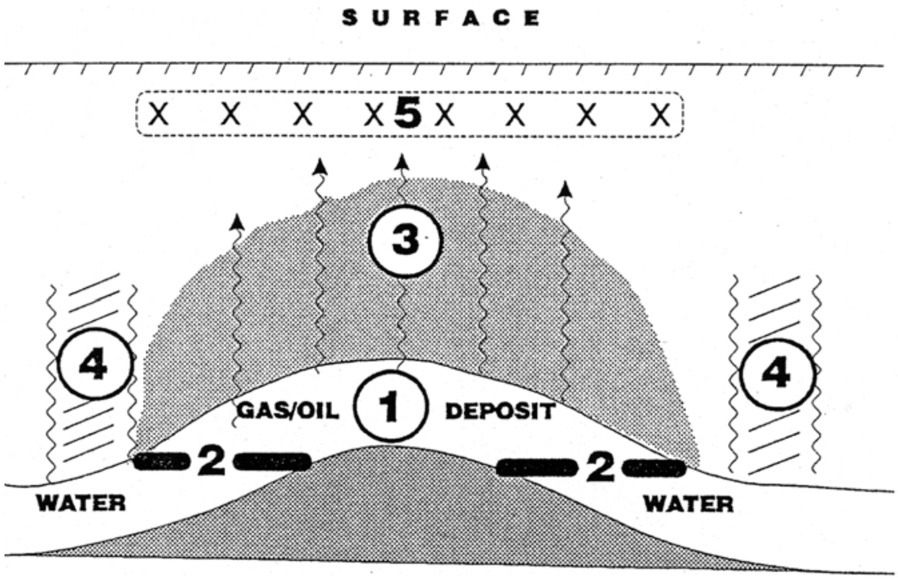

Figure 10. Idealised illustration of the migration-related alteration concept (after Hughes et al., 1985b; Karus et al., 1985). The key elements of the model are: the zone of hydrocarbon accumulation (1), the gas/oil-water contact zone (2), the hydrocarbon invasion halo or chimney (3), steep annular zone at the edge of the oil/gas accumulation (4), and characteristic near-surface zone above the oil/gas field (5).

1981b), the most definitive published work are those of Conoco Inc. (e.g., Oehler and Sternberg, 1982, 1984) for North American oil fields and of Haren (1984) and Haren and Reeves (1983) for Australian fields. Interesting work on the subject was also reported by major contracting companies such as Zonge Engineering and Research Organisation (e.g., Carlson et al., 1981; Zonge and Hughes, 1981; Ostrander et al., 1983; Hughes, 1983; Hughes et al., 1982, 1984a, b, 1985a, b) and Phoenix Geophysics Ltd (e.g., Klein, 1983; Sill, 1983). The deep probing EM and IP tools, especially those that furnish apparent resistivity and phase information, were favoured for alteration mapping in these investigations (see Table V). In Figure 11 is shown an example of time-domain IP survey over an oil field in Northwest China (Zhang et al., 1986). The oil-bearing zones lie between borehole positions 6202 and 193 in this figure. The survey employed the Schlumberger array with a source electrode separation of 1000 metres and transmitter current on-times of 2 sec and 8 sec. The effective depth of investigation for this current electrode separation would be about 220 m (Meju, 1995) and thus sampled above the oil-bearing zone. Notice that the apparent resistivity profile (labelled ρ_a in the top plot) suggests similar resistivity values (about 10 Ωm) in the near-surface zone over the known reservoir and much further down-dip outside the prospect. In contrast, however, the apparent chargeability (M_a) and apparent metal factor (J_a) profiles show anomalous high values that correlate with the location of the reservoir.

TABLE V

Some case histories of structural, lithologic and geochemical alteration mapping using GEM methods in frontier basins and seismic poor-record areas.

Target feature	Country/locality	GEM method used	Investigators
Basalt-covered sediments	Columbia Plateau, USA	MT/gravity/magnetics	Prieto et al. (1985)
	Parana Basin, Brazil	MT	Stanley et al. (1985)
	Parana Basin, Brazil	MT	Beamish and Travassos (1992b)
Overthrust carbonate sequences	Italy	MT	Orange (1989)
	Papua New Guinea	MT/gravity/magnetics	Billings and Thomas (1990)
	Papua New Guinea	MT	Christopherson (1991)
Alluvium-covered marine carbonates	Lower Yangtze, China	Seismics/MT/gravity/aeromagnetics	Deng and Ou (1995)
Salt plug/diapir	The Netherlands	CSMT/TEM	den Boer et al. (200)
Alteration haloes over gas and oil fileds	Surrat basin, Australia	IP	Haren (1983, 1984)
	Arkoma basin, Oklahoma	IP/downhole logging	Oehler and Sternberg (1984)
	Arkoma basin, Oklahoma	CSMT	Hughes et al. (1985b)
	Eromanga basin, Queensland	CSMT	Zonge Engineering (1985)
	Rocky Mt foothills, Alberta	IP	Duckworth (1987)
	Gunnedah basin, Australia	IP/TEM/seismics/magnetics	Webster and Woods (1988)
	Northwest China	IP	Zhang et al. (1986)
	China	IP	Nie Xinwu et al. (1989)
	Kisalfold basin, Hungary	CSMT	Beke et al. (1991)
Oil-water contact	USSR	TEM	Spies (1983)
	USA	TEM	Wightman et al. (1983)
Gas-water contact	Australia	TEM	Bertin et al. (1983)
Stratigraphic/structural traps	France/Germany	LOTEM	Strack et al. (1989, 1991)
	Northern Ireland	TEM/MT	Meju (1994)
Offshore traps	San Diego Trough, USA	MT	Constable et al. (1998)
	Gulf of Mexico, USA	MT	Hoversten et al. (1998)

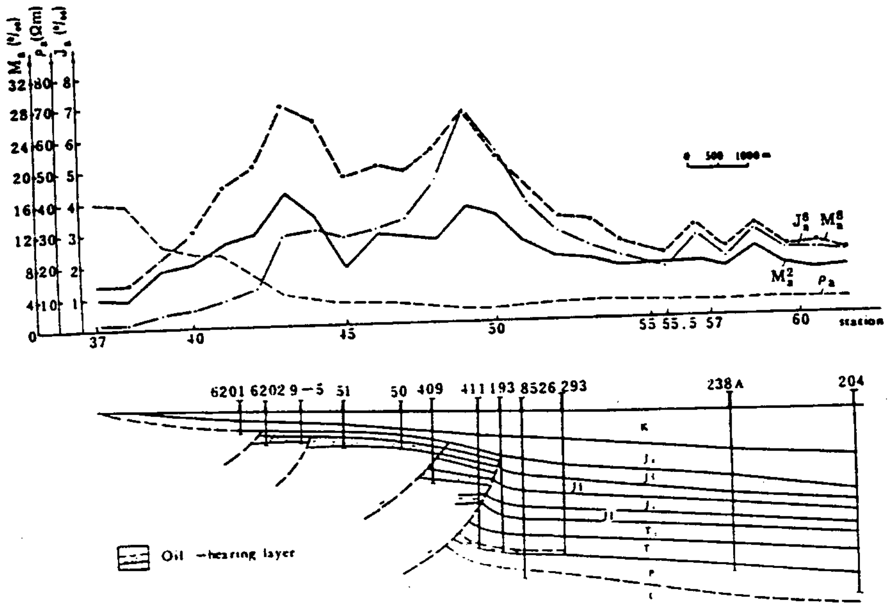

Figure 11. Results of IP survey over an oil field in China (Zhang et al., 1986). The site geological section derived from borehole data is shown in the bottom diagram. The IP chargeability (M_a), current density (J_a) and apparent resistivity (Ω_a) profiles are shown in the upper diagram. The oil-bearing zone is positioned between borehole 6202 and borehole 193.

Although careful attention may have been paid to survey design, the widespread presence of cultural features such as pipelines and well-casings in most of the oil and gas fields used for these alteration-based pilot studies places some limit on the real significance of the results. Such cultural features can produce significant GEM anomalies (e.g., Parra, 1984; Wait and Williams, 1985). Another limitation of these studies is the linear nature of the survey profiles over the 3D geochemical alteration haloes. It is encouraging that the result of 3-D grid-type CSMT survey by Beke et al. (1991) over a gas field in Kisalfold basin in Hungary appears to provide better geometrical constraints on the nature of these electro-geochemical anomalies and the feasibility of direct detection of hydrocarbons. Beke et al. (1991) found an elliptically shaped zone of increasing resistivity around a gas producing well only at a depth interval (2470–2570 m) that encompasses the productive zone (2519–2525 m). This zone, representing areas with resistivity changes greater than 15% but less than 25%, was found to be in agreement with the trace of the field limits and was interpreted as the altered zone at the periphery of the gas field by Beke et al (1991); a dry well within this zone was taken as lending credence to this interpretation. However, the simplistic 1D depth transformation of the sounding data is a major weakness of this study and we cannot rule out the possibility that the evinced resistive anomaly may be a fortuitous discovery; 3D data imaging would be more appropriate but was not available then. This study nonetheless demonstrates the wealth of information derivable from 3D controlled source EM surveys. Such a survey could be done over a seismically defined structure as a prospect development check or as a direct hydrocarbon indicator over aeromagnetically defined prospects in seismic poor-record areas.

4.3.2. *Structural and stratigraphic mapping*

The deep-probing EM techniques (MT, EMAP, CSMT, TEM) have been applied to structural and stratigraphic mapping for hydrocarbon exploration in many parts of the world (see Table V). Discrete soundings were commonly used in the 1980s for hydrocarbon exploration and are still popular in regional or reconnaissance exploration programmes (e.g., Stanley et al., 1992). MT and TEM prospecting for hydrocarbons take a high profile in Russia and the former Soviet Union but there are very little published accounts in western literature (e.g., Berdichevsky, 1994). In these regions, MT data have served for producing regional tectonic maps of sedimentary basins with petroliferous potential (Obukhov et al., 1983); conductance maps are prepared from high density MT soundings and correlated with existing oil and gas fields. The Urengoy Gas Field in Western Siberia, one of the largest gas fields in the world, was discovered when an associated basement arch detected by MT was drilled (see Berdichevsky, 1994). China is currently one of the greatest users of MT in hydrocarbon exploration and some unpublished symposia presentations suggest that MT has played a pivotal role in the discovery of some fields; however, it remains to see such reports in the public domain.

Some of the world's hydrocarbon provinces are concealed beneath thick layers of volcanic or volcano-sedimentary materials. Seismic exploration methods do not always work well in such environments because of the dispersive nature of the volcanics and the decrease in acoustic velocity at the base of the volcanic-cover. Such areas have been known for some time to be favourable for the application of the MT method (e.g., Stanley et al., 1985) which may then provide data to supplement the seismic information (e.g., Berkman et al., 1983). Warren and Srnka (1992) evaluate the EMAP method at basalt-covered sites in the Columbia River basin in the USA (Whiskey Mountain, Saddle Mountain and Page sites in Figure 12). EMAP surveys were conducted in the vicinity of three boreholes and successfully mapped intra-basalt conductors (Figure 13). EMAP results are commonly presented as resistivity cross-sections derived from 1D Bostick inversion of the spatially filtered continuous dipole profiling data; however, Warren and Srnka (1992) suggest the use of the derivative of the 1D resistivity model under each dipole as an aid to interpretation, yielding the cross-sections shown in Figure 13. Notice that the resistivity gradient interpretations for the Whiskey Mountain survey (upper diagram in Figure 13) and Page survey (lower diagram in Figure 13) closely resemble the known subsurface geology. The base of the volcanics was accurately located and the underlying conductive rocks mapped on two of the three test lines. The presence of faulting in the conductive horizons was also inferred from these sections. The use of 1D inversion limited model resolution in these EMAP surveys. There was a notable

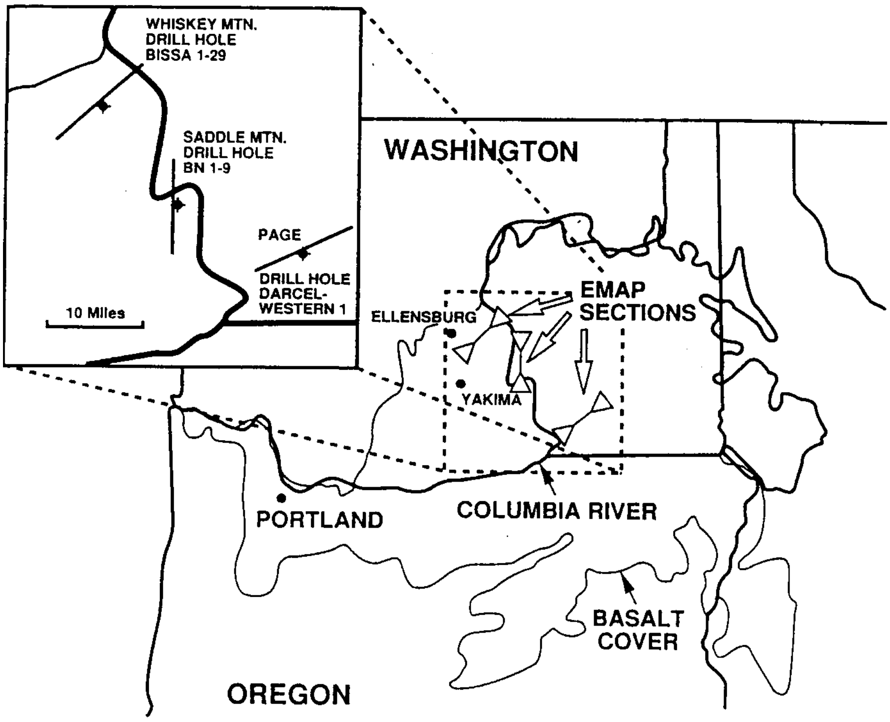

Figure 12. Location map for EMAP test surveys over basalt-covered sediments (after Warren and Srnka, 1992). The results for the Whiskey Mountain and Page transects are shown in Figure 13.

disagreement between the EMAP section and the induction well log below 1 km depth at the Page test site, ascribed to the possible presence of a heterogeneous conductor at depth. Shoham et al. (1992) examine EMAP and three controlled-source EM (TEM, LOTEM and FEM) surveys over the same area and suggest that the EMAP survey is the most cost-effective since it provided much more detailed information about the subsurface resistivity distribution than the other techniques that employed discrete soundings. However, Shoham et al. (1992) note that, for each of the tested EM methods, 2D or 3D inversion of the field data is required for realistic geological correlations.

Gravity and magnetic measurements have been used to provide useful constraints on the interpretation of discrete MT soundings in basalt-covered areas (e.g., Prieto et al., 1985). The major problem faced by discrete MT depth probes in such environments is static distortion necessitating the use of complementary TEM soundings (e.g., Sternberg et al., 1988; Pellerin and Hohmann, 1990; Meju, 1994, 1996a), borehole control (e.g., Beamish and Travassos, 1992a, b) or the EMAP technique if costs permit. Withers et al. (1994) present an integrated case study of hydrocarbon exploration in a basalt-covered terrain in north-central Oregon where gravity modelling identified a basin model but required the information furnished

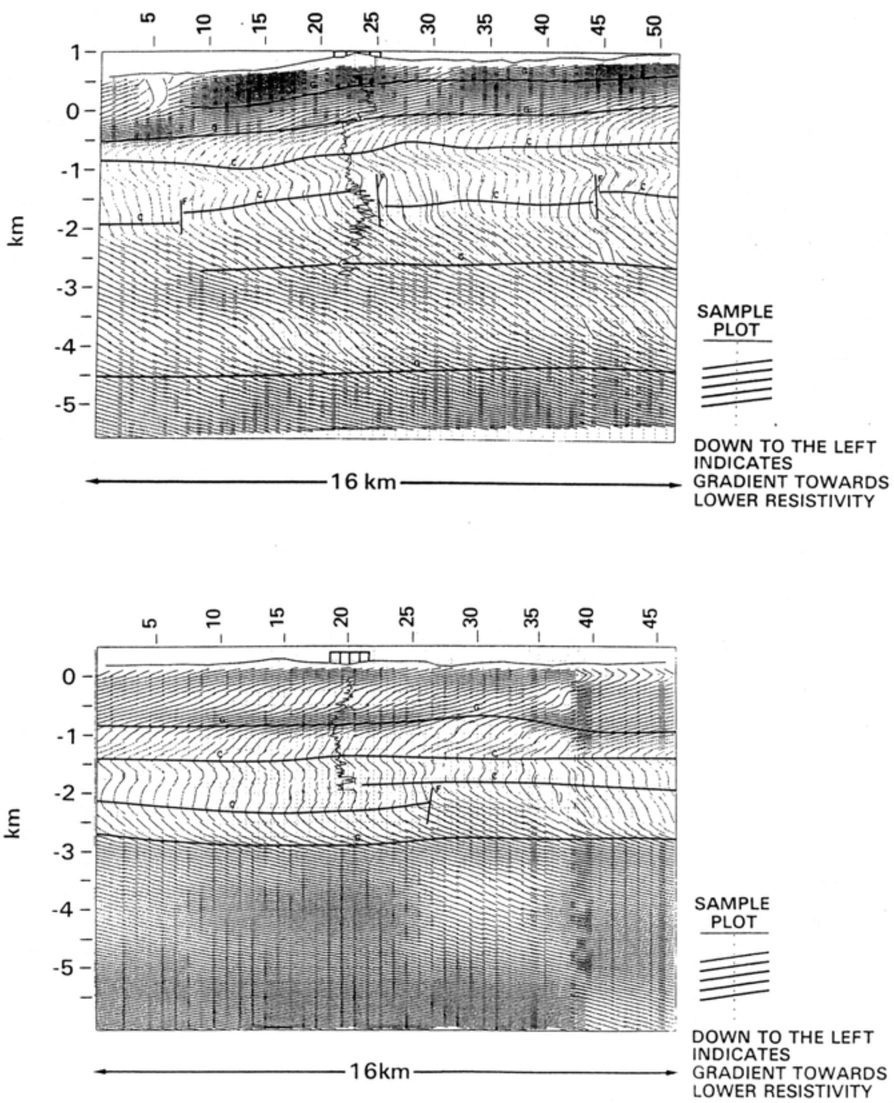

Figure 13. EMAP resistivity gradient section for the Whiskey Mountain and Page profiles. The available deep induction well logs, plotted on a logarithmic amplitude scale, are superimposed on the resistivity sections for comparison (Warren and Srnka, 1992).

by discrete MT soundings to constrain the thickness of the basalt cover. The MT data were corrected for static shift using TEM soundings. Although a well drilled over the sub-basalt prospect identified using the integrated approach was found to be dry, it confirmed the existence of the hitherto unexplored tectonic basin; seismic reflection surveys produced poor results for this particular prospect (Withers et al., 1994).

In prospective overthrust terrains, massive segments of originally deep-lying rocks are typically thrust over younger sedimentary rocks cutting out several potentially petroliferous rock formations. The thrust plate may contain resistive, high velocity rocks especially in carbonate terrains, while the underlying sediments may be characterised by lower velocity and resistivity. It is often difficult to obtain good quality seismic data in such terrains whereas MT has had some success in mapping the thrust plate, the underlying sediments and the resistive basement such as in the Appenines (see e.g., Orange, 1989), Papua New Guinea (Billings and Thomas, 1990; Christopherson, 1991), and Northwest Colorado (Word et al., 1992). In the case of the frontier area of Papua New Guinea (PNG), the prospective mountainous fold belt is characterised by the presence of thick karstic Miocene limestone at the surface causing problems for seismic reflection surveys. The Darai limestone overlies prospective sediments of the Ieru Formation. The Ieru Formation is of fairly constant thickness and contains the target reservoir known as the Toro sandstone. In some areas, double thrusting of the Darai limestone has resulted in complex duplexes. Sample result of high-resolution seismic reflection survey across an anticlinal structure in PNG (the Hides anticline) is shown in Figure 14. The base of the Darai limestone is indicated in this section, but notice that there are no coherent events yielding a characteristic sugary texture in the seismogram. The resistivity and sonic logs from a well drilled on the Hides anticline are shown in Figure 15. There are good velocity and resistivity contrasts at the base of the Darai limestone (such a velocity contrast would be expected to produce a reflection at about 0.8 s while the sole of the thrust may have enhanced conductivity and hence serve as a GEM marker horizon). Christopherson (1991) describe the use of MT to map the base of the resistive Darai limestone and image the conductive Ieru Formation (by virtue of its uniform thickness). There is no significant resistivity contrast between the Toro sandstone and the shaly members of the Ieru Formation precluding direct reservoir mapping using MT imaging. Billings and Thomas (1990) show the contribution of MT in integrated 2D interpretation involving potential field data in the PNG setting. Note that in these reported MT surveys, the interpretation of the field data was limited to 2D forward modelling incorporating the available a priori information. Hoversten (1992) shows that the base of the Darai could be mapped using 1D and 2D MT analyses for a survey across the Hides anticline. However, for the MT survey over an adjacent structural high (Angore anticline), for which drilling revealed the presence of double thrusting of Darai limestone, 2D inversions of data and good control on static shift were found necessary to map the base of the limestone duplex (Hoversten, 1992). Large volumes of continuous array profiling (EMAP) data have been acquired in various hydrocarbon exploration campaigns, and capability for large-scale 2D inversion of EMAP data is now available. It will be interesting to reprocess some of the past data sets (e.g., Shohan et al., 1992; Warren and Srnka, 1992) using robust 2D inversion schemes to see whether any significant improvements in geological correlation can be obtained.

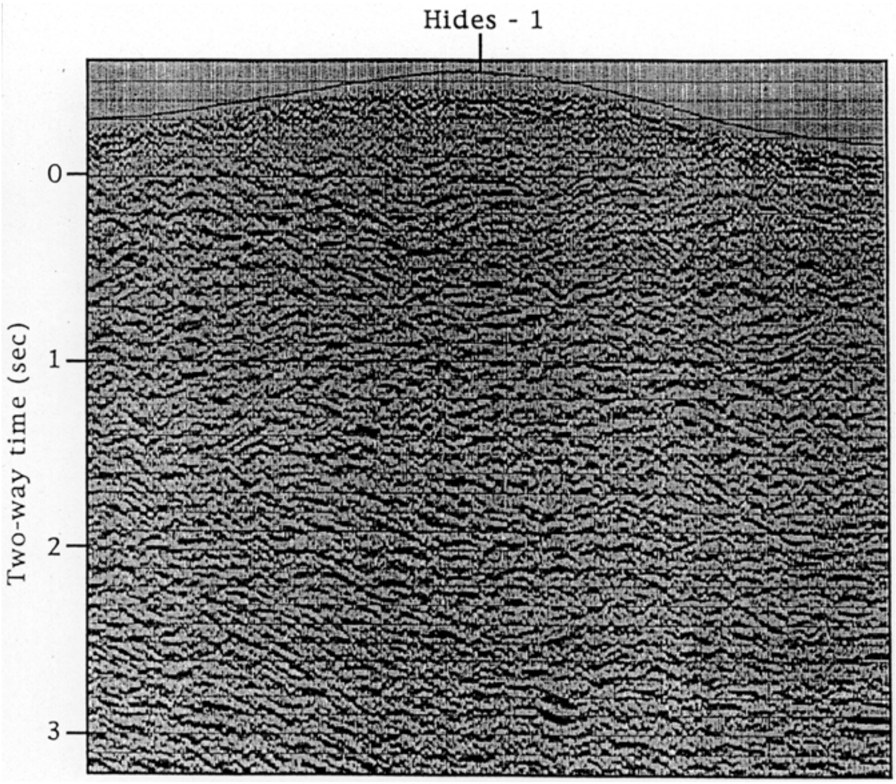

Figure 14. High resolution seismic reflection section for survey across the Hides anticline in Papua New Guinea (Hoversten, 1992). The position of the Hides-1 well is shown.

Stewart et al. (1996) describe an interesting use of discrete MT soundings to shed some light on a stratigraphic problem in central Saudi Arabia. In the study area, the prospective sedimentary section beneath a Permian carbonate (Khuff) formation is poorly defined by conventional seismic data. The pre-Khuff section (i.e., between the Precambrian basement and the base of the Khuff carbonate) has significant potential for hydrocarbon exploration and data from about 500 MT soundings on a 2-D grid were interpreted, with control provided by available well log data and seismic interpretation of the shallow section. The resulting interpretative resistivity models suggest the presence of significant pre-Khuff section over basement and indicated 'pinch-out' areas (where the pre-Khuff is inferred to be thin or absent) that warrant further detailed or specialised seismic exploration for stratigraphic traps.

A remarkable development is the use of the information provided by GEM models to aid seismic data processing and interpretation. Warren (1992) shows examples of surveys in three test areas in the Western USA demonstrating the use of EMAP as an exploration tool, and suggested that the information from EMAP

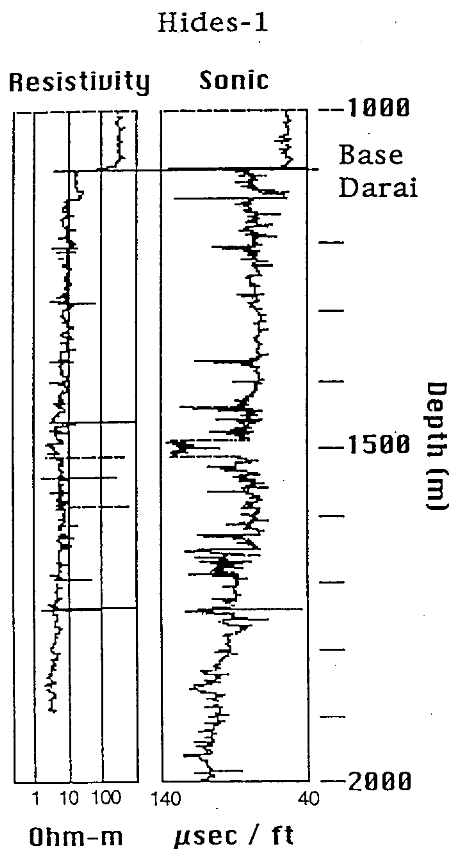

Figure 15. The Hides-1 resistivity and sonic logs (Hoversten, 1992). The base of the Darai limestone is at a depth of 1100 m and shows marked resistivity and velocity changes.

sections can be used to control the depth migration of seismic data whose stacking velocities may otherwise be erroneous. Basically, the Faust equation

$$\text{Velocity} = A \cdot (\text{Resistivity} \times \text{Depth})^B \tag{7}$$

was used to calculate seismic velocity from the resistivity-versus-depth information. The constants A and B in Equation (8) are determined, by calibration, for the EMAP dipole closest to a check-shot well and then applied to all the dipoles on the EMAP line. den Boer et al. (2000) demonstrate the utility of high-density CSMT/TEM data acquisition and 2D CSMT inversion technique in imaging the top and flanks of the Ommelanderwijk and Broek salt domes in the Netherlands. den Boer et al. (2000) also show how GEM results aided prestack migration of seismic data. The results of recent studies by Constable et al. (1998) and Hoversten et al. (1998) appear to suggest that MT may soon become a practical tool for offshore hydrocarbon exploration.

4.4. Challenges ahead

The three basic requirements in subsurface exploration for hydrocarbons are the delineation of any existing basins and description of their age, lithological make-up and depositional environments. Although GEM borehole logs are established as powerful tools for oil field correlations, the conventional usage and resolution limits of surface GEM methods do not lend them easily to the characterisation of lithological types and depositional environments or facies. Accurate stratigraphic mapping is still an outstanding problem in ground-based GEM exploration. The problem is compounded further by the fact that the source of resistivity variation for GEM methods could be fluid salinity instead of lithology (see e.g., Burgett et al., 1992). Joint GEM and Seismic inversion might help to overcome this problem (cf. Strack et al., 1991). Thus, the development of cost-effective 3D acquisition systems and robust software tools for joint multi-dimensional inversion of EM and seismic data should be seen as pressing challenges in hydrocarbon exploration. With such developments in place, the concepts of geoelectrostratigraphic or electrofacies classification of basinal environments may become physically realisable for continuous profiling data systems; for example, unconformities (surfaces of non-deposition or ancient erosion) which are important time-stratigraphic markers can be mapped and used as paleo-environmental marker horizons in geoelectrostratigraphy. The development of multi-dimensional joint GEM-seismic inversion will also have implications for the feasibility of direct detection of hydrocarbon, improved prediction of reservoir properties and improved mapping of seepage-related geochemical alterations. Note that the more common MT and TEM techniques are generally biased towards low-resistivity parts of the subsurface since they sense predominantly horizontal current flow. Grounded wire EM transmitters and electric field receivers (e.g., Strack et al., 1989; Strack, 1992) allow the effects of vertical current flow and charges at the boundaries of resistive zones to be detected (Eadie, 1981), and appear to provide useful additional data for resolving zones of enhanced resistivity due to carbonate alteration. The continuous array profiling variants of these artificial-source EM techniques may thus be the ones to combine with seismics in joint multi-dimensional inversion but will require the development of improved forward models for non-planar source fields.

5. Volcanic-Associated Massive Sulphide Deposits

5.1. Geological setting of VMS deposits

Volcanic-associated massive sulphide (VMS) deposits are small- to large-size concentrations of base metal mineralisations in host sequences dominated by submarine volcanics. They occur in a variety of geological environments that include divergent plate margins, convergent plate boundaries, intraplate oceanic islands and

Precambrian structures known as Archaean greenstone belts. The most characteristic feature of VMS deposits is that they occur, and appear to have been formed, as lenses parallel to the primary layering of their volcanic and volcano-sedimentary country rocks (Stanton, 1986). Being closely associated with volcanic lavas and pyroclastic rocks, they are commonly found clustered around old volcanic centres and along volcanic rifts, and they tend to occur in or close to one or two favourable horizons in the relevant volcano-sedimentary stratigraphic succession as in the Iberian Pyrite belt (e.g., Strauss et al., 1977), Noranda and Bathurst districts in Canada (Holyk, 1956; Spence and de Rosen-Spence, 1975) and Kuroko province of Japan. Graphitic shales are typically present between the volcanic sequences. There is an association of particular ore types with particular rock types: pyritic copper ores (of Cyprus type) with deep-sea basaltic volcanism and pyritic lead-zinc ores (of Kuroko type) with island arc andesite-dacite-rhyolite volcanism (Clarke, 1971). VMS deposits commonly show a chemical-mineralogical stratigraphy with predominantly iron and copper sulphides at the basal part and grading upwards into a zinc-rich zone followed by a lead-rich zone and then a barite-rich capping zone that may contain silver and lead; this zonation is best developed in deposits of felsic volcanic association (Stanton, 1986). In general, the deposits may be mound-shaped, blanket- or extensive sheet-like, or pipe-like in shape. However, the classic model of a VMS deposit is that of a stratiform lensoid or tabular zinc-rich massive sulphide body underlain by a discordant copper-rich massive sulphide zone or stockwork mineralisation (mostly stringer sulphide ore) within hydrothermally altered wall rocks (Sangster 1972; Sawkins 1976) as illustrated in Figure 16. Such an idealised VMS deposit may be characterised by a distinct zonation of the ore, gangue and hydrothermally altered minerals. The zonation is usually outward and upward from the base of the stockwork zone and the base of the massive sulphide lenses.

5.2. Electrical properties of massive sulphide ores and host rocks

The resistivities of the common sulphide ore minerals are summarised in Table VI. It can be seen that these minerals, except sphalerite, have high electrical conductivities. The detectability of these minerals using remote GEM methods depends very strongly on their quantity and the degree of connection between the various mineral grains or veins in the relevant host rock. Many massive sulphide deposits are typically single bodies with cross-sectional areas of over 100 m^2 and containing greater than 50% metallic mineralisation (which may include pyrrhotite and pyrite). Pyrrhotite typically forms elongated veinlets that serve as good geoelectrical conduction paths so that when present, even in small quantities, can greatly influence the overall electrical conductivity signature of a sulphide body (Gaucher, 1983). Massive pyrite is highly conductive but the mineral often occurs as unconnected blobs (Palacky, 1987) such that a pyrite-rich deposit may only be of

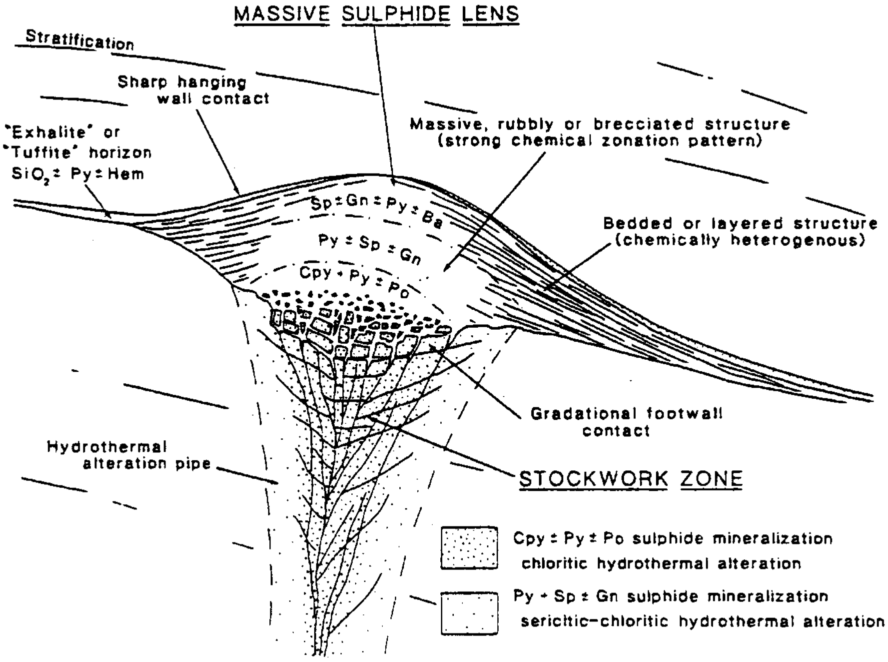

Figure 16. The structure of an idealised VMS deposit showing mineral and alteration zoning (after Sawkins, 1976).

moderate resistivity (20–40 Ωm). Chalcopyrite is highly conductive but usually constitutes only a small part of the total sulphide volume in many deposits.

Sample published data from systematic petrophysical measurements on some of the world's major VMS deposits and host rocks are given in Table VII. The main features of these massive sulphides are their low electrical resistivity. The effectiveness of GEM methods in detecting such deposits depends upon the existence of adequate contrast in these physical properties between the ore bodies and their host rocks. There are strong contrasts in resistivity between the massive sulphides and host rocks in many of the deposits listed in this table. Considering the deeply weathered Elura orebody (Emerson, 1980), there are marked differences between the electrical properties of weathered and fresh materials. The 2.5 m thick soil/hardpan layer has a resistivity of 71–305 Ωm. The limonitic gossan over the deposit is resistive (70–300 Ωm). The underlying saprolite zone has a resistivity of 10 Ωm and is 75 to 105 m thick. The zone of partially weathered materials has resistivities in the range 150 to 500 Ωm and rests on fresh host rock of about 1500 Ωm resistivity. The fresh pyritic and pyrrhotitic zones have resistivities of 0.3 and 0.1 Ωm respectively. Notice that the resistivity characteristics of this deeply weathered ore-body are in accord with the weathering model developed earlier in Section 2.1.

TABLE VI

Resistivities of the typical minerals in massive sulphide deposits (after Ward, 1966).

Mineral	Resistivity (Ωm)
Pyrrhotite	0.001–0.1
Pyrite	0.001–100
Marcasite	0.01–10
Chalcopyrite	0.0001–1
Sphalerite	1–10000
Galena	0.001–0.1
Arsenopyrite	0.1
Chalcocite	0.001–1
Bornite	0.01–1
Haematite	0.001–100000
Magnetite	0.01–10

We expect an idealised VMS deposit to be characterised by high electrical conductivity, high chargeability bordering zones (the deposit may be surrounded by an alteration halo of lower sulphide content that is amenable to detection by induced polarisation methods), and associated magnetite and pyrrhotite (or magnetic marker units such as banded iron formations) noting that sediments (such as graphitic shales) will be more conductive than the associated felsic volcanics. It may be noted that hydrothermal alteration and shearing in basic and ultrabasic rocks typically lead to the formation of talc and serpentine minerals which are electrically conductive. It is also of interest that major faults, fracture zones, and related structural control features in VMS prospects may be saturated with saline fluids, as in the case of Elura Orebody (e.g., Emerson, 1980), making them electrically conductive.

5.3. Case histories of exploration for massive sulphides

GEM methods are the central tools in the search for massive sulphides. TEM, IP, CSMT, mise-a-la-masse and MMR techniques find wide applications especially in Australia (e.g., Smith, 1980; Tyne et al., 1980, 1981; Fritz and Sheehan, 1984; Gunn and Chisholm, 1984; Buselli et al., 1986; Staltari, 1986; Smith and Pridmore, 1989; Boyd and Frankcombe, 1994; Lebel and Fallon, 1994), Canada (see Palacky, 1987 and references therein) and the Trans-Iberian Pyrite Belt (e.g., Leca, 1990; Van Ngoc and Daniele, 1992; Oliveira et al., 1993; Hopgood and Hungerford, 1994). They are also popular in the search for Cyprus-style VMS deposits (e.g.,

TABLE VII

Summary of some published data on the electrical properties of some VMS ores and host rock (after Hone, 1980; Schneider and Emerson, 1980; Tyne et al., 1981; Bishop and Lewis, 1992; Hopgood and Hungerford, 1994).

Locality/material	Resistivity Ωm	Chargeability mV/V (or ms)	IP effect (% freq. effect)
Aguas Tenidas East, Spain:			
Acid lavas	1500–4000 3–8		
Acid tuffs	500–800	5–10	
Diabase	1000	2–5	
Shale	100–600	10–25	
Massive pyrite	0.01–0.05	60+	
Complex banded sulphides	0.2–1	20–100	
Dissemin. Sulphides	0.5–1	20–80	
Woodlawn, Australia:			
Massive sulphide	0.01–5		25–30
Mineralized volcanics	0.1–10		<30
Dolerite	6800		2–7
Rhyolite	10000		1
Acid tuff	100+		2–10
Tuffaceous shale	1000		2–4
Gossan overburden	40-200+		0
Elura, Australia:			
Gossan (limonite)	70-300+		Small
Massive pyritic ore	0.3	80	25
Massive pyrrhotite ore	0.1	50	15
Semi-mass. siliceous ore	35		220
Weathered siltstone	10-20	1.6	Very small
Slightly weath. siltstone	150-500+		Minor
Fresh siltstone	1500+	12.5	Minor
Soil/hard-pan	71-305	4.2-6.7	
Red Dog, Alaska:			
Sulphide ore	20-90	(20-110)	
Country rock	50-1000		

Maliotis and Khan, 1980; Al Azry et al., 1993; Cooper and Swift, 1994) and Besshi-type deposits (e.g., Ogilvy, 1983, 1986; Bowker and Hill, 1987). Although deep EM methods have generally been successful in mapping stratiform and discordant conductive mineralised zones, the EM signatures may be dominated by contributions from undesirable ionic conductors or shielded by siliceous alteration in some terrains (e.g., Gunn and Chisholm, 1984; Cooper and Swift, 1994). In such cases, the IP method has been much more effective especially in mapping the stringer or disseminated sulphide zones connected to the massive orebodies (e.g., Maliotis and Khan, 1980). The various roles of GEM methods in the search for solutions to current problems related to VMS exploration and development are summarised in Table VIII. The availability of efficient 2D inversion software (except for TEM method) has added value to GEM exploration for VMS targets. Improved acquisition of 3D controlled source GEM data and a matching improvement of inverse modelling capability are highly desirable in VMS exploration. GEM deployment in mining sites remains a challenge.

6. Porphyry Copper Deposits

6.1. Regional geologic setting of PCDs

Porphyry copper deposits (PCDs) are high-tonnage, low-grade copper occurrences that are associated with specific tectonic environments and petrology. They are the dominant source (about 50%) of the world's copper and usually carry minor gold and silver. PCDs are known to occur in subduction related settings (Figure 17) within island arc magmatic belts, and mountain belts of Mesozoic and Tertiary ages, e.g., the Andean subduction zone. The deposits are found to be located on the accretionary plate-side in close association with porphyritic igneous plutonic rocks with a calc- alkaline compositional trend. The mineralization within these deposits is centred upon a vertical cylinderical stock that may be about 1 km to 2 km in diameter. Typical host lithologies are granitic to dioritic (I-type granites), with tonalite and quartz-monzonite being important hosts. Intrusions are often associated with volcanism. The distribution of these deposits is closely controlled by major regional structures. The deposits therefore show marked regional zonation in the form of clustering as typified by those in the mining districts of Southwest U.S.A. (e.g., Lorne, Ely and Bingham deposits), Papua New Guinea (e.g., Ok Tedi and Bougainville deposits), Philippines and the numerous deposits associated with the Andean subduction zone. Mineralization is hypogene and may occur within the country rocks, within the host stock, and across both the host and country rocks to the surface. Mineralization is generally concentrically zoned within the host stock and the sulphides occur as finely disseminated and stockwork forms (see Lowell and Guilbert, 1970). The mineralogy is pyrite, chalcopyrite, bornite, and molybdenum, often with associated secondary gold or silver.

TABLE VIII
Summry of common applications of GEM techniques to VHS exploration problems.

GEM method	Target features in VMS prospects
EM	
Airborne EM	Structural framework, linear or clustered conductive features, gossan detection.
TEM/FEM(HLEM,CSMT,MT)	Faults, shear zones, weathering profile, alteration halo, conductive or resistive mineralization, concealed intrusive bodies.
Electrical	Mapping of lithology, weathering profiles, relict brine ponds, faults, mineralization, bedrock depth and sulphide content.
Spectral IP/complex resistivity	Detection of resistive horizons, altered sequences and mineralisation.
Time-domain IP	Graphite-massive sulphide discrimination, mapping of disseminated ore zones.
Magnetic IP	Mapping of mineralised zones in “EM poor-record” terrains and disseminated sulphides.
SP	Mapping of shallow massive sulphides, quartz-sericite-pyrite alterations.
Mise-a-la-masse	Mapping lateral dimensions and continuity of massive orebodies.
Borehole surveys	Lithologic identification, stratigraphic correlation, in situ rock properties, detection of off-axis mineralisation, ore quality and reserve assessment.
Petrophysical measurements (core)	Lithostratigraphic correlation, interpretation of surface geophysical exploration data.

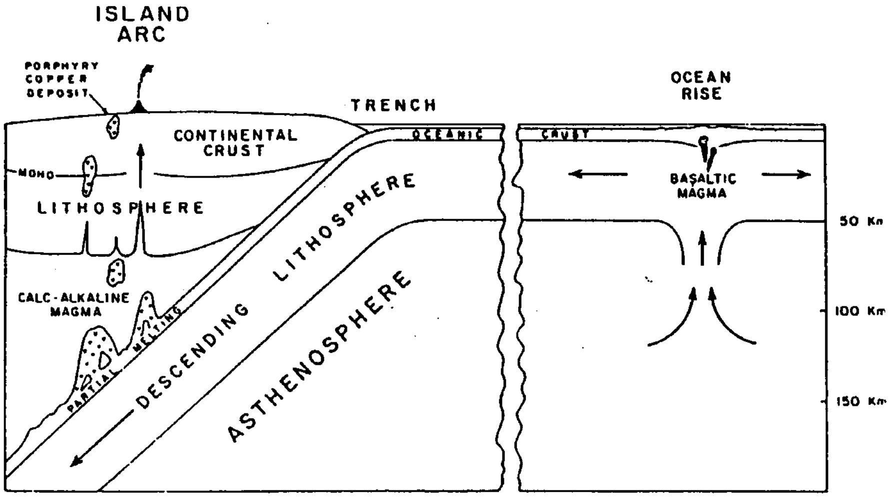

Figure 17. Sketch depicting subduction-related tension fractures and genesis of PCDs (Isaacs, 1968; Sillitoe, 1972).

The zones of mineralization and the host lithology may be overprinted by hydrothermal alterations (Guilbert and Lowell, 1974). Essentially, these are ramifications of heat and fluid transport in fracture-controlled geothermal systems, possibly driven by episodic seismogenic events, and have important implications for the geoelectromagnetic responses. Up to four zones of hydrothermally altered rock may be recognised in a typical porphyry copper deposit (Figure 18). The potassic zone, the result of metasomatic alteration, occurs in the core but may not always be present. The characteristic minerals are biotite, orthoclase feldspar and quartz with accessory albite, anhydrite, and apatite. Magnetite may also be present with pyrite and bornite. The potassic zone is sourrounded by a zone of sericitic alteration called the phyllic zone and characterised by quartz, sericite and pyrite minerals resulting from the leaching of magnesium and calcium from the host alumino-silicate rocks. Chlorite, illite and rutile may be present as minor minerals in this zone. This zone shows the best development of mineralization and much silicification. The Argillic zone which is marked by the development of new clay minerals (typically montmorilonite, illite, chlorite, kaolinite) and pyrite veinlets may surround the phyllic zone. The outer zone of propylitic alteration is always present and the characteristic mineral assemblages are chlorite, epidote and calcite; there is extensive alteration of mafic minerals to chlorite and carbonate in this zone. Haematite, apatite and anhydrite may occur as minor minerals.

6.2. Resistivity characteristics of PCDs

PCDs are fossil geothermal systems, *sensu stricto*. Depending on the characteristics of the country rocks, the erosional level and degree of geochemical alteration, the GEM responses across a typical deposit may show recognisable trends. Since

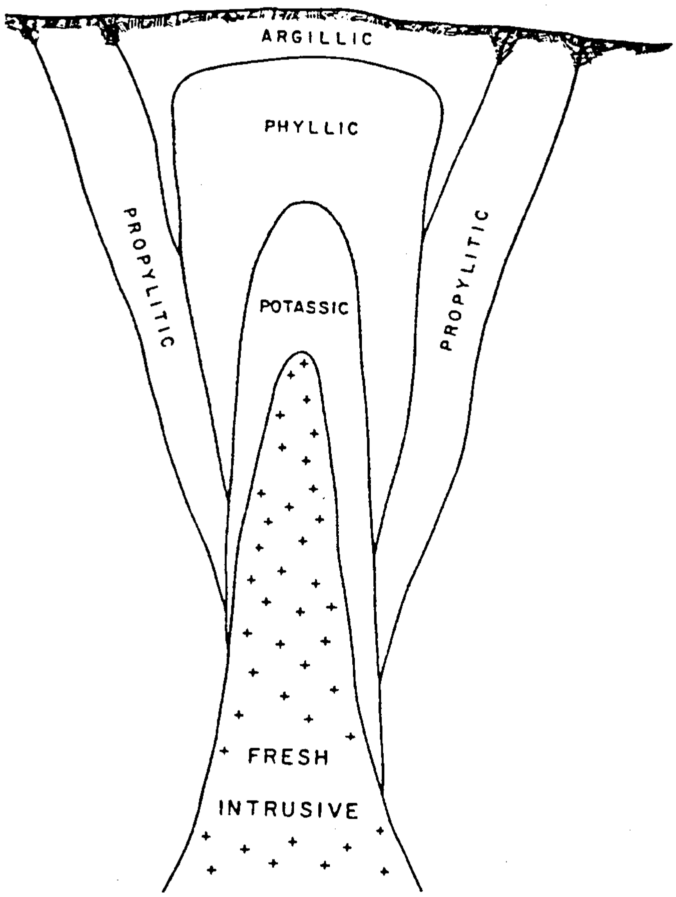

Figure 18. A simplified diagram of the alteration zoning in a typical porphyry copper deposit (Hollister et al., 1974).

the parent intrusive bodies are usually injected into country rocks along zones of weakness (faults or shear zones) in the region, there might be present some significant structures related to the disruption of the physical state of the pre-existing rocks. These structurally controlled intrusions may thus be characterised by notable crustal and upper mantle anomalies or lateral inhomogeneities. The region containing the porphyry body might be characterised by hot, molten material at depth and a doming of the mantle. A low resistivity zone may thus be apparent on deep GEM images. The composite GEM signature across an exposed PCD could consist of a broad signature corresponding to the intrusive stock with superposed anomalous conductive zones over the sulphide and clay rich alteration zones. There is usually a broad zone of high IP responses across a PCD since the deposit consists of disseminated mineralizations. The skarn mineralization (where the mineralization takes the form of stringers and veinlets) and zones of supergene enrichment would be associated with low resistivities (Table IX). Corry (1985) suggest that the

TABLE IX
Distinguishing features of PCDs and applicable GEM methods.

Physico-chemical features	GEM exploration approach
Major regional structures (lineaments, faults)	AEM + ground TEM, CSMT
Moho offsets, deep intrusives, partial melt	MT, LOTEM
Disseminated sulphide mineralisations, stockworks	IP
Supergene-enrichment zones, skarn, stockworks	TEM, FEM(CSMT), IP, SP
Gossan	AEM, shallow ground FEM/TEM, gradient IP
Argillic and chloritic alterations; magnetite destruction (reduced resistivity)	AEM + ground FEM (CSMT), TEM, dc resistivity
Silicic and carbonate alterations (increased resistivity)	CSMT, TEM (LOTEM), dc resistivity
Quartz-sericite-pyrite alteration halo (unoxidised)	SP

quartz-sericite-pyrite alteration zone with associated pyrrhotite would give rise to significant SP anomalies.

6.3. Exploration for PCDs

GEM techniques are the dominant tools in the search for porphyry copper deposits. Regional airborne and follow-up ground investigations are common-place (see e.g., Witherly, 1977). The current areas of application of GEM methods to PCD exploration are given in Table X. The induced polarisation method has the highest potential for direct detection of the disseminated mineralization and the reader is referred to the classic case studies by Pelton and Smith (1979). The other GEM methods are indirect search techniques, in every sense. Corry (1985) presents interesting field examples showing that the SP method is useful for finding the quartz-sericite-pyrite alteration zone. Ground electromagnetic methods are useful for locating associated skarn mineralization where the mineralization takes the form of stringers and veinlets and for locating linear conductors and zones of supergene enrichment. Dc resistivity techniques may contribute some useful information in the form of background resistivity distribution but are not hugely popular in the search for porphyry copper deposits.

LOTEM (employing electrical and magnetic field measurements) and CSMT surveys have enhanced capability for high resolution mapping of alteration zones when compared to natural source MT, magnetic-field based TEM, and dc resistivity techniques. However, tensor MT surveys can provide deep images of the crust enabling prospect ranking and adequate mapping of structural controls on mineralization in prospective regions.

TABLE X

Current uses of GEM methods in the exploration for PCDs.

GEM method	Exploration targets
Electrical	
SP	Quartz-sericite-pyrite alteration, heat flow, fluid flow in stockworks.
IP	Structure, disseminated and fracture-fill mineralization, geochemical alterations.
Dc resistivity	Faults, lineaments, silicic alteration.
MMR	Structure, skarn mineralization, alterations.
Electromagnetic	
AEM, shallow FEM	Lineaments, faults, regional conductivity trends, gossans.
TEM/CSMT	Deep structure, alterations, skarn, supergene-enriched zones, stockworks, shallow intrusive stocks.
MT/LOTEM	Regional controls, deep intrusives, partial melt, conductivity distribution, alterations.
Downhole methods	Sulphide distribution, alterations, off-axis mineralization.

7. Gold Deposits

7.1. Geological setting of gold deposits

Gold deposits represent a complex array of deposit styles, ranging from large disseminated deposits to thin quartz veins and stockworks. The main gold producing areas are in the Precambrian shields (e.g., South Africa, Canada, Australia and Brazil), Palaeozoic fold belts, and Mesozoic to Quaternary volcanic arcs such as in the Pacific rim (Doyle, 1990). This wide variety of geological environments in which gold deposits are found makes GEM prospecting a challenging task especially since the various environments exhibit a wide range of resistivity or polarizability characteristics. Doyle (1990) notes that although gold has high electrical conductivity (5×10^7 S/m), this property is masked by the low grades in typical deposits (of the order of grammes per tonne) ruling out direct detection by GEM methods except in the special circumstances where EM detectors are used to locate individual shallow-lying nuggets. Any indirect approach to gold prospecting would require a good understanding of the geological controls on mineralization.

It is of exploration interest that while gold deposits are hosted by a variety of lithologies, there appears to be some association with particular host rocks, marker beds (e.g., banded iron formations or magnetic quartzites, magnetic dolerites, magnetite-rich shales or other carbonaceous units, pyritic and other metallic sulphide horizons, and zones of silicic or argillic alteration), and structures (faults and shear zones) that may be geoelectromagnetically responsive (cf. Doyle, 1990). There appears to be some structural controls on the distribution of gold deposits; most deposits are within a few kilometres of major shear zones as in the Abitibi subprovince of Canada (see e.g., Robert, 1991). The precise structural controls on location of gold mineralization is poorly understood but it is known that the prospective regions are characterised by primary linear through-going structures and second or third order extensional features. It is becoming accepted that the large primary faults serve for channelling ore fluids and do not provide adequate collection points for ore. Cox et al. (1991, 1995) suggest that is the second or third order structures (faults, shear zones and related fracture systems) that are spatially associated with the large crustal-scale shear zones, and are of limited lateral extent (dead end pores in Figure 19), which serve for deposition of significant ore. Localised deformation (bending, splaying etc) along the major faults, shear zones and their associated fracture systems leads to preferential focussing of mineralising fluids in the resulting connected second order structures (Cox et al., 1991, 1995). This conceptual model would dictate that a multi-phase GEM approach is essential for effective gold prospecting (comprising of the initial identification of lineaments and favourable lithologies, follow-up exploration for small-scale second-order extensional features and detailed localised search for mineralised targets). Although there are several types of gold deposits on account of the various geological settings (see Boyle, 1984; Doyle, 1990), only the Archaean granite-

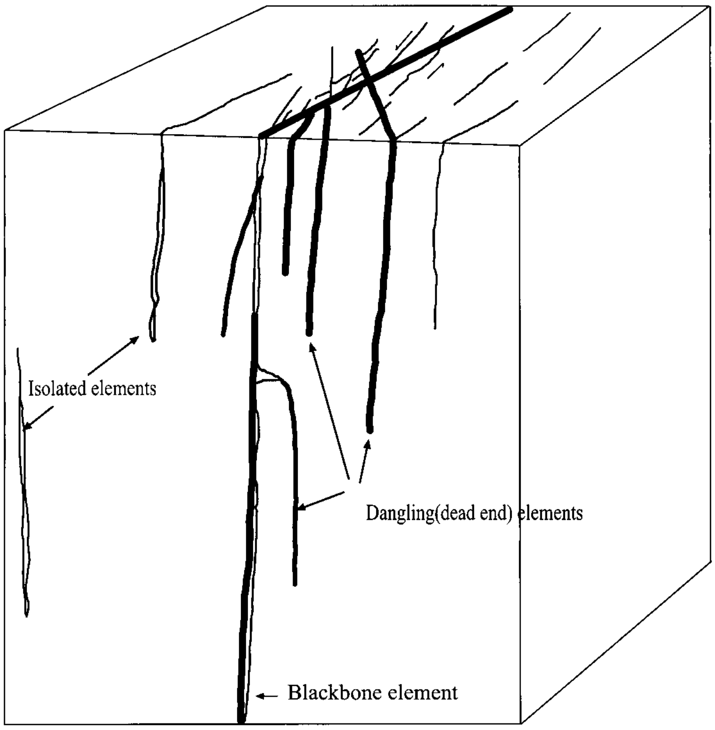

Figure 19. Cox's model showing effective sites of gold localisation in a fracture-controlled system. The dark-shading indicates the accessible sites for potential ore-beearing fluids. Those isolated elements not connected to the backbone element (main carrier) are barren. The dangling (dead end) elements with links to the backbone element are the prospective sites for gold deposition.

greenstone belt and Mesozoic-Quaternary epithermal deposits will be discussed here. The relevant characteristics for model development include the structural controls, important host rocks, mineralization and alteration styles and the size of ore-shoots or deposits.

7.2. Exploration model for epithermal gold deposits

GEM exploration for Mesozoic-Quaternary epithermal gold systems is a difficult task since much depends on the nature of the host rocks, structural controls on the mineralization and level of erosion. The distinguishing features of epithermal gold deposits are listed in Table XI and an ideal geological model is shown in Figure 20. Silicic and argillic alteration patterns are commonly mapped using electrical and EM methods. In some prospects, these alterations may be associated with useful mineralization. The GEM responses would tend to vary with the level of erosion of the deposit (see Table XII). Johnson and Fujita (1985) present examples of the use of airborne EM surveys to map faults and shear zones that may be associated

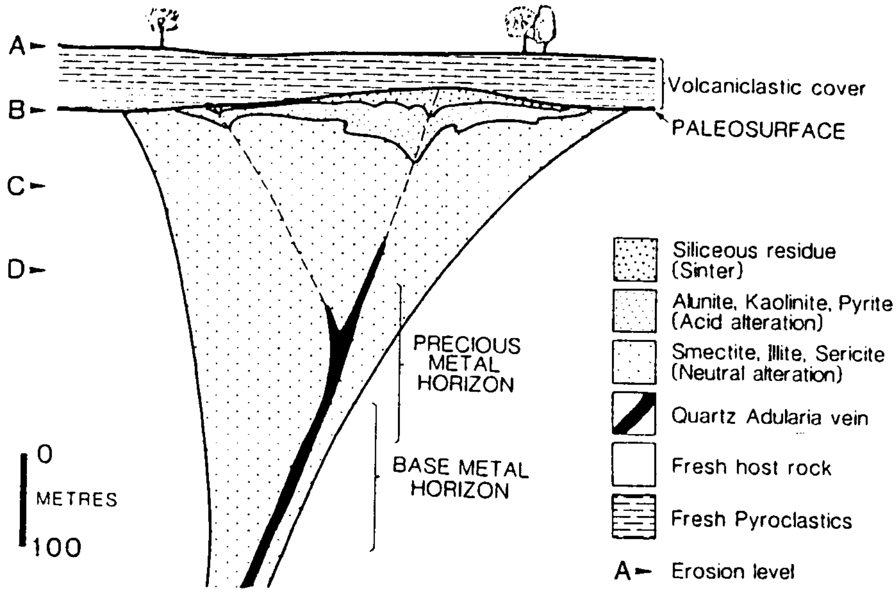

Figure 20. An idealised model for epithermal gold deposits (Irvine and Smith, 1990). The symbols A, B, C and D denote hypothetical levels of exhumation of the deposit by surface erosion. The anticipated responses at these sequential erosional levels are given in Table XII.

with gold mineralization in a prospective region selected on the basis of available geological and/or remote sensing data.

7.3. Exploration for granite-greenstone belt gold deposits

Archaean greenstone belt gold deposits present extreme difficulties in exploration due to the variation in size, morphology and sulphide mineralogy of ore-shoots (Doyle, 1990). The extent and heterogeneity of iron-sulphide and carbonate alteration, and the extent of magnetite (and/or ilmenite) consumption in alteration reactions would affect the overall GEM response of a deposit. The characteristic features of greenstone gold deposits of relevance to GEM exploration are given in Table XIII.

The most common feature of greenstone belt gold deposits is their close spatial association with major crustal-scale deformation or shear zones extending for tens to several hundred kilometres (Eisenlohr et al., 1989). The ore is typically in second or third order structures of the major shear zones especially in bends, splays and offsets that indicate a local tensional regime. The major structures may have served for channelling the ore forming solutions but it would appear that the secondary or tertiary short-wavelength (<10 km) fracture zones are the effective collection sites of the potential auriferous ores. The deposits occur in all rock types (mafic, ultramafic, banded iron formations, sedimentary, granitoids) but mafic rocks appear to be favoured. In Australia, for example, gold lodes occur mostly in mafic

TABLE XI

Distinctive features of epithermal environments and GEM exploration approach (adapted from Irvine and Smith, 1990, Table 1).

Physico-chemical features	GEM exploration approach
Major structural controls – faults, fold: (deep resistivity anisotropy)	Remote-sensing + AEM (follow-up regional LOTEM/MT)
Favourable host lithologies	AEM resistivity + geology
Deep intrusives, congealed magma, Moho offsets (deep resistivity anisotropy)	MT, LOTEM
Argillic alteration, magnetite destruction (reduced resistivity)	AEM resistivity + ground FEM/TEM (+ magnetics), dc resistivity/MMR and MT/CSMT
Carbonate or silicic alteration, quartz veining and pegmatite formation (increased resistivity)	High resolution inductive source resistivity (TEM, LOTEM, CSMT), dc resistivity
High sulphide content (increased polarizability, reduced resistivity)	IP, FEM/TEM, MMR

TABLE XII

Anticipated GEM responses for various levels of exhumation of an ideal epithermal deposit (modified from Irvine and Smith, 1990, Table 2). Note that the response may be modified by the presence of a sinter at or near the present topographic surface.

Erosional level of Prospective target	Shallow FEM/AEM	CSMT, TEM	IP	Dc resistivity
A – target covered by young volcaniclastics	Nil or weak response	Weak broad conductor	Nil or weak response	Nil or weak conductor
B – hydrothermal palaeosurface	Strong broad conductor	Strong broad conductor	Moderate broad response	Strong broad conductor
C – subcropping vein system at 50 to 150 m depth	Distinct conductor	Strong conductor within which narrow resistor may be resolved	Moderate response	Strong conductor within which narrow resistor is unlikely to be resolved
D – outcropping vein system	Narrow multiple conductors	Narrow strong resistor flanked by strong conductors	Weak narrow response	Narrow strong resistor flanked by strong conductors

TABLE XIII

Distinctive structural, lithologic and alteration characteristics of greenstone belt gold deposits and effective GEM methods for mapping them (adapted from Hoover and Heran, 1993).

Physico-chemical features	Size of target features	GEM exploration approach
Structural control (faults, folds, lineaments):		
a. Close spatial association of ore with major shear or deformation zones	10 to several 100 km long and several km wide	Remote-sensing, regional AEM, CSMT/MT, TEM, IP
b. Folding may have provided extensional zones for ore deposition	All scales	Regional and detailed AEM, CSMT/MT(EMAP), TEM/LOTEM
c. Deposits found in second or third order structures of the major shear zones especially in extensional zones	Structures up to 10 km long and several tens of metres wide; ore bodies up to 1 km long and tens of metres wide	Detailed AEM and follow-up CSMT, TEM, IP, MMR
Geological environment:		
a. PreCambrian granitoid-greenstone belts	Elongate folded belts about 10 to >100 km long	Regional AEM, FEM
b. Favourable host rocks are commonly mafic	All scales	Detailed AEM, FEM, CSMT
c. Carbonaceous sediments form associated marker horizons	All scales	AEM + detailed IP/MMR, TEM/CSMT
Hydrothermal alteration:		
a. Carbonatization is extensive and most common		CSMT (+ radiometrics)
b. Sulphidation is important		AEM resistivity mapping
c. Silicic alteration		IP/MMR, CSMT/LOTEM/TEM, SP
d. Haloes of small size	Up to a few 100 m around ore	Detailed ground and borehole surveys

volcanics and intrusives (e.g., dolerite) and banded iron formations (BIF). Greenstone gold deposits are commonly found associated with carbonaceous (shaly or graphitic) materials (in potential marker horizons) and wall-rock alteration is a characteristic feature. The alteration haloes are of small size and may consist of inner zones of Fe-sulphide surrounded by K-mica and siderite-ankerite-dolomite alteration, with wider carbonate (calcite) alteration in some areas depending on the host rocks.

Airborne EM and ground HLEM methods have been effective in defining major crustal-scale linear structures in several parts of the world and such zones are sometimes the sites of pre- or post-mineralization igneous intrusions (e.g., Isles and Cooke, 1992) with possible attendant enhancement of GEM signatures. At the prospect scale, detailed airborne and ground GEM methods are commonly used by the mining industry to map lithologies and identify small faults at bends or splays of major lineaments in greenstone terrains. Hoover and Heran (1993) suggest that mafic and BIF hosted deposits tend to have higher sulphide content making them good targets for GEM (especially IP) methods. Graphitic and shaly marker horizons associated with greenstone gold deposits are very conductive, and Reinhardt and Davidson (1990) show that they can be traced using GEM methods. GEM methods play an important role in alteration mapping and detailed ground and borehole surveys are necessary because of the typical small size of the haloes. Many deposits are associated with sulphidation and extensive carbonate alteration. Sulphidation alteration (increased sulphide content) presents a natural target for IP, MMR and high resolution inductive resistivity methods. Silicic and carbonate alterations may lead to increased resistivity so that GEM methods can be used to map the haloes. However, carbonation halo may not always have a significant resistivity enhancement and it is logical in this case to integrate GEM and gamma-ray spectrometry for carbonate alteration mapping since the zone may have enriched potassium (e.g., Melo, 1990). It is opined that more research studies need to be carried out to define precisely the GEM signatures of the main structural controls, mineralization styles and alteration zoning in greenstone belts gold deposits. It is also suggested that GEM methods can be integrated with structural geology and fluid inclusion studies to understand better the deformational controls on the dynamics of fluid flow in mesothermal and epithermal gold systems.

8. Diamondiferous Kimberlites

8.1. Geological setting of kimberlites

Economic concentrations of diamonds occur in alluvial (placer) deposits or in their primary host rocks known as kimberlites and lamproites. Kimberlites are considered to be the major host rocks. They occur in a variety of geological environments as hybrid rocks with extremely variable composition but are mostly found in ancient shield regions (Bardet, 1964) associated with major crustal lineaments (Dawson, 1971). The parent magma is mantle-derived and intruded as pipes, dykes and (rarely) sills along deep-reaching zones of weakness in the Earth's crust or at the intersection of major faults. Kimberlites vary in form and size from small volcanic vents or thin dykes to pipes less than 2 km across, and may extend vertically for several hundred metres. The emplacement mechanism is characterised by rapid transport by gas fluidisation and vent enlargement at shallow levels (<2 km depth) culminating in an explosive breakthrough to the surface at structurally controlled points such as the intersections of deep fractures (Macnae, 1979). The pressure release accompanying this explosive event results in geochemical alteration of the upper parts of the intruded magma (principally, serpentinisation of olivine) and there may be some silicification of the wall rocks. The cooling process leads to substantial fracturing and settling creating a crater on the surface surrounded by volcanoclastic debris (ejectamenta or tuff ring). A crater lake often results and the subsequent sedimentation in this small structural basin is characterised by mixed sediment infill comprising of locally derived clastics and the volcanoclastic deposits dubbed epiclastic kimberlites (Hawthorne, 1975). In most cases, the underlying (primary) kimberlite pipe (or diatreme) is oval in outline with a carrot shaped extension at depth and a feeder dyke or plug at the basal part (Figure 21). Diatremes are typically steep sided, with the dip of the inward wall ranging from 79° to 85° and may be a few hundred metres in diameter at the surface. Apophyses or satellite bodies may be present with different diamond grades. The whole structure is relatively porous (with porosity decreasing with depth). Kimberlites tend to occur in clusters of 2 to 40 pipes, each cluster occupying an area up to 40 km in diameter (cf. Kamara, 1981). An individual pipe might be re-intruded during subsequent volcanic episodes, and it is not uncommon to find pipe clusters or plugs with different petrographic characteristics (i.e., marked heterogeneity).

Not all kimberlites are diamondiferous (Dawson, 1971). Diamondiferous kimberlites appear to be confined to centres of ancient shields or cratons that have not experienced major orogenic activities in the past 1500 Ma (cf. Kirkley et al., 1991). Diamonds are considered to result from partial melting of carbonated peridotite at depths of over 150 km in the Earth's mantle underneath regions of thick, stable continental crust, i.e., cratons with deep crustal roots (Kirkley et al., 1991) where the source rock is molten and enormous pressure squeezes the carbon atoms into a tetrahedral crystal structure. Their source rocks are considered to be eclogite and garnet peridotite that are present in mantle roots at depths of about 150 to 200 km beneath such regions. Almost all known kimberlite pipes containing economic quantities of diamond were emplaced in those parts of the cratons that are of Archaean age (>2500 Ma). Interestingly, diamonds often are found to be much older (900 to 3,300 Ma) than the enclosing kimberlite (e.g., 50 to 560 Ma in the Northwest Territories of Canada; 100 to 1,200 Ma in known world occurrences). This suggests that the host kimberlite may not be the source of the diamonds, which could have crystallised from a different melt and were preserved over a long

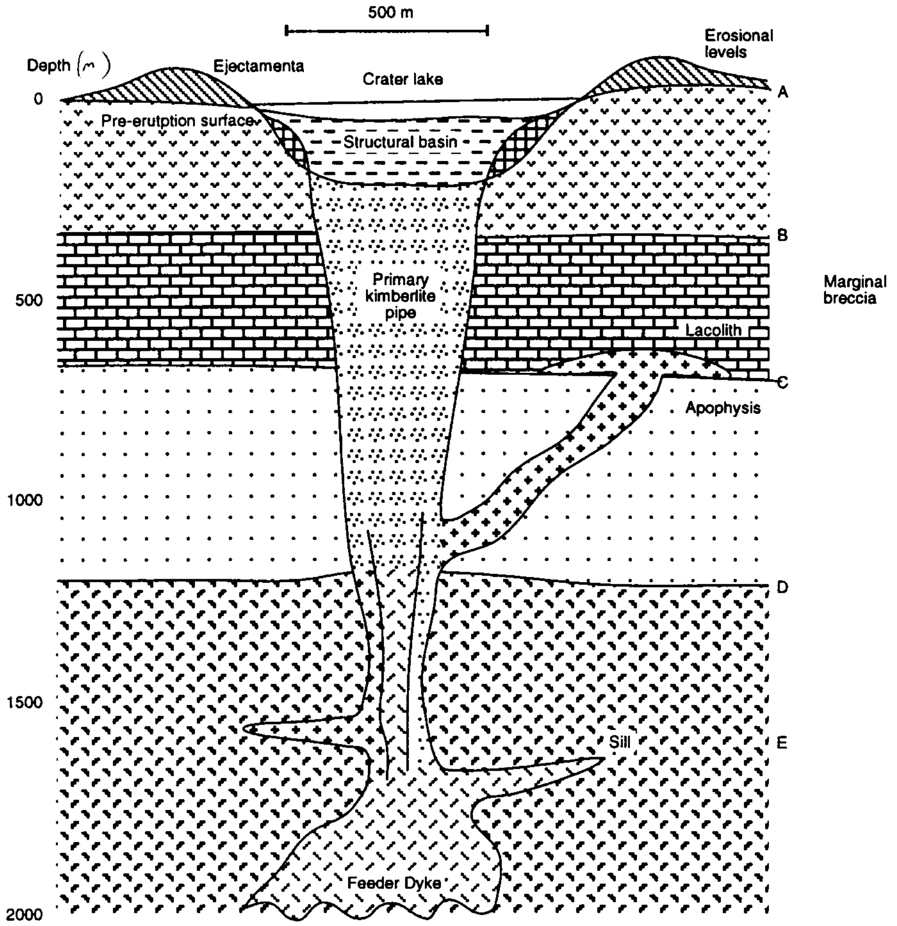

Figure 21. Kimberlite pipe morphology soon after emplacement (adapted from Dawson, 1971; Hawthorne, 1975).

period of time in regions of high pressure and relatively cool temperatures before being transported to the near-surface by kimberlitic magma. There is no GEM method for direct detection of diamonds, but under favourable local conditions, it is possible to delineate weathered kimberlite pipes that can serve as pathfinders for diamond mineralisation. It is also of geophysical exploration significance that the prospective cratons are typically associated with thick (>150 km) lithosphere.

Kimberlite is a porphyritic alkalic peridotite. Fresh kimberlite is a hard, blue or dark grey rock but it is very susceptible to weathering, and especially with its high porosity and permeability. Thus at a given level of erosion, the typical weathering profile of kimberlite would consist of: (i) an upper leached zone in which the original kimberlite has been completely hydrated and oxidized into friable clayey materials; the thickness of this zone (dubbed the yellow ground) varies from 2 to 50 m, and nontronite and montmorillonite are the dominant clay minerals (da Costa, 1989); (ii) a transition zone of serpentinised kimberlite (blue ground), about 20 to over 300 m thick (Wagner, 1914), and often containing masses of relatively unweathered kimberlite; it may also show a marked depletion in Fe (magnetite destruction by conversion to limonite and other hydroxides of iron) and enhancement in CaO and CO_2 leached from the overlying yellow ground as in the Finsch kimberlite in South Africa (Ruotsala, 1975); and (iii) fresh kimberlite (termed hardebank). For the attendant *in situ* weathering process, deeper profiles will be expected over regions with a long period of non-deposition. Also, an initially exposed and weathered kimberlite may become gouged out by glacial action and covered by glacial till or alluvium during a later phase of deposition.

8.2. Resistivity characteristics of kimberlites

Fresh kimberlite contains about 5 to 10 percent Fe in the form of magnetite and ilmenite (Litinskii, 1963; Fesq et al., 1975). Both of these minerals occur as primary constituents in kimberlites but magnetite is also formed as a secondary mineral during the process of serpentinization. A fresh kimberlite may thus give rise to significant IP anomalies, depending on the degree of heterogeneity of the pipe (the pulses of intrusions and ingestion of pre-existing rocks may lead to a confused anomaly pattern) and host rock composition. Clays are common in deeply weathered kimberlites. The clay-rich yellow ground and the serpentinized blue ground are typically conductive while the hardebank is usually resistive (see Table XIV). Thus in some situations, the weathered pipes may provide a relatively conductive (disc-shaped) target or marker horizon for geoelectromagnetic exploration.

However, the detectability of kimberlite pipes would depend on the contrast in resistivity between the kimberlite and the surrounding country rock, and also between their weathering products. Weathered kimberlite pipes are known to be more conductive than their granitic country rocks in Tanzania and Sierra Leone only because the pipes weather to nontronite and montmorillonite while the granite weathers to kaolinite clay (Gerryts, 1967; Kamara, 1981). There are environments in which the country rock weathers into more conductive products than the intruded kimberlite pipe which is then a relatively resistive target (cf. Jenke, 1983). And, we would expect to see different GEM responses depending on whether yellow ground or hardebank is exposed. In glaciated terrains, the weathered section might be eroded away exposing relatively resistive kimberlite or become covered with conductive glacial till and lake sediments as in the Northwest Territories (NWT) and other parts of the Canadian Shield affected by Pleistocene glaciation. A weathered kimberlite pipe may be covered by younger granular deposits of comparable resistivity and variable thickness. Through-going fracture-zones (i.e., transecting the entire crustal thickness and offsetting the Moho) can be expected in prospective terrains and the structurally controlled kimberlite intrusions may thus be associ-

TABLE XIV

Typical resistivities of kimberlite material and country rocks from Lesotho and South Africa. (Data from Burley and Greenwood, 1972; Kamara, 1981; da Costa, 1989.)

Locality/depth range (m)	Material sampled	Electrical resistivity (Ωm)
Lesotho:		
9–24	Yellow kimberlite	10–20
	Soft, partially weathered kimberlite	10–20
	Basalt/dolerite (non-amygdaloidal)	500–1000
9–19+	Hard fresh kimberlite	100–1000+
South Africa:		
3–8	Yellow kimberlite	10–20
29–44	Soft blue kimberlite	10–20
	Fresh kimberlite	100–200
	Weathered norite (country rock)	260
	Fresh norite (country rock)	1500–2500

ated with notable crustal and upper mantle conductivity anomalies or strong lateral heterogeneity.

TABLE XV

Main features of kimberlites and GEM exploration approach.

Target features	GEM exploration approach
Major structure (parallel or intersecting lineaments), circular or elliptical depressions (crater lake sites), pipe clusters	Landsat imagery/photogeology + AEM
Weathered kimberlite (conductive)	AEM + ground FEM/TEM, IP/dc resistivity
Fresh kimberlite (resistive)	IP, CSMT (sedimentary host rock)
Geochemical alterations:	
Serpentinization of olivine, magnetite destruction (reduced resistivity)	AEM + TEM, CSMT, dc resistivity/IP
Silicification of wall rock (increased resistivity)	CSMT, TEM (LOTEM), IP/dc resistivity
Deep intrusives (diatremes, apophyses, dykes), through-going fracture-zones, Moho offsets	MT, CSMT or LOTEM

8.3. Case studies and developments in the exploration for kimberlite pipes

Kimberlites present some exploration problems (Table XV) since the anticipated GEM responses tend to vary with the pipe and host rock chemistry and petrography, the level of erosion and degree of weathering (or the post-emplacement sedimentation history). GEM methods are popular for mapping deeply weathered kimberlites (see e.g., da Costa, 1989). Since the initial phase of exploration is concerned with the efficient and cost-effective assessment of the potential of a given area to host kimberlite pipes, a combined airborne EM/magnetics approach appears to be favoured for reconnaissance surveys (Macnae, 1979; da Costa, 1989; Smith et al., 1996). The combined approach is also adopted in follow-up ground or airborne investigations to refine the position of any detected anomalies and to provide details on the size, shape and internal structure of the target. The survey parameters (line spacing, instrument recording bandwidth, sampling rate and sensor height) are often optimised to the prevailing field conditions. Lines spaced 200 to 250 m apart are commonly used in airborne reconnaissance surveys for pipes with anticipated diameters of a few hundred metres. Smith et al. (1996) suggest that a conservative approach would be to use a flight-line spacing equal to the expected target size. Smith et al. (1996) also describe the modifications to a time-domain AEM/magnetics field system which resulted in improved anomaly detection over the Point Lake discovery pipe in Lac de Gras area and another nearby prospect in the Slave Structural Province, NWT of Canada where glaciation may have removed parts of the originally weathered pipes. They ascribe the AEM anomaly to enhanced conductivity due to the presence of thicker lake sediments above the kimberlite, greater fluid content in the porous target, or alteration to serpentine and clay minerals.

It would appear that time-domain AEM surveys incorporating measurements during transmitter on- and off-times (Smith et al., 1996) offer improved capability for detecting weathered pipes but an integrated approach is essential for a successful exploration. An important criterion in the selection of kimberlite targets from AEM survey results is the presence of isolated conductors with associated magnetic signatures (Figure 22) which may mark the positions of potential weathered pipes (Macnae, 1979; Smith et al., 1996). Lateral profiling on the ground is often done to delimit the concealed conductive section of a weathered pipe (da Costa, 1989). Note that there are combined surveys with no diagnostic AEM responses such that exploration decisions were based mainly on the magnetic data. Reed and Sinclair (1991) describe an exploration program in the James Bay lowlands of Ontario (Canada) where the prospective epiclastic breccia-pipes, discovered based on their magnetic signatures, had AEM responses that were either weak or indistinguishable from those of the surrounding glacial till. Removal of the presumed weathered zones of these bodies by Pleistocene glaciation is a plausible explanation for the paucity of AEM anomalies in this Canadian terrain (Reed and Sinclair, 1991).

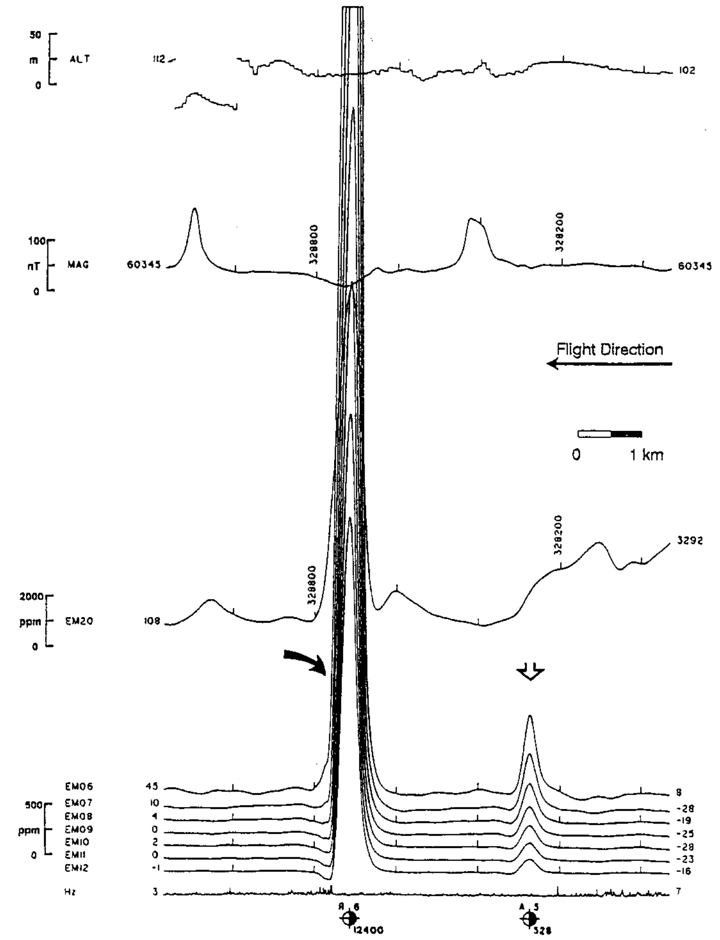

Figure 22. Multi-channel AEM profiles across the Point Lake (Lac de Gras) kimberlite pipe (Smith et al., 1996). The aircraft altimeter (ALT), the flight direction (east to west), and the magnetic profile (MAG) are also shown. The solid arrow marks the Point Lake response (strong AEM anomalies and a coincident weak magnetic low). The open arrow marks another weaker AEM anomaly with no coincident magnetic anomaly.

In Western Australia where the overburden is very conductive, only 60% of the anomalies present in magnetic survey data had associated AEM signatures (Jenke, 1983; Atkinson, 1986).

Although less common in traditional kimberlite exploration programmes, the deep-probing MT and LOTEM methods can be fruitfully applied to the search for kimberlites (see Table XV). They may be pivotal to the recent spurt of exciting developments in kimberlite exploration philosophy, practice and promise. Jones et al. (1996) note that, since only those kimberlite pipes originating from about 150 km deep in the Earth may contain diamonds in commercial quantities, knowledge of the thickness and internal structure of the upper mantle such as derivable from long period MT (or teleseismic) measurements would help optimise exploration strategies for kimberlites or lamproites that may have formed in the diamond stability field. Jones et al. (2000) demonstrate that the MT method can identify regional structures that may have controlled the emplacement of the kimberlite pipes in Lac de Gras region of NWT. The MT responses sampling 50–150 km depths show a maximum spatial correlation with the diamond field and the resistivity models show a spatially confined anomalous conductor (<30 Ωm) at depths of 80–120 km in the upper mantle beneath the Lac de Gras region. The crust and upper mantle above the conductor are more heterogeneous here than in other regions of the Slave Craton possibly indicative of disruption during kimberlite emplacement (Jones et al., 2000). It cannot be emphasised enough that the results of these recent MT surveys over the Eocene kimberlite field in Lac de Gras area (Jones et al., 2000) are exciting and hold good promise for regional GEM mapping of prospective kimberlite fields in comparable terrains.

9. Discussions and Conclusion

New advances in digital technology and concurrent developments in multi-dimensional numerical modelling and instrumentation have led to improved GEM data acquisition and interpretation techniques as well as brought these popular methods within range of their theoretical resolving capability in natural resources investigations. It is now possible to collect field data sets of the highest achievable quality and invert them to produce geologically significant resistivity images of prospective geological targets. However, much work needs to be done in the areas of efficient 3D surveying and bulk data inversion, and integrating resistivity, geological and geochemcial data. In this paper, an attempt has been made to provide an overview of the problems and prospects of GEM exploration methods. Effort was also made to show the possible correspondence between geological processes and geoelectromagnetic signatures of economic subsurface targets. It is stressed that most resource targets and their controlling structures are associated with clays and hydrothermal features. Hydrated clay minerals are an important source of conductivity anomalies in GEM prospecting. They provide targets for GEM exploration for geothermal resources and the epithermal gold deposits (which are essentially fossil geothermal systems) and which also form the uppermost (epithermal) parts of porphyry copper deposits. The presence of clays is often the determining factor in the hydraulic conductivity of many groundwater aquifers. It is thus logical that clays and hydrothermal processes may be used to provide a unifying framework for GEM exploration as recognised in this paper. While it is desirable to develop a somewhat consistent investigative approach, it is mooted that no single model may suffice for each of the exploration problems discussed above. A flexible approach is desirable in many situations and a detailed 3D conductivity map is often of considerable value in itself, irrespective of whether the resource target is directly or indirectly detected.

Acknowledgements

The constructive comments from the reviewers, especially T. Grant Caldwell, are gratefully acknowledged. They helped improve the quality of this paper.

References

Al Azry, H., Webster, S.S., Isles, D., Al Zubaidy H., and Witham, W.: 1993, Exploration for Cyprus style copper deposits, Sultanate of Oman: A case study, *Explor. Geophys.* **24**, 315–322.

Ander, M., Goss, R., and Strangway, D.W.: 1984, A detailed magnetotelluric/audiomagnetotellurics study of the Jemez Volcanic Zone, New Mexico, *J. Geophys. Res.* **89**, 3335–3353.

Annan, A.P., Smith, R.S., Lemieux, J., O'Connell, M.D., and Pedersen, R.N.: 1996, Resistive-limit, time-domain AEM apparent conductivity, *Geophysics* **61**, 93–99.

Archie, G.E.: 1942, The electrical resistivity log as an aid in determining some reservoir characteristics, *Amer. Inst. Mining Metall. Eng. Trans.* **146**, 54–62.

Aristodemou, E. and Thomas-Betts, A.: 2000, DC resistivity and induced polarisation investigations at a waste disposal site and its environments, *J. Applied Geophys.* **44**, 275–302.

Atekwana, E.A., Sauck, W.A., and Werkema, D.A.: 2000, Investigations of geoelectrical signatures at a hydrocarbon contaminated site, *J. Applied Geophys.* **44**, 167–180.

Atkinson, W.J.: 1986, Diamond exploration philosophy, practice and promises: A review, in J. Ross (ed.), *Kimberlites and Related Rocks*, Vol. 2, Proc. 4th Int. Kimberlite Conf., Geol. Soc. Austral., Spec. Publ., Vol. 14, pp. 1075–1107.

Bai, D., Liao, Z., Zhao, G., and Wang, X.: 1994, The inference of magmatic heat source beneath the Rehai (Hot Sea) Field of Tengchong from the results of magnetotelluric sounding, *Chinese Science Bulletin* **39**, 572–577.

Bai, D., Meju, M.A., and Liao, Z.: 2001, Magnetotelluric images of deep crustal structure of the Rehai geothermal field near Tengchong, southern China, *Geophys. J. Int.* **147**, 677–687.

Bardet, M.G.: 1964, Controle geotechtonique de la repartition des venues diamantiferes dans le monde: role structural des platesformes et des fractures tres fondes, *Chronique Mine Rech. Min.* **328/329**, 67–89.

Barker, R.D.: 1981, The offset system of electrical resistivity sounding and its use with a multi-core cable, *Geophys. Prosp.* **29**, 128–143.

Barnett, C.T.: 1984, Simple inversion of time-domain electromagnetic data, *Geophysics* **49**, 925–933.

Beamish, D. and Travassos, J.M.: 1992a, Magnetotelluric imaging of basalt-covered sediments, *First Break* **10**, 345–357.

Beamish, D. and Travassos, J.M.: 1992b, A study of static shift removal from magnetotelluric data, *J. Applied Geophys.* **29**, 157–178.

Beeson, S. and Jones, C.R.C.: 1988, The combined EMT/VES geophysical method for siting boreholes, *Ground Water* **26**, 54–63.

Beke, B., Csorgei, J., Formanne-Gulyas, C., Lada, F., Nagy, T., and Nagy, Z.: 1991, Non-seismic methods used to delineate hydrocarbon deposits in Hungary, Paper presented at AAPG Internat. Conference and Exhibition, September 29–October 2.

Berdichevsky, M.N.: 1994, Role of geoelectric methods in hydrocarbon and deep structural investigations in Russia, *Geophys. Trans. (Hung.)* **39**, 3–33.

Berkman, E., Orange, A., and Smith, R.D.: 1983, Seismics and magnetotellurics combined: A case history of the South Clay Basin Prospect, *53rd Annual Internat. SEG Meeting*, Extended Abstracts, pp. 65–67.

Berktold, A.: 1983, Electromagnetic studies in geothermal regions, *Geophys. Surv.* **6**, 173–200.

Berktold, A., Haenel, R., and Wohlenberg, J.: 1982, A model of the Urach geothermal anomaly as derived from geophysical investigations, in R. Haenel (ed.), *The Urach Geothermal Project*, E. Schweizerbart'sche Verlagsbuchhandlung, pp. 401–412.

Beres, M. and Haeni, F.P.: 1991, Application of ground-penetrating-radar methods in hydrogeologic studies, *Ground Water* **29**, 375–386.

Bertin, J., Farabolini, W., Gole, R., and Roudot, M.: 1983, The transient method applied to hydrocarbon exploration: A statistical study of its results (abstract), *Explor. Geophys.* **14**, 189–190.

Bibby, H.M., Caldwell, T.G., Davey, F.J., and Webb, T.H.: 1995, Geophysical evidence on the structure of the Taupo Vocanic Zone and its hydrothermal circulation, *J. Volcan. Geotherm. Res.* **68**, 29–58.

Billings, A.J. and Thomas, J.H.: 1990, The use and limitations of non-seismic geophysics in the Papuan Thrust Belt, *Proceedings of the First PNG Petroleum Convention, Port Moresby*, 12–14 February 1990, pp. 51–62.

Bishop, J.R. and Lewis, R.J.G.: 1992, Geophysical signatures of Australian volcanic- hosted massive sulfide deposits, *Econ. Geol.* **87**, 913–930.

Boyd, G. and Frankcombe, K.F.: 1994, Geophysical responses over the Scuddles VMS deposit, in *Geophysical Signatures of Western Australian Mineral Deposits*, Geology and Geophysics Dept. (Key Centre) & UWA Extension, The Univ. Western Australia, Publication No. 26, pp. 133–144.

Boyle, R.W.: 1984, Gold deposits: Their geology, geochemistry and origin, in R.P. Foster (ed.), *Gold'82: The Geology, Geochemistry and Genesis of Gold Deposits*,Proc. Symp. Gold'82, University of Zimbabwe, pp. 183–189.

Bowker, A.M. and Hill, I.A.: 1987, Geophysical study of Kerry Road orebody, Gairloch, *Trans. Inst. Min. Metall.* **96**(B), 213–220.

Bromley, C.: 1993, Tensor CSAMT study of the fault zone between Waikite and Te Kopia geothermal fields, *J. Geomag. Geoelectr.* **45**, 887–896.

Burgett, W.A., Orange, A., and Sigal, R.F.: 1992, *Integration of MT, Seismic, Gravity and Magetic Data for Reconnaissance of the Columbian Amazon*, 54th EAEG Meeting, Paris, Technical Abstracts, pp. 428–429.

Burley, A.J. and Greenwood, P.G.: 1972, Geophysical surveys over kimberlite pipes in Lesotho, Applied Geophysics Unit, Institute of Geological Sciences, Geophysical Division Report, London, pp. 1–32.

Buselli, G., McCracken, K.G., and Thorburn, M.: 1986, Transient electromagnetic measurements of the Teutonic Bore orebody, *Geophysics* **51**, 957–963.

Buselli, G. Barber, C., and Zerilli, A.: 1988, The mapping of groundwater contamination with TEM and DC methods, *Explor. Geophys.* **19**, 240–248.

Buselli, G., Barber, C., Davis, G.B., and Salama, R.B.: 1990, Detection of groundwater contamination near waste disposal sites with transient electromagnetic and electrical methods, in S.H. Ward (ed.), *Geotechnical and Environmental Geophysics*, Vol. II, SEG Publ. Tulsa, OK, pp. 27–39.

Buselli, G., Davis, G.B., Barber, C., Height, M.I., and Howard, S.H.D.: 1992, The application of electromagnetic and electrical methods to groundwater pollution problems in urban environments, *Explor. Geophys.* **23**, 543–556.

Carlson, N.R., Hughes, L.J., and Zonge, K.L.: 1981, Hydrocarbon exploration using induced polarization, apparent resistivity and electromagnetic scattering, Technical Papers, 51st Annual Internat. SEG Meeting and Exposition, Vol. 3, pp. 1339–1358.

Carrasquilla, A., Posani, M.J., and Tavares, A.: 1997, Prospeccao de agues subterraneas no Alto Xingu-Para com metodos geofisicos eletromagneticos, *Revista Brasileira de Geociencias* **27**, 221–228.

Christensen, N.B.: 1995, 1D imaging of central loop transient electromagnetic soundings, *J. Env. Eng. Geophys.* **0**, 53–66.

Christensen, N.B. and Soresen, K.I.: 1994, Integrated use of electromagnetic methods for hydrogeological investigations, in *Proc. EEGS Symposium on Applications of Geophysics to Engineering & Environmental Problems*, Boston, March 1994, pp. 163–176.

Christopherson, K.R.: 1991, Applications of magnetotellurics to petroleum exploration in Papua new Guinea: A model for frontier areas, *The Leading Edge* **10**(4), 21–27.

Clarke, L.A.: 1971, Volacnogenic ores: Comparison of cupriferous pyrite deposits of Cyprus and Japanese Kuroko deposits, in Y. Takeuchi (ed.), *Proc. IMA-IAGOD Meetings '70*, AIGOD volume, (Soc. of Mining Geologists of Japan, Tokyo), Spec. Issue No. 3, pp. 206–215.

Constable, S.C., Parker, R.L., and Constable, C.G.: 1987, Occam's inversion: A practical algorithm for generating smooth models from electromagnetic sounding data, *Geophysics* **52**, 289–300.

Constable, S.C., Orange, A., Hoversten, G.M., and Morrison, H.F.: 1998, Marine magnetotellurics for petroleum exploration, Part II: A sea-floor equipment system, *Geophysics* **63**, 816–825.

Cooper, N.J. and Swift, R.: 1994, The application of TEM to Cyprus-type massive sulphide exploration in Cyprus, *Geophysics,* **59**, 202–214.

Corry, C.E.: 1985, Spontaneous polarization associated with porphyry sulphide systems, *Geophysics* **50**, 1020–1034.

Cox, S.F., Wall, V.J., Etheridge, M.A., and Potter, T.F.: 1991, Deformational and metamorphic processes in the formation of mesothermal gold deposits – examples from the Lachlan Fold Belt in central Victoria, Australia, *Ore Geology Review* **6**, 391–423.

Cox, S.F., Sun, S.-S., Etheridge, M.A., Wall, V.J., and Potter, T.F.: 1995, Structural and geochemical controls on the development of turbidite-hosted gold-quartz vein deposits, Wattle Gully Mine, central Victoria, Australia, *Econ. Geol.* **90**, 1722–1746.

da Costa, A.J.M.: 1989, Palmietfontein kimberlite pipe, South Africa – A case study, *Geophysics* **54**, 689–700.

Dawson, J.B.: 1971, Advances in kimberlite geology, *Earth-Sci. Rev.* **7**,187–214.

Dawson, J.B.: 1968, Recent researches on kimberlite and diamond geology, *Econ. Geol.* **63**, 504–511.

DeGroot-Hedlin, C. and Constable, S.: 1990, Occam's inversion to generate smooth two-dimensional models from magnetotelluric data, *Geophysics* **55**, 1613–1624.

den Boer, E., Eikelboom, J., van Driel, P., and Watts, D.: 2000, Resistivity imaging of shallow salt with magnetotellurics as an aid to prestack depth migration, *First Break* **18**(1), 19–26.

Deng, D. and Ou, Q.: 1995, Geophysical prospecting for petroleum in marine carbonate areas of the lower Yagtze region of southern China, *Geophysics* **60**, 1306–1312.

Domenico, P.A. and Schwartz, F.W.: 1990, *Physical and Chemical Hydrogeology*. John Wiley and Sons, New York.

Donaldson, I.G.: 1962, Temperature gradients in the upper layers of the Earth's crust due to convective water flows, *J. Geophys. Res.* **67**, 3449–3459.

Donaldson, I.G.: 1970, The simulation of geothermal systems with a simple convective model, *Geothermics*, (Spec. Issue 2), **2**(1), 649–654.

Donovan, T.J.: 1974, Petroleum microseepage at Cement, Oklahoma – evidence and mechanism, *Amer. Assoc. Petrol. Geol. Bull.* **58**, 429–446.

Donovan, T.J., Roberts, A.A., and Dalziel, M.C.: 1981, Epigenetic zoning in surface and near-surface rocks resulting from seepage-induced, redox gradients, Velma Oil Field, Oklahoma: A synopsis, *The Shale Shaker* **32**, 1–7.

Doyle, H.: 1996, Geophysical exploration for gold – a review, *Geophysics* **55**, 134–146.

Duckworth, K.: 1987, Lithologically discordant resistivity and IP anomalies associated with hydrocarbons in the Rocky Mountain foothills of Alberta, Canada, *Explor. Geophys.* **18**, 31–34.

Druskin, V.L. and Knizhnerman, L.A.: 1988, A spectral semi-discrete method for the numerical solution of 3-D nonstationary problems in electrical prospecting, *Phys. Solid Earth* **24**, 63–74.

Druskin, V.L., Knizhnerman, L.A., and Lee, P.: 1999, New spectral Lanczos decomposition method for induction modelling in arbitrary 3-D geometry, *Geophysics* **64**, 701–706.

Eadie, T.: 1981, Detection of hydrocarbon accumulations by surface electrical methods, *Research in Applied Geophysics*, Vol. 15, University of Toronto.

Ebraheem, M.W., Bayless, E.R., and Krothe, N.C.: 1990, A study of acid mine drainage using earth resistivity measurements, *Ground Water* **28**, 361–368.

Edet, A.E.: 1990, Application of photogeologic and electromagnetic techniques to groundwater exploration in Northwestern Nigeria, *J. African Earth Sciences* **11**, 321–328.

Eisenlohr, B.N., Groves, D., and Partington, G.A.: 1989, Crustal-scale shear zones and their significance to Archean gold mineralization in Western Australia, *Mineral Deposits* **24**, 1–8.

Ellis, R.G. and Oldenburg, D.W.: 1994, The pole-pole 3-D dc-resistivity inverse problem: A conjugate gradient approach, *Geophys. J. Int.* **119**, 187–194.

Emerson, D.W. (ed.): 1980, The geophysics of the Elura orebody, Cobar, New South Wales, *Bull. Austral. Soc. Explor. Geophys.* **11**, 143–347.

Fesq, H.W., Kable, E.J.D., and Gurney, J.J.: 1975, Aspects of the geochemistry of kimberlites from the Premier mine, and other selected South Africa occurrences with particular reference to the rare earth elements, *Phys. Chem. Earth* **9**, 687–707.

Fitterman, D.V. and Neev, D.K.: 1985, Transient sounding investigation of the Newberry Volcano, Oregon, Geothermal Resources Council, Transactions, Vol. 9, Part II, pp. 407–410.

Fitterman, D.V. and Stewart, M.T.: 1986, Transient electromagnetic sounding for groundwater, *Geophysics* **51**, 995–1005.

Fokin, A.F.: 1971, *Method perekhodnikh protsessov pri poickakh mestorozdeniy sulfidnikh rud*, Nedra, Leningrad.

Fontes, S.L., Meju, M.A., Lima, J.P.R., Carvalho, R.M., La Terra, E.F., Germano, C.R., and Metelo, M.: 1997, Geophysical investigation of major structural controls on groundwater distribution, north of São Raimundo Nonato, Piaui State, *5th Internat. Congr. Brazil*. Geophys. Soc., Expanded Abstracts, pp. 766–769.

Fouques, J.P., Fowler, M., Knipping, H.D., and Schimann, K.: 1986, The Cigar Lake Uranium deposit: Discovery and general characteristics, *Can. Inst. Min. Metall. Bull.* **79**(886), 70–86.

Freeze, R.A. and Cherry, J.A.: 1979, *Groundwater*, Prentice-Hall Inc., Englewood Cliffs, New Jersey, 604 pp.

Fritz, F.P. and Sheehan, G.M.: 1984, The geophysical signature of the Teutonic Bore Cu-Zn-Ag massive sulphide deposit, *Explor. Geophys.* **15**, 127–142.

Frohlich, R.K., Fisher, J.J., and Summerly, E.: 1996, Electric-hydraulic conductivity correlation in fractured crystalline bedrock: Central Landfill, Rhode Island, USA, *J. Applied Geophys.* **35**, 249–259.

Furlong, K.P. and Fountain, D.M.: 1986, Lithospheric evolution with underplating: Thermal considerations and seismic-petrologic consequences, *J. Geophys. Res.* **91**, 8285–8294.

Galanopoulos, D., Hutton, V.R.S., and Dawes, G.J.K.: 1991, The Milos geothermal field: Modelling and interpretation of electromagnetic induction studies, *Phys. Earth Plan. Int.* **66**, 76–91.

Gaucher, E.: 1983, Estimation of sulphide content of a potential orebody from surface observations and its role in optimising exploration programmes, in A.A. Fitch (ed.), *Developments in Geophysical Exploration Methods*, Applied Sci. Publ. Ltd., pp. 1–37.

Gerryts, E.: 1967, Diamond prospecting by geophysical methods – a review of current practice, in L.W. Morley (ed.), *Mining and Groundwater Geophysics*, Geological Survey of Canada, pp. 439–446.

Goebuchi, T., Shima, H., and Hara, T.: 1988, A new resistivity meter, featuring fully automatic measurement and a built in analysis program, *Explor. Geophys.* **19**, 276–280.

Goff, F.E. and Gardner, J.N.: 1994, Evolution of a mineralized geothermal system, Valles Caldera, New Mexico, *Econ. Geol.* **89**, 1803–1832.

Goldman, M., Du Plooy, D., and Eckard, M.: 1994, On reducing ambiguity in the interpretation of transient electromagnetic sounding data, *Geophys. Prosp.* **42**, 3–25.

Goldman, M., Gilad, D., Ronen, A., and Melloul, A.: 1991, Mapping of seawater intrusion into the coastal aquifer of Isreal by the transient electromagnetic method, *Geoexploration* **28**, 153–174.

Griffiths, D.H., Turnbull, J., and Olayinka, A.I.: 1990, Two-dimensional resistivity mapping with a computer-controlled array, *First Break* **8**, 121–129.

Guilbert, J.M. and Lowell, J.D.: 1974, Variations in zoning patterns in porphyry ore deposits, *CIM Bull.* **67**, 99–109.

Gunn, P.J. and Chisholm, J.: 1984, Non-conductive volcanogenic massive sulphide mineralisation in the Pilbara area of Western Australia, *Explor. Geophys.* **15**, 143–153.

Haak, V., Ritter, O., and Ritter, P.: 1989, Mapping the geothermal anomaly on the island of Milos by magnetotellurics, *Geothermics* **18**, 533–546.

Halvorsen, M.O., Kingman, J.E.E. and Corbet, D.: 1988, Advances in IP technology, telluric cancellation and high spatial resolution arrays, in G.D. Garland (ed.), *Exploration '87 Symposium*, Toronto, Geol. Survey of Canada Publication.

Haren, R.J.: 1983, Electrical petroliferous exploration down under, *51st Annual Internat. SEG Meeting and Exposition*, Expanded Abstracts, pp. 1319–1338.

Haren, R.J. and Reeves, J.A.: 1983, Electrical petroliferous exploration in Australia, *Explor. Geophys.* **14**, 185–189.

Haren, R.J.: 1984, An evaluation of electrical methods applied to petroleum exploration in Australia, *Explor. Geophys.* **15**, 197–212.

Hawkins, T.R.W. and Chadha, D.S.: 1990, Locating the Sherwood Sandstone aquifer with the aid of resistivity surveying in the Vale of York, *Quart. J. Eng. Geol.* **23**, 229–241.

Hawthorne, J.B.: 1975, Model of kimberlite pipe, *Phys. Chem. Earth* **9**, 1–16.

Hazell, J.R.T., Cratchley, C.R., and Preston, A.M.: 1988, The location of aquifers in crystalline rocks and alluvium in Northern Nigeria using combined electromagnetic and resistivity techniques, *Quart. J. Eng. Geol.* **21**, 159–175.

Hersir, G.P., Bjornsson, A., and Pedersen, L.B.: 1984, Magnetotelluric survey across the active spreading zone on Southwest Iceland, *J. Volcan. Geotherm. Res.* **20**, 253–265.

Hollister, V.F., Potter, R.R., and Barker, A.L.: 1974, Porphyry-type deposits of the Appalachian orogen, *Econ. Geol.* **69**, 618–630.

Holyk, W.: 1956, Mineralization and structural relations in Northern New Brunswick, *Northern Miner* **41**(49), 27.

Hone, I.G.: 1980, Geoelectric properties of the Elura prospect, Cobar, NSW, *Explor. Geophys.* **11**, 178–182.

Hoover, D.B. and Heran, W.D.: 1993, Geophysics in gold exploration: Application to greenstone belt gold deposits, *3rd Internat. Congr. Brazil*. Geophys. Soc., Expanded Abstracts, pp. 451–454.

Hopgood, J.D. and Hungerford, N.: 1994, Geophysical case history of the discovery of the Aguas Tenidas East massive sulphide deposit, SW Spain, *Explor. Geophys.* **25**, 1–17.

Hoversten, G.M.: 1992, Papua New Guinea MT: Looking where seismic is blind, *54th EAEG Meeting, Paris*, Technical Abstracts, pp. 430–431.

Hoversten, G.M., Morrison, H.F., and Constable, S.C.: 1998, Marine magnetotellurics for petroleum exploration, Part II: Numerical analysis of subsalt resolution, *Geophysics* **63**, 826–840.

Hughes, L.J., Nosal, E.A., Carlson, N.R., and Zonge, K.L.: 1982, Distinguishing well casing from structural effects in electrical anomalies over hydrocarbons: A case history, *52nd Annual Internat. SEG Meeting and Exposition*, Extended Abstracts, pp. 443–445.

Hughes, L.J.: 1983, *Case Histories of an Electromagnetic Method for Petroleum Exploration*, Zonge Engineering and Research Organization, Inc, Tucson.

Hughes, L.J., Carlson, N.R., and Ostrander, A.G.: 1984a. Applications of CSAMT in mapping structure and alteration associated with petroleum, *54th Annual Internat. SEG Meeting and Exposition*, Expanded Abstracts, pp. 102–104.

Hughes, L.J., Ostrander, A.G., Reed, E.V., and Zonge, K.L.: 1984b, Structure and alteration mapping with CSAMT, CR, and TEM in Australian basins: A feasibility study, *Proceedings of 2nd Australian Petroleum Geophysics Symposium*, pp. 162–178.

Hughes, L.J., Carlson, N.R., and Zonge, K.L.: 1985a, Applications of electrical techniques in an integrated petroleum exploration program, Paper presented at the China Petroleum Society/SEG Joint Meeting on Seismic Exploration, Beijing, PRC. April 16, 1985.

Hughes, L.J., Zonge, K.L., and Carlson, N.R.: 1985b, The application of electrical techniques in mapping hydrocarbon-related alteration, in M.J. Davidson (ed.), *Unconventional Methods in Exploration for Petroleum and Natural Gas IV*, Southern Methodist University Press, Dallas.

Hutton, V.R.S., Dawes, G.J.K., Devlin, T., and Roberts, R.: 1985, A broadband tensorial magnetotelluric study in the Travale geothermal Field, *Geothermics* **14**, 645–652.

Ingham, M.R.: 1991, Electrical conductivity structure of the Broadlands–Ohaaki geothermal field, New Zealand, *Phys. Earth Plan. Int.* **66**, 62–75.

Irvine, R.J. and Smith, M.J.: 1990, Geophysical exploration for epithermal gold deposits, *J. Geochem. Explor.* **36**, 375–412.

Isacks, B., Oliver, J., and Sykes, L.R.: 1968, Seismology and the new global tectonics, *J. Geophys. Res.* **73**, 5855–5900.

Isles, D.J. and Cooke, A.C.: 1992, Archean gold deposits and Proterozoic dolerite dykes – a symbiotic relationship, *Australian Soc. Explor. Geophysics Preview* **36**, 5–7.

Jenke, G.: 1983, The role of geophysics in the discovery of the Ellendale and Fitzroy kimberlites, *3rd Biennial Conf., Austral., Soc. Explor. Geophys.*, Abstracts, pp. 66–72.

Jiracek, G.R., Kinn, C.R., Scott, C.L., Curran, S.A., and Kuykendall, M.G.: 1993, Magnetotelluric mapping of upper crustal isotherms beneath the Valles Caldera hydrothermal system, *EOS*, Trans. Amer. Geophys. Union, Fall Supplement, p. 229.

Johnson, I.M. and Fugita, M.: 1985, The Hishikari gold deposit: An airborne E.M. discovery, *Can. Inst. Min. Bull.* **78**, 61–66.

Jones, A.G.: 1988, Static shift of magnetotelluric data and its removal in a sedimentary basin environment, *Geophysics* **53**, 967–978.

Jones, A.G., Eaton, D.W., White, D., Bostock, M., Mareschal, M., and Cassidy, J.: 1996, Geophysical measurements for lithospheric parameters, in A.N. LeCheminant, R.N.W. DiLabio, and K.A. Richardson (eds.), *Searching for Diamonds in Canada*, Geol. Surv. Canada, Open File 3228, pp. 243–250.

Jones, A.G., Ferguson, I.J., Chave, A.D., Evans, R.L., and McNeice, G.W.: 2000, The electric lithosphere of the Slave Craton. Abstracts of the 15th EM Inducton Workshop, Cabo Frio, Brazil, August 19–26, 2000, pp. 27–28.

Jones, M.: 1985, The weathered zone aquifers of the Basement Complex areas of Africa, *Quart. J. Eng. Geol.* **18**, 35–46.

Karus, E.W., Kuznetsov, O.L., Kirichek, M.A., and Petukhov, A.V.: 1985, Direct prospecting of gas-oil deposits including complex of geophysical and geochemical techniques, *Proc. 30th Internat. Geophysical Symposium*, Moscow, Part I, pp. 23–28.

Kamara, A.Y.S., 1981, Review: Geophysical methods for kimberlite prospecting, *Explor. Geophys.* **12**, 43–51.

Kirkley, M.B., Gurney, J.J., and Levinson, A.A.: 1991, Age, origin, and emplacement of diamonds: Scientific advances in the last decade, *Gems and Gemology* **27**(1), 2–25.

Klein, J.D.: 1983, Spectral induced polarization survey, David Field, Alberta, Paper presented at the 36th Annual Meeting of the Midwest Society of Exploration Geophysicists, Denver, CO.

Lane, J.W., Jr., Haeni, F.P., and Watson, W.M.: 1995, Use of a square-array direct-current resistivity method to detect fractures in crystalline basement in New Hampshire, *Ground Water* **33**, 476–485.

Lattiman, L.A. and Parizek, R.R.: 1964, Relationship between fracture traces and the occurrence of ground water in carbonate rocks, *J. Hydrol.* **2**, 73–91.

Lebel, A. and Fallon, G.N.: 1994, Geophysical signature of the Mons Cupri VMS deposit, Western Australia, in *Geophysical Signatures of Western Australian Mineral Deposits*, Geology and Geophysics Dept. (Key Centre) & UWA Extension, The Univ. Western Australia, Publication No. 26, pp. 145–154.

Leca, X.: 1990, Discovery of concealed massive sulphide bodies at Neves-Corvo, southern Portugal, *Trans. Inst. Min. Metall.* **99**(B), 139–152.

Lindqvist, J.G.: 1987, Use of electromagnetic techniques for groundwater exploration in Africa, *Geophysics* **52**, 456–458.

Litinskii, V.A.: 1963, Measurement of magnetic susceptibility in prospecting for kimberlite pipes, *The Mining Magazine* **109**, 137–146.

Loke, M.H. and Barker, R.D.: 1996, Rapid least-squares inversion of apparent resistivity pseudosections by a quasi-Newton method, *Geophys. Prosp.* **44**, 131–152.

Lowell, J.D. and Guilbert, J.M.: 1970, Lateral and vertical alteration-mineralization zoning in porphyry copper deposits, *Econ. Geol.* **65**, 373–408.

Mackie, R.L.: 1996, Two dimensional inversion of magnetotelluric data: Software, Internet site: MTNET "http://nazca.cg.emr.ca/mtnet/mtnet.html".

Mackie, R.L. and Madden, T.R.: 1993, Three-dimensional magnetotelluric inversion using conjugate gradients, *Geophys. J. Int.* **115**, 215–229.

Macnae, J.C.: 1979, Kimberlites and exploration geophysics, *Geophysics* **44**, 1395–1416.

Macnae, J.C.: 1984, Survey design for multicomponent electromagnetic systems, *Geophysics* **49**, 265–273.

Maliotis, G. and Khan, M.A.: 1980, The applicability of the induced polarization method of geophysical exploration in the search for sulphide mineralization within the Troodos ophiolite complex of Cyprus, *Proc. International Ophiolite Symposium Cyprus 1979*, Cyprus Geological Survey Department, pp. 129–138.

Martinez-Garcia, M.: 1992, Electromagnetic induction studies in geothermal fields and volcanic belts, *Surveys in Geophysics* **13**, 409–434.

Mathers, S. and Zalasiewicz, J.: 1994, A guide to the sedimentology of unconsolidated sedimentary aquifers (UNSAs), British Geological Survey Technical Report WC/93/32.

McKenzie, D.P.: 1978, Some remarks on the development of sedimentary basins, *Earth and Plan. Sci. Lett.* **40**, 25–32.

McNeill, J.D.: 1987, Advances in electromagnetic methods for groundwater studies, *Proceedings of Exploration '87: Applications of Geophysics and Geochemistry*, Geol. Survey of Canada Special Publication, pp. 678–702.

Meekes, J.A.C., and van Will, M.F.P.: 1991, Comparison of seismic reflection and combined TEM/VES methods for hydrogeological mapping, *First Break* **9**, 543–551.

Meju, M.A.: 1994, Joint TEM and AMT surveys: Cost-effective exploration in frontier basin regions, *Proc. 10th Petroleum Congress and Exhibition of Turkey*, April 11–15, 1994, Ankara, Geophysics volume, pp. 157–176.

Meju, M.A.: 1995, Simple effective resistivity-depth transformations for infield or real-time data processing, *Comp. & Geosci.* **21**, 985–992.

Meju, M.A.: 1996a, Joint inversion of TEM and distorted MT soundings: Some effective practical considerations, *Geophysics* **61**, 56–65.

Meju, M.A.: 1996b, Geoelectromagnetics, geology and the environment: Understanding electrical images of the subsurface, Presented at the 20th Ann. United Kingdom Geophysical Assembly, Newcastle-upon-Tyne, April 1996.

Meju, M.A.: 1998, A simple method of transient electromagnetic data analysis, *Geophysics* **63**, 405–410.

Meju, M.A., 2000a, Environmental geophysics: the tasks ahead, *J. Applied Geophys.* **44**, 63–65.

Meju, M.A.: 2000b, Geoelectrical investigation of old/abandoned, covered landfill sites in urban areas: Model development with a genetic diagnosis approach, *J. Applied Geophys.* **44**, 115–166.

Meju, M.A. and Montague, M.: 1995, Basis for a flexible low-cost automated resistivity data acquisition and analysis system. *Comp. & Geosci.* **21**, 993–999.

Meju, M.A., Fontes, S.L., Oliveira, M.F.B., Lima, J.P.R., Ulugergerli, E.U., and Carrasquilla, A.A.: 1999, Regional aquifer mapping using combined VES-TEM-AMT/EMAP methods in the semiarid eastern margin of Parnaiba Basin, Brazil, *Geophysics* **64**, 337–356.

Meju, M.A., Fenning, P.J., and Hawkins, T.R.W.: 2000, Evaluation of small-loop transient electromagnetic soundings to locate the Sherwood Sandstone aquifer and confining formations at well sites in the Vale of York, England, *J. Applied Geophys.* **44**, 217–236.

Meju, M.A., Fontes, S.L., Ulugergerli, E.U., La Terra, E.F., Germano, C.R., and Carvalho, R.M.: 2001, A joint TEM-HLEM geophysical approach to borehole siting in deeply weathered granitic terrains, *Ground Water* **39**, 554–567.

Melo, G. Jr.: 1990, Geochemical investigations of the hydrothermal alteration zone surrounding the greenstone-hosted Fazenda Brasileiro gold deposit, Bahia, Brazil, Unpublished Ph.D thesis, Colorado School of Mines, 547 pp.

Moskowitz, B. and Norton, D.: 1977, A preliminary analysis of intrinsic fluid and rock resisitivity in active hydrothermal systems, *J. Geophys. Res.* **82**, 5787–5795.

Muffler, L.J.P.: 1975, Tectonic and hydrologic control of the nature and distribution of geothermal resources, in *Proc. 2nd United Nations Symposium on the Development and Use of Geothermal Resources*, San Francisco, 20–29 May 1975, pp. 499–508.

Mwenifumbo, C.J.: 1993, Borehole geophysics in environmental applications, *CIM Bulletin* **86**(966), 43-49.

Nekut, A.G. and Spies, B.R.: 1989, Petroleum exploration using controlled-source electromagnetic methods, *Proc. Inst. Electr. Electron. Eng.* **77**, 338–362.

Newman, G.A., Anderson, W.L., and Hohmann, G.W.: 1987, Interpretation of transient electromagnetic soundings over three-dimensional structures for the central-loop configuration, Geophys, *J. R. Astr. Soc.* **89**, 889–914.

Newman, G.A., Hohmann, G.W., and Anderson, W.L.: 1986, Transient electromagnetic response of a three-dimensional body in a layered-earth, *Geophysics* **51**, 1608–1627.

Newman, G.A., Wannamaker, P.E., and Hohmann, G.W.: 1985, On the detetectability of crustal magma chambers using the magnetotelluric method, *Geophysics* **50**, 1136–1143.

Nichols, A.E., Morrison, H.F., and Lee, S.: 1994, Controlled source magnetotellurics for groundwater, *64th Annual Internat. SEG Meeting and Exposition*, Extended Abstracts.

Nie X., Zhou, A., Yang, G., Zhang, Sa., Jian, A., and Zhang, Sh.: 1989, Exploration for oil and gas with IP method – A discussion on the results and the anomaly model, in J. Zhoa, (ed.), *An Overview of Exploration Geophysics in China - 1988*, Society of Exploration Geophysicists Series 3, pp. 273–301.

Obukhov, G.G., Chernjavsky, G.A., and Jakovlev, J.A.: 1983, *Magnetotelluric Prospecting in Oil Potential Regions of the USSR*, Moscow, Nedra (in Russian).

Oehler, D.Z. and Sternberg, B.K.: 1984, Seepage-induced anomalies, "false" anomalies, and implications for electrical prospecting, *Amer. Assoc. Petrol. Geol. Bull.* **68**, 1121–1145.

Oehler, D.Z. and Sternberg, B.K.: 1982, Induced polarization for hydrocarbon exploration: Geochemical/geological interpretation, *52nd Annual Internat. SEG Meeting and Exposition*, Extended Abstracts, pp. 445–448.

Ogilvy, R.D.: 1983, Application of down-hole pulse electromagnetic surveys for off-hole mineral exploration, *Trans. Inst. Min. Metall.* **92**(B), 148–153.

Ogilvy, R.D.: 1986, Transient electromagnetic studies over a Cu-Zn-Au mineral prospect, Gairloch, Scotland, *J. Geol. Soc. Lond.* **143**, 551–568.

Olayinka, A.I. and Barker, R.D.: 1990, Borehole siting in crystalline basement areas of Nigeria with a micro-processor controlled resistivity traversing system, *Ground Water* **28**, 178–183.

Oldenburg, D.W. and Li, Y.: 1994, Inversion of induced polarisation data, *Geophysics* **59**, 1327–1341.

Olhoeft, G.: 1981, Electrical properties of rocks, in Y.S. Touloukian and C.Y. Ho (eds.), *Physical Properties of Rrocks and Minerals*, McGraw-Hill/CINDAS data series on material properties, II-2, pp. 257–297.

Oliveira, V.M.J., Matos, J.X., Bengala, J.A.M., Silva, M.C.N., Sousa, P.O., and Tores, L.M.M.: 1993, Lagoa Salgada um novo deposito na faixa piritosa iberica Bacia terciaria do Sado, *Estudos, Notas e Trabalhos, Inst. Geologico e Mineiro* **35**, 55–89.

Orange, A.S.: 1989, Magnetotelluric exploration for hydrocarbons, *Proc. Inst. Electr. Electron. Eng.* **77**, 287–317.

Ostrander, A.G., Carlson, N.C., and Zonge, K.L.: 1983, Further evidence of electrical anomalies over hydrocarbon accumulations using CSAMT, *53rd Annual Internat. SEG Meeting and Exposition, Las Vegas*, Expanded Abstracts, pp. 60–63.

Palacky, G.J.: 1987, Resistivity characteristics of geological targets, in M.N. Nabighian (ed.), *Electromagnetic Methods in Applied Geophysics - Theory*, Vol. 1, pp. 53–129, Soc. Expl. Geophys., Investigations in Geophysics Series, No. 3.

Palacky, G.J., Ritsema, I.L., and De Jong, S.J.: 1981, Electromagnetic prospecting for groundwater in precambrian terrains in the Republic of Upper Volta, *Geophys. Prosp.* **29**, 932–955.

Panissod, C., Dabas, M., Hesse, A., Jolivet, A., Tabbagh, J., and Tabbagh, A.: 1998, Recent developments in shallow-depth electrical and electrostatic prospecting using mobile arrays, *Geophysics* **63**, 1542–1550.

Parra, J.O.: 1984, Effects of pipelines on spectral induced polarisation surveys, *Geophysics* **49**, 1979–1992.

Pellerin, L., Johnston, J.M., and Hohmann, G.W.: 1996, A numerical evaluation of electromagnetic methods in geothermal exploration, *Geophysics* **61**, 121–130.

Pelton, W.H. and Smith, P.K.: 1979, Mapping porphyry copper deposits in the Philippines with IP, *Geophysics*, **41**, 106–122.

Peric, M.: 1981, Exploration of Burundi nickeliferous laterites by electrical methods, *Geophys. Prosp.* **29**, 274–287.

Peters, W.S. and de Angelis, M.: 1987, The Radio Hill Ni-Cu massive sulphide deposit: A geophysical case history, *Explor. Geophys.* **18**, 160–166.

Petrick, W.R., Pelton, W.H., and Ward, S.H.: 1977, Ridge regression inversion applied to crustal resistivity sounding data from South Africa, *Geophysics* **42**, 995–1005.

Powell, J.A.: 1981, Electrical transient surveys for hydrocarbon. *50th Annual Internat. SEG Meeting and Exposition*, Expanded Abstracts, pp. 1773–1794.

Prieto, C., Perkins, C., and Berkman, E.: 1985, Columbia River Basalt Plateau – An integrated approach to interpretation of basalt-covered areas, *Geophysics* **50**, 2709–2719.

Raiche, A.P., Jupp, D.L.B., Rutter, H., and Vozoff, K.: 1985, The joint use of coincident loop transient electromagnetic and Schlumberger sounding to resolve layered structures, *Geophysics* **50**, 1618–1627.

Reed, L.E. and Sinclair, I.G.L.: 1991, The search for kimberlites in the James Bay lowlands of Ontario, *Can. Inst. Min. Bull.* **84**(947), 132–139.

Reinhardt, M.C. and Davidson, I.: 1990, Structural and lithologic controls on gold deposition in the shear-zone hosted Fazenda Brasileiro mine, Bahia state, Northeast Brazil, *Econ. Geol.* **85**, 952–967.

Rijo, L.: 1993, Three-dimensional transient electromagnetic modelling of complex conductive earth, *3rd Internat. Congr. Brazil. Geophys. Soc.*, Expanded Abstracts, pp. 1367–1372.

Ritzi, R.W. and Andolsek, R.H.: 1992, Relation between anisotropic transmissivity and azimuthal resistivity surveys of fractured, carbonate flow systems, *Ground Water* **30**, 774–780.

Robert, F.: 1991, Gold metallogeny of greenstone belts – considerations from the eastern Abitibi Subprovince, Canada, in E.A. Ladeira (ed.), Brazil Gold'91, pp. 31–48.

Ross, H.P., Mackelprang, C.E., and Wright, P.M.: 1990. Dipole-dipole electrical resistivity surveys at waste disposal study sites in Northern Utah, in S.H. Ward (ed.), *Geotechnical and Environmental Geophysics*, Vol. 2, Society of Exploration Geophysicists, pp. 145–152.

Ross, H.P. and Moore, J.N.: 1985, Geophysical investigations of the Cove Fort – Sulphurdale geothermal system, Utah, *Geophysics* **50**, 1732–1745.

Ruotsala, A.P.: 1975, Alteration of the Finsch kimberlite pipe, South Africa, *Econ. Geol.* **70**, 587-590.

Sandberg, S.K.: 1993, Examples of resolution improvement in geoelectrical soundings applied to groundwater investigations, *Geophys. Prosp.* **41**, 207–227.

Sangster, D.F.: 1972, Precambrian volcanogenic massive sulphide deposits in Canada: A review, Canada Geol. Survey Paper 72-22, 44 pp.

Sasaki, Y.: 2001, Full 3-D inversion of electromagnetic data on PC, *J. Applied Geophys.* **46**, 45–54.

Sassen, R.: 1980, Biodegradation of crude oil and mineral deposition in a shallow Gulf Coast salt dome, *Organic Geochemistry* **2**, 153–166.

Sawkins, F.J.: 1976, Massive sulphide deposits in relation to geotectonics, in D.F. Strong (ed.), *Metallogeny and Plate Tectonics*, Geological Association of Canada, Spec. Paper, 14, pp. 221–240.

Schneider, M.N. and Emerson, D.W.: 1980, Physical properties of the Elura prospect, Cobar, NSW, *Bull. Aust. Soc. Explor. Geophys.* **11**, 184–185.

Schwartz, G., Haak, V., and Rath, V.: 1985, Electrical conductivity studies in the Travale geothermal field, Italy, *Geothermics* **14**, 653–661. Sengpiel, K.-P. and Siemon, B., 1998, Examples of 1-D inversion of multifrequency HEM data from 3-D resistivity distributions, *Explor. Geophys.* **29**, 133–141.

Shima, H., Sakashita, S., and Kobayashi, T.: 1996, Development of non-contact data acquisition techniques in electrical and electromagnetic explorations. *J. Applied Geophys.* **35**, 167–173.

Shoham, Y., Morrison, F., and Torres-Verdin, C.: 1992, Electromagnetic mapping of electrical conductivity beneath the Columbia basalt, *54th EAEG Meeting, Paris*, Technical Abstracts, pp. 418–419.

Shtivelman, V. and Goldman, M.: 2000, Integration of shallow reflection seismics and time domain electromagnetics for detailed study of the coastal aquifer in the Nitzanim area of Isreal, *J. Applied Geophys.* **44**, 197–215.

Sill, W.R.: 1983, Cultural effects in induced polarization data, in *Electrical Methods in Oil and Gas Exploration*, University of Utah Research Institute, Earth Science Laboratory, Salt Lake City.

Sillitoe, R. H., 1972, A plate tectonic model for the origin of porphyry copper deposits, *Econ. Geol.* **67**, 184–197.

Sinha, A.K.: 1990, Stratigraphic mapping of sedimentary formations in southern Ontario by ground electromagnetic methods, *Geophysics* **55**, 1148–1157.

Smith, M.J.: 1980, Experimental controlled source audiomagnetotelluric measurements on the Elura orebody, NSW, *Explor. Geophys.* **11**, 261–263.

Smith, R.S., Annan, A.P., Lemieux, J., and Pedersen, R.N.: 1996, Application of a modified GEOTEM system to reconnaissance exploration for kimberlites in the Point Lake Area, NWT, Canada, *Geophysics* **61**, 82–92.

Smith, J.T. and Booker, J.R., 1991, Rapid inversion of two- and three-dimensional magnetotelluric data, *J. Geophys. Res.* **96**, 3905–3922.

Smith, R.S. and Keating, P.B.: 1996, The usefulness of multicomponent, time-domain airborne electromagnetic measurements, *Geophysics* **61**, 74–81.

Smith, R.J. and Pridmore, D.F.: 1989, Electromagnetic exploration for sulphides in Australia, in G.D. Garland (ed.), *Proc. Exploration'87*, Spec. Vol. 3, Ontario Geological Survey, Toronto, pp. 504–516.

Snyder, D.D., Kolvoord, R.W., Frangos, W., and Bajwa, Y.L.: 1981a, Exploration for petroleum using complex resistivity measurements, *Geophysics* **46**, 431.

Snyder, D.D., Kolvoord, R.W., Frangos, W., Bajwa, Y., Fleming, D.B., and Tasci, M.T.: 1981b, Exploration for petroleum using complex resistivity measurements, in *Advances In Induced Polarization and Complex Resistivity*, University of Arizona Press, Tucson, pp. 209–253.

Sorensen, K.I.: 1996, Pulled array continuous electric profiling, *First Break* **14**, 85–90.

Sorensen, K.I.: 1997, The pulled array transient electromagnetic method, *Proc. 3rd Meeting of EEGS-ES*, Aarhus, Demark, pp. 135–138.

Sorensen, K.I., Efferso, F., and Christensen, A.J.: 1995, Pulled array transient electromagnetic method (PATEM), *Proc. SAGEEP Conference*, Orlando, pp. 899–904.

Spence, C.D. and de Rosen-Spence, A.F.: 1975, The place of sulfide mineralization in the volcanic sequence at Noranda, Quebec, *Econ. Geol.* **70**, 90–101.

Spies, B.R.: 1983, Recent developments in the use of surface electrical methods for oil and gas exploration in the Soviet Union, *Geophysics* **48**, 1102–1112.

Spies, B.R.: 1988, Local noise prediction filtering for central induction transient electromagnetic sounding, *Geophysics* **53**, 1068–1080.

Spies, B.R. and Eggers, D.E.: 1986, The use and misuse of apparent resistivity in electromagnetic methods, *Geophysics* **51**, 1462–1471.

Spitzer, K.: 1993, Dreidimensionale geoelektrische modellrechnungen nach der methode der finiten differenzen. Bericht 111551, Niedersachsisches Landesamt fur Bodenforschung, Hanover, Germany.

Staltari, G.: 1986, The Que River TEM case study, *Explor. Geophys.* **17**, 125–128.

Stanley, W.D., Boehl, J.E., Bostick, F.X., and Smith, H.W.: 1982, Geothermal significance of magnetotelluric sounding of the eastern Snake River Plain – Yellowstone region, *J. Geophys. Res.* **82**, 2501-2514.

Stanley, W.D., Saad, A.R., and Ohofugi, W.: 1985, Regional magnetotelluric surveys in hydrocarbon exploration, Parana Basin, Brazil, *Bull. Amer. Assoc. Petrol. Geol.* **69**, 346–360.

Stanley, W.D., Gwilliam, W.J., Latham, G., and Westhusing, K.: 1992, The southern Washington Cascades Conductor – a previously unrecognised thick sedimentary sequence?, *Bull. Amer. Assoc. Petrol. Geol.* **76**, 1569–1585.

Stanton, R.L.: 1986, Stratiform ores and geological processes, *Trans. Inst. Min. Metall.* **95**(B), 167–178.

Sternberg, B.K., Washburne, J.C., and Pellerin, L.: 1988, Correction of static shift in magnetotellurics using transient electromagnetic soundings, *Geophysics* **53**, 1459–1468.

Stewart, I.C.F., Connally, T.C., and Copley, J.H.: 1996, Stratigraphic interpretation of magnetotelluric data in central Saudi Arabia, *GeoArabia* **1**(1), 52–63.

Stewart, M.T.: 1982, Evaluation of electromagnetic methods for rapid mapping of salt- water interfaces in coastal aquifers, *Ground Water* **20**, 538–545.

Stewart, M.T. and Gay, M.C.: 1986, Evaluation of transient electromagnetic soundings for deep detection of conductive fluids, *Ground Water* **24**, 351–356.

Strack, K.-M., 1992, *Exploration with Deep Transient Electromagnetics*, Elsevier Science Publ.

Strack, K.-M., LeBrocq, T., Moss, D.C., Vozoff, K., and Wolfgram, P.A.: 1989, Case histories of LOTEM surveys in hydrocarbon prospective areas, *First Break* **7**, 467–477.

Strack, K.-M., Luschen, E., and Kotz, A.W.: 1990, Long-offset transient electromagnetic (LOTEM) depth soundings applied to crustal studies in the Black Forest and Swabian Alb, Federal Republic of Germany, *Geophysics* **55**, 834–842.

Strack, K.-M., Hoerdt, A., Wolfgram, P.A., and Vozoff, K.: 1991, Integrated electromagnetic and seismic methods for petroleum exploration, *Explor. Geophys.* **22**, 375–378.

Strauss, G.K., Madel, J., and Fdez Alonso, F.: 1977, Exploration practice for strata-bound volcanogenic sulphide deposits in the Spanish-Portuguese Pyrite Belt: Geology, geophysics and geochemistry, in D.D. Klemm and H.J. Shneider (eds.), *Time- and Strata-Bound Ore Deposits*, Springer-Verlag.

Sugeng, F., Raiche, A. and Rijo, L.: 1993, Comparing the time-domain EM response of 2-D and elongated 3-D conductors excited by a rectangular loop source, *J. Geomag. Geoelectr.* **45**, 873–885.

Tagomori, K., Ushijima, K., and Kinoshita, Y.: 1984, Direct detection of geothermal reservoir at the Hatchobaru Geothermal Field by the Mise-a-la-masse measurement, *Geothermal Resources Council, Transactions* **8**, 513–516.

Thanassoulas, C., Tselentis, G.-A., and Kolios, N., 1986, Geothermal prospecting by geoelectric soundings in NE Greece, *Geophys. Prosp.* **34**, 83–97.

Torres-Verdin, C. and Bostick, F.X., Jr., 1992, Principles of spatial surface electric field filtering in magnetotellurics: Electromagnetic array profiling (EMAP), *Geophysics* **57**, 603–622.

Tyne, E.D., Idnurm, M., and Malone, E.J.: 1981, Physical properties of the Woodlawn orebody and surrounding rocks, in R.J. Whiteley (ed.), *Geophysical Case Study of the Woodlawn Orebody, New South Wales, Australia*, Pergamon Press, pp. 99–111.

Tyne, E.D., Haren, R.J., and Webster, S.S.: 1980, A computer model evaluation of the resistivity and IP response of the Elura deposit, *Explor. Geophys.* **11**, 208–216.

Uchida, T. and Murakami, Y.: 1990, Development of a FORTRAN code for the two-dimensional Sclumberger inversion, Geol. Surv. Japan, Open-file Report No. 150.

Unsworth, M., Xinyou, L., and Watts, M.D.: 1997, Site characterisation for radioactive waste disposal using CSAMT, *67th Annual Internat. SEG Meeting*, Extended Abstracts, Paper 97a.

Ushijima, K., Noritomi, K., Tagomori, K., and Kinoshita, Y.: 1986, Magnetotelluric interpretation of the Hatchobaru geothermal area (I), *Butsuri-Tausa (Geophysical Exploration)* **39**(5), 24–41.

van Lisa, R.V., van Maanen, H.R.J., and Odera, F.W.: 1987, The use of remote sensing and geophysics for groundwater exploration in Nyanza Province – Kenya. Paper presented at the African Water Technology Conference, Nairobi, February 1987.

Van Ngoc, P. and Daniele, B.: 1992, *Mesures magneto-telluriques sur le secteur de Lagoa Salgada, Relatorio interno*. Dep. Geomagnetisme, Inst. Physique du Globe de Paris, 20 pp.

Vogelsang, D.: 1987, Examples of electromagnetic prospecting for karst and fault systems, *Geophys. Prosp.* **35**, 604–617.

Vozoff, K.: 1972, The magnetotelluric method in the exploration of sedimentary basins, *Geophysics* **37**, 98–141.

Vozoff, K.: 1991, The magnetotelluric method, in M.N. Nabighian (ed.), *Electromagnetic Methods in Applied Geophysics*, Vol. 2B, Application: Society of Exploration Geophysicists, pp. 641–711.

Wagner, P.A.: 1914, *The Diamond Fields of Southern Africa, The Transvaal Leader* (2nd impression, C. Struik (Pty) Ltd).

Wait, J.R. and Williams, J.T.: 1985, EM and IP response of a steel well casing for a four-electrode surface array: Part I, theory, *Geophys. Prosp.* **33**, 723–735.

Wannamaker, P.E.: 1983, Resistivity structure of the Northern Basin and Range, in *The Role of Heat in the Development of Energy and Mineral Resources in Northern Basin and Range*, Geothermal Resources Council, Special Rep. 13, pp. 345–362.

Wannamaker, P.E.: 1991, Advances in three-dimensional magnetotelluric modelling using integral equations, *Geophysics* **56**, 1716–1728.

Wannamaker, P.E.: 1997a, Tensor CSAMT survey over the Sulphur Springs thermal area, Valles Caldera, New Mexico, U.S.A., Part I: Implications for structure of the western caldera, *Geophysics* **62**, 451–465.

Wannamaker, P.E.: 1997b, Tensor CSAMT survey over the Sulphur Springs thermal area, Valles Caldera, New Mexico, U.S.A., Part II: Implications for CSAMT methodology, *Geophysics* **62**, 466–476.

Ward, S. H.: 1966, The search for massive sulphides – Introduction, in *Mining Geophysics I*, Society of Exploration Geophysicists, pp. 117–129.

Warner, M.M.: 1975, Special aspects of Cenozoic history of southern Idaho and their geothermal implications, in *Proc. 2nd United Nations Symposium on the Development and Use of Geothermal Resources*, San Francisco, 20–29 May 1975, pp. 653–664.

Warren, R.K.: 1992, Subsurface imaging with EMAP – an aid to seismic processing and interpretation, *54th EAEG Meeting, Paris*, Technical Abstracts, pp. 432–433.

Warren, R.K. and Srnka, L.J.: 1992, Exploration in the basalt-covered areas of the Columbia River Basin, Washington, using electromagnetic array profiling (EMAP), *Geophysics* **57**, 986–993.

Webster, S.S. and Woods, K.T.: 1988, Field trials of non-seismic geophysical techniques for petroleum exploration in New South Wales, *Explor. Geophys.* **19**, 193–198.

Weller, A., Frangos, W., and Seichter, M.: 2000, Three-dimensional inversion of induced polarization data from simulated waste, *J. Applied Geophys.* **44**, 67–83.

White, D.E.: 1973, Characteristics of geothermal resources, in P. Kruger and C. Otte (eds.), *Geothermal Energy*, Stanford University Press, Stanford, CA, pp. 69–94.

White, D.E. and Williams, D.L. (eds.): 1975, *Assessment of Geothermal Resources of the United States – 1975*, Geol. Surv. Circ. 726.

Wightman, W.E., Kaufman, A.A., and Hoeskra, P.: 1983, Mapping gas-water contacts in shallow producing formations with transient EM, *52nd Annual Internat. SEG Meeting and Exposition*, Expanded Abstracts, pp. 59–60.

Wilt, M.J. and Williams, J.P.: 1989, Layered model inversion of central-loop EM soundings near a geological contact, *Explor. Geophys.* **20**, 71–73.

Wilt, M., Goldstein, N.E., Stark, M., Haught, J.R., and Morrison, H.F.: 1983, Experience with the EM-60 electromagnetic system for geothermal exploration in Nevada, *Geophysics* **48**, 1090–1101.

Witherly, K.E.: 1977, Geophysical and geochemical methods used in the discovery of the Island Copper deposits, Vancouver Island, British Columbia, in P.J. Hood (ed.), *Geophysics and Geochemistry in the Search for Metallic Ores*, Geological Survey of Canada Economic Geology Report 31.

Withers, R., Eggers, D., Fox, T., and Crebs, T.: 1994, A case study of integrated hydrocarbon exploration through basalt, *Geophysics* **59**, 1666–1679.

Word, D.R., Rosen, R., Horita, J., and Ishihra, K.: 1992, EMAP (Electromagnetic Array Profiling) Part I: An introduction to EMAP and some case studies in oil and gas fields, *Butsuri-Tansa* **45**, 224–233.

Wright, P.M., Ward, S.H., Ross, H.P., and West, R.C.: 1985, State of the art geophysical exploration for geothermal resources, *Geophysics* **50**, 2666–2696.

Yang, C.-H., Tong, L.-T., and Huang, C.-F.: 1999, Combined application of dc and TEM to sea-water intrusion mapping, *Geophysics* **64**, 417–425.

Zhang, J., Mackie, R.L., and Madden, T.R.: 1995, 3-D resistivity forward modelling and inversion using conjugate gradients, *Geophysics* **60**, 1313–1325.

Zhang, Sa., Z., Li, Y., Zhou, J., Nie, X., Zhou, A., and Yang, G.: 1986, The induced polarisation (IP) method in oil exploration - The cause of the IP and its relation to oil reservoirs, *Acta Geophys. Sinica* **29**, 597–612 (in Chinese).

Zhdanov, M.S., Traynin, P.N., and Portniaguine, O.: 1995, Resistivity imaging by time-domain electromagnetic migration, *Explor. Geophys.* **26**, 186–194.

Zonge Engineering: 1985, Delineation of oil and gas fields using CSAMT – a case history: Bodalla South and Mount Bellalie, Eromanga Basin, Queensland, Zonge Engineering and Research Organisation (Australia) Company document.

Zonge, K.L. and Hughes, L.J.: 1981, The complex resistivity method, in *Advances In Induced Polarization and Complex Resistivity*, University of Arizona Press, Tucson, pp. 163–208.